ErbB1-dependent signalling and vesicular trafficking in primary afferent nociceptors associated with hypersensitivity in neuropathic pain

ErbB1-dependent signalling and vesicular trafficking in primary afferent nociceptors associated with hypersensitivity in neuropathic pain.

Rory Mitchell[1], Marta Mikolajczak[1], Christian Kersten[2], Sue Fleetwood-Walker[1]*

[1] Centre for Discovery Brain Sciences, Edinburgh Medical School, College of Medicine & Veterinary Medicine, University of Edinburgh, Edinburgh, UK; & [2] Center for Cancer Treatment, Sorlandet Hospital, Pb 416, 4604 Kristiansand, Norway.

Correspondence should be sent to:

Sue Fleetwood-Walker, Centre for Discovery Brain Sciences, Edinburgh Medical School: Biomedical Sciences, Hugh Robson Building, George Square, University of Edinburgh, Edinburgh EH8 9XD, UK.

Telephone: (+44) 131 651 1696
Email: s.m.fleetwood-walker@ed.ac.uk

Graphical Abstract

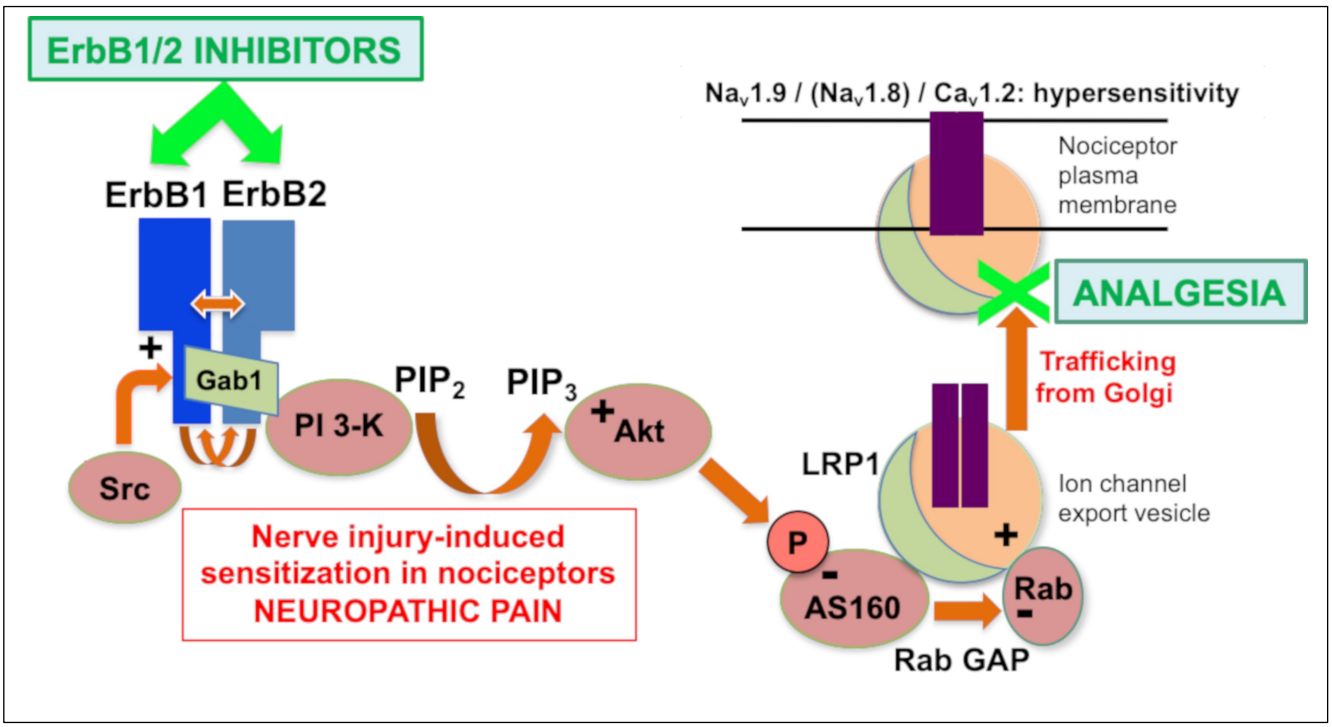

Highlights

- ErbB1 inhibitors reverse hypersensitivity in neuropathic pain models, as clinically
- Nociceptors in DRG selectively express ErbB1 and ErbB2 but not ErbB3 or ErbB4
- ErbB1 drives Akt- /AS160-dependent trafficking of nociceptor Na^+ and Ca^{2+} channels
- ErbB1- and Akt-inhibitors prevent channel trafficking and hypersensitivity
- Dual blockade of the ErbB1/2 signalling hub produces synergistic analgesia

Abstract

Effective analgesic treatment for neuropathic pain remains an unmet need, so previous evidence that epidermal growth factor receptor inhibitors (EGFRIs) provide unexpected rapid pain relief in a clinical setting points to a novel therapeutic opportunity. The present study utilises rodent models to address the cellular and molecular basis for the findings, focusing on primary sensory neurons because clinical pain relief is provided not only by small molecule EGFRIs, but also by the anti-EGFR antibodies cetuximab and panitumumab, which are unlikely to access the central nervous system in therapeutic concentrations. We report robust, rapid and dose-dependent analgesic effects of EGFRIs in two neuropathic pain models, matched by evidence with highly selective antibodies that expression of the EGFR (ErbB1 protein) is limited to small nociceptive afferent neurons. As other ErbB family members can heterodimerise with ErbB1, we investigated their distribution, showing consistent co-expression of ErbB2 but not ErbB3 or ErbB4, with ErbB1 in cell bodies of nociceptors, as well as providing evidence for direct molecular interaction of ErbB1 with ErbB2 in situ. Co-administration of selective ErbB1 and ErbB2 inhibitors produced clear evidence of greater-than-additive, synergistic analgesia; highlighting the prospect of a unique new combination therapy in which enhanced efficacy could be accompanied by minimisation of side-effects. Peripheral (intraplantar) administration of EGF elicited hypersensitivity only following nerve injury and this was reversed by local co-administration of selective inhibitors of either ErbB1 or ErbB2. Investigating how ErbB1 is activated in neuropathic pain, we found evidence for a role of Src tyrosine kinase, which can be activated by signals from inflammatory mediators, chemokines and cytokines during neuroinflammation. Considering downstream consequences of ErbB1 activation in neuropathic pain, we found direct recruitment to ErbB1 of an adapter for PI 3-kinase and Akt signalling together with clear Akt activation and robust analgesia from selective Akt inhibitors. The known Akt target and regulator of vesicular trafficking, AS160 was strongly phosphorylated at a perinuclear location during neuropathic pain in an ErbB1-, ErbB2- and Akt-dependent manner, corresponding to clustering and translocation of an AS160-partner, the vesicular chaperone, LRP1. Exploring whether neuronal ion channels that could contribute to hyperexcitability might be transported by this vesicular trafficking pathway we were able to identify $Na_v1.9$, ($Na_v1.8$) and $Ca_v1.2$ moving towards the plasma membrane or into proximal axonal locations – a process prevented by ErbB1 or Akt inhibitors. Overall these findings newly reveal both upstream and downstream signals to explain how ErbB1 can act as a signalling hub in neuropathic pain models and identify the trafficking of key ion channels to neuronal subcellular locations likely to contribute to hyperexcitability. The new concept of combined treatment with ErbB1 plus ErbB2 blockers is mechanistically validated as a promising strategy for the relief of neuropathic pain.

Keywords

Neuropathic pain, EGF receptor, ErbB1, ErbB2, cetuximab, Src, Akt, vesicular trafficking, $Na_v1.7/1.8/1.9$, $Ca_v1.2$

Introduction

Chronic hypersensitive pain states, especially those due to nerve injury (neuropathic pain) are difficult to treat with current medications, which show limited efficacy and frequently treatment-limiting side effects (Finnerup, Sindrup et al. 2010). There is a clear unmet need to develop new, safe and efficacious analgesics for neuropathic pain through novel targeting strategies. One such approach originated from our serendipitous observation of remarkable pain relief in a rectal cancer patient treated with the anti-epidermal growth factor receptor (EGFR) antibody, cetuximab, despite tumour progression (Kersten and Cameron 2012), which initiated a reverse-translational programme to elucidate the role of the EGFR in pain processing. Clinical follow-up studies on a small case series and then a larger study of patients with neuropathic pain of different origins (both cancer and non-cancer) showed similarly promising results (80% clinically meaningful response) with cetuximab, panitumumab and the small molecule EGFR inhibitors, gefitinib and erlotinib (Kersten, Cameron et al. 2013, Kersten, Cameron et al. 2015). A small-scale randomised proof-of-concept trial of cetuximab in neuropathic pain patients (nerve compression and complex regional pain syndrome), corroborated the idea of a clinically meaningful analgesic signal (Kersten, Cameron et al. 2019). Importantly, many of the patients responding to EGFR inhibitors had pain that had proved refractory to all other interventions, emphasizing the potential of this novel strategy. Some mechanistic insight arises from the efficacy displayed by cetuximab and panitumumab (which are unlikely to penetrate the blood-brain barrier in therapeutic concentrations) and therefore implicates primary sensory afferents as a likely site of action.

Independent support for the idea of EGFR involvement in chronic pain has come from molecular genetics analysis (Martin, Smith et al. 2017, Verma, Khoury et al. 2020) of patients with temporomandibular disorders – a group of conditions associated with chronic pain from joint, muscle or central origins (Cairns 2010). A number of single nucleotide polymorphisms (SNPs) in the genes for epiregulin (an EGFR ligand) and EGFR showed significant differential association with TMD patient and control groups (Martin, Smith et al. 2017, Verma, Khoury et al. 2020). The minor allele of the epiregulin SNP most strongly associated with reduced odds of chronic TMD was matched to lower epiregulin mRNA levels in leukocytes (Martin, Smith et al. 2017). However, the minor allele was also associated with increased numbers of acute pain sites in TMD patients (Verma, Khoury et al. 2020). Rodent chronic pain models have provided further support for a role of the EGFR in pain processing. The hypersensitivity due to nerve injury, inflammation or direct compression injury to DRG (CCD) was attenuated by EGFR-selective inhibitors (although across a range of potencies) and also (in the case of CCD) by EGFR siRNA (Martin, Smith et al. 2017, Wang, Liu et al. 2019). Furthermore, mice expressing a constitutively activating EGFR mutation show enhanced responses to formalin, while *Drosophila* larvae with EGFR knockdown in peripheral nociceptors display impaired thermal nociception (Martin, Smith et al. 2017).

The EGFR (ErbB1) is one of a family of 4 receptor tyrosine kinases (RTKs), which display sequence homology and a common structural organisation (Olayioye, Neve et al. 2000). ErbB2 is thought to lack a physiological ligand yet act as the preferred heterodimerisation partner for all other ErbB receptors (Graus-Porta, Beerli et al. 1997, Tzahar, Pinkas-Kramarski et al. 1997) and can enable constitutive functional activity (Garrett, McKern et al. 2003), while ErbB3 has ligands but displays minimal levels of tyrosine kinase catalytic activity (around 1000-fold less than ErbB1) (Shi, Telesco et al. 2010). The functional importance of ErbB1:ErbB2 heterodimers is emphasised, for example, by the elevated basal phosphorylation of both ErbB1 and ErbB2 in co-transfected cells and the potent inhibition of ErbB2-overexpressing tumour and cell line proliferation by highly selective ErbB1 inhibitors (Moasser, Basso et al. 2001). ErbB dimerisation generally comes about as a result of ligand-induced conformational changes stabilising an extended configuration of extracellular domains (Dawson, Berger et al. 2005). The chimeric human/murine monoclonal antibody, cetuximab (Kim, Khuri et al. 2001, Harding and Burtness 2005) binds to an extracellular domain of ErbB1 that partly occludes the ligand binding site and also inhibits transition to the extended configuration necessary for dimerisation (Li, Schmitz et al. 2005, Berger, Krengel et al. 2011) but importantly results in down-regulation of EGFR expression (Perez-Torres, Guix et al. 2006). Although the classical paradigm for ErbB receptor activation centres on ligand-induced initiation of dimerisation, there is evidence for ligand-independent formation of homo- and hetero-dimers (including ErbB1:ErbB2) and in some cases for their initial assembly in the endoplasmic reticulum (Verveer, Wouters et al. 2000, Moriki, Maruyama et al. 2001, Sawano, Takayama et al. 2002, Yu, Sharma et al. 2002, Kumagai, Katsumata et al. 2003, Tao and Maruyama 2008, Junttila, Akita et al. 2009).

ErbB receptors undergo constant internalisation, intracellular shuttling and recycling (Wiley 2003). Although ErbB1 is predominantly localised at the cell surface in fibroblasts, other cell types maintain large intracellular pools of unliganded receptor (Burke and Wiley 1999, Kim, Khuri et al. 2001). In the case of cetuximab binding to ErbB1, the internalised complex is resistant to dissociation in the acidified environment of endosomes and is therefore targeted for lysosomal degradation rather than recycling, thereby quickly depleting the shuttling pool of ErbB1 receptor protein (Jimeno, Rubio-Viqueira et al. 2005, Li, Schmitz et al. 2005). Neuronal ErbB1 expression has been reported in both the CNS and dorsal root ganglia (DRG) (Gomez-Pinilla, Knauer et al. 1988, Ferrer, Alcantara et al. 1996, Xian and Zhou 1999). In DRG, expression has been reported to be preferentially in smaller neurons (Huerta, Diaz-Trelles et al. 1996, Xian and Zhou 1999), whereas other studies have suggested a widespread neuronal localisation (Andres, Meyer et al. 2010, Martin, Smith et al. 2017) or preferential expression in medium/large myelinated neurons and minimal co-expression with markers of small unmyelinated neurons (Wang, Liu et al. 2019). Some studies also report ErbB1 expression in glial cells within DRG (Andres, Meyer et al. 2010, Wang, Liu et al. 2019). Expression of other ErbB family members has also been reported in DRG neurons (Pearson and Carroll 2004).

ErbB receptors achieve diverse signalling outcomes by trans- or autophosphorylation of Tyr residues in their intracellular carboxy-terminal domains, which act as high affinity docking sites for various signalling and adapter proteins (Olayioye, Neve et al. 2000). ErbB1 autophosphorylation at Tyr1068 primarily leads to the recruitment of signalling adapters, Grb2 (to regulate the ERK MAP kinase pathway) and Gab1 (to enable PI 3-kinase binding and activation, then downstream activation of Akt) (Lowenstein, Daly et al. 1992, Downward 1994, Holgado-Madruga, Emlet et al. 1996, Rodrigues, Falasca et al. 2000, Mattoon, Lamothe et al. 2004, Cao, Huang et al. 2009). In endothelial cells stably transfected with ErbB1 or ErbB1 plus ErbB2, there is evidence for ligand-independent activation as shown by significant basal phosphorylation of ErbB1, ErbB2 and ERK (Berger, Krengel et al. 2011). In this model, cetuximab markedly reduced not only EGF-induced responses, but also basal, unstimulated ERK phosphorylation, clearly impacting on ligand-independent downstream signalling from ErbB1/2.

In view of the clinical findings pointing to the potential of EGFR inhibition as a strategy for alleviation of chronic hypersensitive pain, we sought to corroborate this in a controlled laboratory setting and explore some of the underlying mechanisms. Although the humanised/human monoclonal antibodies, cetuximab and panitumumab, would not be useful tools in rodent studies due to immune incompatibility, many small molecule inhibitors of different ErbB family receptors have been developed because of their therapeutic potential in oncology (Roskoski 2014, Kavuri, Jain et al. 2015). A number of these tyrosine kinase inhibitors (TKIs) are very highly selective for particular ErbB receptors, against other ErbB family members and panels of other protein kinases (Fabian, Biggs et al. 2005, Anastassiadis, Deacon et al. 2011, Davis, Hunt et al. 2011).

Material and Methods

Animals

All animal breeding, maintenance and experimental procedures complied with ARRIVE guidelines and were carried out in accordance with the UK Animals (Scientific Procedures) Act 1986, with approval from the University of Edinburgh's Local Ethical Review Board. Animals were housed under a 12h light-dark cycle and given access to food and water *ad libitum*. Most experiments were carried out on adult Sprague-Dawley rats (200-350g in weight, which were male unless otherwise indicated). The sciatic nerve chronic constriction injury (CCI) preparation was used as a model of chronic neuropathic pain in rats (Bennett and Xie 1988). Animals were anaesthetised with a 4% isoflurane/oxygen mixture (Zeneca, Cheshire, UK) before exposure of the sciatic nerve, proximal to the trifurcation at mid-thigh level. Four loose ligatures of chromic catgut (SMI AG, Hunningen, Belgium) were tied around the nerve, separated by 1mm. CCI rats consistently developed ipsilateral thermal reflex hypersensitivity, which peaked between days 8 and 12 post-surgery, when experiments were carried out. Some experiments were carried out in adult male C57/Bl6J mice (25-35g in

weight), using an oxaliplatin model of chemotherapy-induced peripheral neuropathy (CIPN) (Zhao, Isami et al. 2012). Oxaliplatin (Abcam) in 5% glucose vehicle was injected intraperitoneally (under light isoflurane anaesthesia) at a dose of 7mg/kg (100μl/mouse) and experiments carried out 3-7days later when mechanical hypersensitivity was fully developed.

Quantitative sensory testing in vivo

Mechanical and thermal nociceptive sensitivity were assessed using standard behavioural tests, during which, the investigator was blinded to drug treatment. Mechanical nociception was assessed as Paw Withdrawal Threshold (PWT; in g) from force-calibrated von Frey nylon filaments (Stoelting, Illinois). Nociceptive heat sensitivity was measured as Paw Withdrawal Latency (PWL; in sec) using Hargreaves' infrared apparatus (Linton Instrumentation), set to a maximum temperature of 52^{o}C and a cut-off time of 20sec. Testing was always separated by at least 5min to avoid sensitisation of responses. Nociceptive cold sensitivity was measured as Suspended Paw Elevation Time using a shallow water bath at the temperature of iced water (~4^{o}C) (Garry, Moss et al. 2003). Animals were initially habituated to the sensory testing environments to establish consistent responses.

Drug administration in vivo

Small molecule agents were obtained from MedChem Express, Selleckchem, Key Organics or Axon MedChem. Murine EGF, purified from submaxilliary gland and recombinant human neuregulin1-β1 EGF domain (NRG1) were obtained from Sigma-Aldrich and R & D Systems, respectively. For intraperitoneal administration (200μl/rat and 100μl/mouse) agents were dissolved in 10% dimethylsulphoxide, 40% polyethylene glycol-400 and 50% propylene glycol. For intraplantar administration (50μl/rat) agents were dissolved in normal saline with 0.3% dimethylsulphoxide. Vehicle controls showed no discernible change in pain-associated behavioural responses. Doses of pharmacological agents were selected on the basis of those showing clear efficacy/target coverage (producing at least 80-90% maximal effects) in literature reports, wherever possible, or their reported potency in vitro compared to that of the benchmark, erlotinib.

Immunofluorescence histochemistry

DRGs from spinal segments L4-6 were dissected, rapidly embedded in cryo-sectioning medium (Thermo Scientific) and frozen on dry ice. 18μm sections were cut by cryostat and mounted onto poly-L-lysine coated slides (Thermo Scientific). Sections were washed in Tris-Buffered Saline (TBS) pH7.60 and then incubated for 1h at room temperature in blocking buffer (10% normal donkey serum, 4% fish skin gelatin, 0.2% Triton X-100 in TBS) prior to overnight incubation at 4°C with a combination of primary antibodies in buffer (4% normal donkey serum, 4% fish skin gelatin and 0.2% Triton X-100 in TBS). The primary antibodies used are listed in Table 1. Sections were washed in TBS and incubated for 1h at room temperature with a combination of

extensively cross-adsorbed, fluorescent secondary antibodies or Alexa Fluor-488 conjugated isolectin IB4 (Invitrogen; I21411; 1:3000) in buffer (4% normal donkey serum, 4% fish skin gelatin in TBS). Donkey anti-mouse, rabbit, chicken or guinea pig secondary antibodies, labelled with 633/647, 568, 488 or 405 nm-emitting fluorophores in appropriate permutations, and all highly cross-adsorbed against other relevant species, were obtained from Biotium via Sigma-Aldrich and were used at a dilution of 1:600. Sections were washed three further times in TBS and then mounted in ProLong® Gold Antifade (Life Technologies). Standard primary antibody omission or blocking peptide controls, wherever possible, confirmed that non-specific staining was minimal. Both concentration-dependence of staining and association with peripherin-positive or NF-200-positive cellular profiles, where appropriate, corroborated specificity.

Confocal microscopy and image analysis

Fluorescence signals were acquired using a Nikon A1R confocal microscope at 1024 × 1024 pixel size frame, 12 bits per pixel images, with a pinhole size 1AU calculated for 488, using objectives 10X Plan Fluor/NA0.3, 20X Plan Apo VC/NA 0.8, or 60X Plan Apo VC/NA1.4 (oil immersion). In all cases, emissions for each fluorophore were obtained sequentially to avoid channel bleed-through. Z-stacks were acquired covering the whole thickness of each section at a low power magnification (acquired with 10X or 20X objectives; 5μm and 2μm step size between planes) and maximum intensity projections were generated using ImageJ/Fiji. All cells positive for markers of interest were blind-counted manually (using ImageJ/Fiji software plugin), usually versus ErbB1 or peripherin across the whole section in each case. Mean percentage expression values were generated over sections from at least 4 separate animals. Antigen distribution within single cells (collected at a high power with optical zoom at 0.09x0.09 pixel size) was analysed by measuring fluorescence intensity using Plot Profile tool in ImageJ/Fiji in single plane images (at the centre of each cell) and drawing a transect from the nuclear perimeter to the neuronal apex, that was then divided into 50 bins. Visualisation and three-dimensional reconstruction of images was performed using IMARIS (Bitplane). In the case of phospho-AS160 (Thr642), which was clustered tightly in a peri-nuclear location, only the proximal part of the transect (covering all the discernible fluorescence signal) was analysed by division into 50x0.09μm bins starting at the nuclear perimeter, and fluorescence intensity recorded at each. In order to facilitate comparisons between transect profiles, values were normalised. If the mean intensity from the naïve and CCI datasets differed by more than 40% (as might be anticipated for newly evoked changes such as target phosphorylation or clustering of previously dispersed target proteins into aggregates), normalisation was carried out to the overall mean intensity of the entire data set. This enabled detection of changes in relative intensity as well as the location of any changes. If this value was less than 40% (consistent with simple redistribution of the target protein), normalisation was carried out to the mean for the individual cell sampled, which enabled clearer analysis of changes in fine subcellular localisation.

Mean values were calculated generally across 8-9 individual cell transects originating from 4 separate animals in each case.

Proximity Ligation Assay

Evidence for *in situ* protein:protein interactions was obtained using the Duolink Proximity Ligation Assay (Sigma-Aldrich) (Fredriksson, Gullberg et al. 2002, Soderberg, Gullberg et al. 2006, Liu, Chen et al. 2013, Rivera-Oliver, Moreno et al. 2019). Rabbit or mouse primary antibodies for potential protein partners are outlined in Table 1. Oligonucleotide-derivatised secondary antibody probes were donkey anti-rabbit PLUS and donkey anti-mouse MINUS. Probe ligation, rolling circle amplification (RCA) and detection of the RCA product by Duolink Orange fluorophore (emission 576nm) were all carried out according to the manufacturer's instructions. An optimised procedure was developed to integrate conventional immunofluorescence counterstaining (with chicken anti-peripherin and donkey anti-chicken 488) into the protocol.

Non-linear curve-fitting and statistical analysis

All data analysis was carried out using GraphPad Prism. Non-linear curve-fitting used a sigmoidal dose-response (variable slope) model. Data in two-group format were analysed statistically by Student's t-test. Comparisons between more than two groups were made by One-Way ANOVA with Tukey's or Dunnett's test, or by Two-Way ANOVA with Bonferroni's test.

Results

ErbB1 involvement in hypersensitive pain behaviours and nociceptor activation following nerve injury

Using the CCI neuropathic pain model, marked nociceptive hypersensitivity was observed in the ipsilateral (but not contralateral) hindlimb 8-12days following nerve injury. This was manifest as a reduction in Paw Withdrawal Threshold (PWT) from von Frey filament mechanical stimuli (Fig. 1A), a reduction in Paw Withdrawal Latency (PWL) from Hargreaves' noxious thermal stimuli (Fig. 1B) and an increase in suspended paw elevation time from 4^{o}C noxious cold stimuli (Fig. 1C). In each case, intraperitoneal administration of the highly selective inhibitor of ErbB1 tyrosine kinase function, erlotinib (Moyer, Barbacci et al. 1997) at a dose of 10mg/kg ip, produced marked rapid reversal of ipsilateral hypersensitivity, which was complete at peak effect and remained statistically significant for 140-160min. No discernible effects were observed on responses from the contralateral limb or from vehicle injection. This time course is consistent with evidence that plasma levels of erlotinib increase rapidly after administration and begin to decline steeply after around 2 hours (Pollack, Savage et al. 1999). The reversal of CCI-induced mechanical hypersensitivity by erlotinib was dose-dependent (with a statistically significant effect at as little as 1mg/kg and an IC_{50} of 1.4 [1.3/1.5] mg/kg ip (mean [95% confidence interval]), (Table 2), corresponding to

the dose range (100-150mg) found to provide effective pain relief in patients (Kersten, Cameron et al. 2015). The effect of erlotinib here was also replicated by further highly selective ErbB1 inhibitors, gefitinib (Moasser, Basso et al. 2001, Pedersen, Pedersen et al. 2005) and AG 1478 (Traxler, Green et al. 1999), with effects similar to erlotinib at corresponding doses (Table 2). Reversal of nerve injury-induced mechanical hypersensitivity by erlotinib was similarly observed in female CCI rats (mean percentage reversal over 20-140min post-injection of 88.9±9.2%, n=4, $p<0.01$, at a dose of 10mg/kg ip).

As most selective ErbB1 inhibitors are based around a common quinazoline core, we tested two further, structurally distinct selective agents, falnidamol (BIBX 3182) (Solca, Baum et al. 2004) and EGFRi 324674 (Zhang, Liu et al. 2006). These contain distinct pyrimidopyrimidine and 4,6-substituted-pyrimidine cores, respectively and at appropriate doses they also produced robust reversal of hypersensitivity through 20-140min post-administration, respectively (n=4, in each case), confirming target-specific efficacy (Table 2). Similar results (demonstrating dose-dependence in each case) were observed in a mouse model of oxaliplatin-induced peripheral neuropathy (Zhao, Isami et al. 2012), with IC_{50} values [95% CI] of 3.2 [3.0/3.3] mg/kg ip for erlotinib, 2.4 [2.3/2.6] mg/kg ip for gefitinib and 3.0 [2.7/3.4] mg/kg ip for AG 1478 (n=4 at 4-5 different doses in each case). In both rat CCI and mouse CIPN models, animals showed no discernible changes in general locomotion or motor function, or evidence of sedation, following administration of ErbB1 inhibitors. The doses of erlotinib producing analgesia in the neuropathic pain models here are similar to, or less than, those necessary to reverse EGF-induced autophosphorylation of ErbB1 in liver and tumour xenografts of athymic mice, consistent with appropriate target-associated potency and coverage (Moyer, Barbacci et al. 1997, Pollack, Savage et al. 1999). Repeated testing with erlotinib (10mg/kg ip) showed no significant attenuation of its ability to reverse CIPN-induced hypersensitivity over 7 daily treatments, similar to observations in the CCD (chronic DRG compression) model (Wang, Liu et al. 2019).

In order to provide an unbiased biomarker of activity in nociceptive afferents we measured levels of phospho-CaM kinase IIα (Thr286) in DRG cells. This marker reflects Ca^{2+}-dependent autophosphorylation of the enzyme to an autonomous form of the enzyme, but both activity and Thr286-phosphorylation diminish rapidly, within minutes, following stimulus removal (Lou, Lloyd et al. 1986, Schworer, Colbran et al. 1986, Lengyel, Voss et al. 2004, Chang, Parra-Bueno et al. 2017). Figure 1D shows that phospho-CaMKII (Thr286) staining in small, peripherin-positive DRG cells was significantly increased ipsilateral to CCI and that this was almost completely reversed by erlotinib (10mg/kg ip, 1hr), indicating that CCI-induced activity in nociceptors is highly dependent on ErbB1 functional activity.

ErbB1 is selectively localised in small, peripherin-positive DRG neurons

As there was some disparity in previous reports over ErbB1 expression in subpopulations of DRG cells (Huerta, Diaz-Trelles et al. 1996, Xian and Zhou 1999, Andres, Meyer et al. 2010, Martin, Smith et al. 2017, Wang, Liu et al. 2019), we

addressed this using extensively characterised ErbB1-specific antibodies. Figure 2A shows results using two antibodies documented to label ErbB1, but not other ErbB family members, revealing very high correlation between staining for ErbB1 and peripherin in small DRG cells that are likely to represent unmyelinated nociceptors (Goldstein, House et al. 1991, Fornaro, Lee et al. 2008). In DRG from naïve and CCI animals similarly, both ErbB1-specific antibodies stained 80-90% of peripherin-positive small cells with minimal staining outwith this population. A third ErbB1 antibody (mouse monoclonal 8G6.2); raised against a distinct intracellular epitope in ErbB1), confirmed these results, staining 84.8±1.2% of peripherin-positive DRG cells from naïve animals (CCI not tested; mean±SEM, n=4). In contrast, co-staining with the myelinated neuronal marker, NF-200 (Goldstein, House et al. 1991, Fornaro, Lee et al. 2008), the satellite glial cell marker, glutamine synthetase (Miller, Richards et al. 2002) and the microglial/recruited macrophage marker, CD68 (Hu and McLachlan 2003) was minimal (Fig. 2B). The pattern and levels of ErbB1 expression in DRG were not significantly altered following CCI.

Within the population of ErbB1-expressing small DRG cells, both presumed peptidergic C-fibres, staining for TRPV1 (Cavanaugh, Lee et al. 2009) and presumed non-peptidergic fibres, labelled with isolectin, IB4 (Dong, Han et al. 2001) were strongly represented, with 87.1±2.1% of TRPV1 (and peripherin)-positive cells, and 88.6±2.1% of IB4 (and peripherin)-positive cells co-staining for ErbB1 (means±SEM, n=12). Similar values were found in CCI animals. These observations are consistent with the idea of ErbB1 playing an important role in nerve injury-induced hypersensitivity throughout the whole C-fibre nociceptor population.

As ErbB1 may heterodimerise with other ErbB family members (Olayioye, Neve et al. 2000), we also investigated the expression in DRG of ErbB2-4, using highly characterised, isotype-specific antibodies. We found ErbB2 to be widely and selectively expressed in small, peripherin-positive DRG cells, like ErbB1, with around 90% of peripherin-positive cells expressing ErbB2 in both naïve and CCI animals (Fig. 2C). Similar results were obtained for ErbB2 expression in ErbB1-positive cells (Fig. 2C) and were confirmed with a second highly characterised ErbB2-specific antibody (mouse monoclonal, UMAB36) which showed staining in 76.2±6.3% and 78.5±4.4% of ErbB1-positive cells in naïve and CCI DRG, respectively (means±SEM, n=4). ErbB3- and ErbB4-specific antibodies showed minimal staining in DRG of naïve and CCI animals; with any staining rarely present in small, peripherin-positive cells, only 3-8% of the population in each case (Fig. 2C). These observations suggested that ErbB2, in addition to ErbB1, could potentially represent an analgesic target in nociceptors; acting either independently or in concert with ErbB1 as a heterodimer; an idea supported by evidence that ErbB2 is the preferred heterodimerisation partner for all of the other ErbB family members (Graus-Porta, Beerli et al. 1997, Tzahar, Pinkas-Kramarski et al. 1997).

Functional evidence for a role of ErbB2 within C-fibre nociceptors in CCI-induced hypersensitivity

Using paw withdrawal threshold in the von Frey test, we showed that several ErbB2 blockers caused marked reversal of CCI-induced mechanical hypersensitivity. The highly selective ErbB2 inhibitors, mubritinib and tucatinib (ARRY-380), both of which show very low affinity for ErbB1 (Nagasawa, Mizokami et al. 2006, Moulder, Borges et al. 2017), each at a dose of 15mg/kg ip, produced marked reversal of CCI-induced hypersensitivity, with complete reversal at peak in each case and both remaining statistically significant for 180min. The mean±SEM percentage reversals of hypersensitivity from 20-140min following administration were 91.5±4.7% (n=6) for mubritinib and 87.1±6.9% (n=4) for tucatinib, respectively (Fig. 3A). This validated ErbB2, in addition to ErbB1, as a potential analgesic target for neuropathic pain. Two dual inhibitors of both ErbB1 and ErbB2, lapatinib (a reversible blocker targeting ErbB1≥ErbB2>ErbB4 (Rusnak, Lackey et al. 2001) at a dose of 20mg/kg ip, and afatinib (an irreversible covalent blocker targeting ErbB1>ErbB2≥ErbB4 (Li, Ambrogio et al. 2008)) at a dose of 2.5mg/kg ip, were both similarly effective, reversing hypersensitivity completely at peak effect and remaining statistically significant for 180 and 140min, respectively. The mean±SEM percentage reversals of hypersensitivity from 20-140min following administration were 94.4±6.9% (n=6) for lapatinib and 75.5±9.0% (n=4) for afatinib, respectively (Fig. 3B). Animals treated with inhibitors of ErbB1, ErbB2 or combinations of these were closely observed and showed no apparent changes in locomotor activity, motor co-ordination or any evidence of sedation.

Evidence for ErbB1:ErbB2 interaction in CCI-induced hypersensitivity

In order to evaluate any direct interaction between ErbB1 and ErbB2 in small DRG cells, we used a Proximity Ligation Assay, which relies on hybridisation between DNA-tagged secondary antibodies to produce an amplified fluorescent signal if the epitopes recognised by two, species-distinct, primary antibodies are in close proximity (Fredriksson, Gullberg et al. 2002). Figure 3C shows that ErbB1:ErbB2 proximity ligation in peripherin-positive DRG cells from naïve animals yielded a low fluorescent signal, which was strongly and significantly increased following CCI. Control experiments using rabbit ErbB1 and mouse ErbB3 or ErbB4 antibodies showed minimal proximity ligation signals from DRG cells of naïve or CCI rats. These findings provide explicit evidence for close interaction of ErbB1 and ErbB2 in nociceptive C-fibres following nerve injury.

In the classical paradigm of ErbB receptor activation, ligand binding induces receptor dimerisation, which leads to activation of the intrinsic tyrosine kinase function of the monomers and autophosphorylation or transphosphorylation of intracellular tyrosine residues (Weiss and Schlessinger 1998). ErbB2 lacks any known direct ligand, but readily heterodimerises with each of the other ErbB monomers (Graus-Porta, Beerli et al. 1997, Tzahar, Pinkas-Kramarski et al. 1997), so may act as a subservient, signalling co-receptor in ErbB1:ErbB2 heterodimers. ErbB2 shows prominent auto-/trans-phosphorylation at Tyr1221/1222 upon activation (Ricci, Lanfrancone et al. 1995). Using a phospho-specific antibody that specifically

recognises ErbB2 phosphorylated at Tyr1221/1222, we showed a marked increase in staining in small, ErbB1-positive DRG cells following CCI, which was reversed by erlotinib treatment (at a dose of 10mg/kg ip, 1hr) (Fig. 3D). This indicates that ErbB2 auto-/trans-phosphorylation occurs through an ErbB1-dependent mechanism following nerve injury; most likely representing the function of ErbB1:ErbB2 heterodimers.

Given the accumulating evidence for ErbB1:ErbB2 co-engagement following nerve injury, we investigated whether ErbB1 and ErbB2 blockers might interact functionally in producing analgesia. We selected very low doses of erlotinib (0.33mg/kg) and mubritinib (1mg/kg) that produced just discernible analgesia, (only 9.9±3.1% and 11.4±3.7% reversal of mechanical hypersensitivity when averaged over 20-140min, n=4 in each case). Administration of these in combination produced clearly greater than additive analgesia (52.9±11.1% reversal of hypersensitivity, $p<0.01$, n=4, with complete reversal at peak effect and statistically significant effects for up to 100min, Fig. 3E). Formal assessment of synergy using Bliss Additivism effect-based modelling (Berenbaum 1981, Borisy, Elliott et al. 2003), for combinations of erlotinib through the range 0.1-3.3mg/kg with mubritinib 1.0mg/kg, showed consistently greater observed responses than those predicted from combining individual effects, with more than 3.8-fold reduction in EC_{50} for observed compared to predicted combination dose-response curves ($p<0.001$ by Extra Sum of Squares F-test; Fig. 3F). Two further, structurally distinct selective ErbB1 and ErbB2 inhibitors, were administered separately at low dose and then in combination, to independently confirm the concept of synergistic analgesic effects from dual ErbB1/ErbB2-targeting. Falnidamol (0.33mg/kg) and tucatinib (1.0mg/kg) individually produced 9.0±1.6% and 13.8±3.8% reversal of mechanical hypersensitivity, whereas in combination they produced 54.9±6.1% reversal over 20-140min following administration, clearly much greater than the 21.6±4.1% predicted from Bliss Additivism modelling ($p<0.01$ by unpaired t-test, n=4, Fig. 3G). These observations fully support the idea that ErbB1 and ErbB2 in C-fibre nociceptors co-operate in leading to nerve injury-induced hypersensitivity and suggest that conjoint administration of agents to block both ErbB1 and ErbB2 may represent a favourable strategy for analgesia.

Evidence that peripheral terminals of nociceptors can be sensitised by an ErbB1-dependent process following CCI.

In naïve rats, intradermal injection of EGF or heparin-binding EGF (another ErbB1-selective ligand) was reported to have no effect, whereas GDNF or NGF caused lasting hypersensitivity in a paw pressure withdrawal test (Andres, Meyer et al. 2010, Ferrari, Bogen et al. 2010). Nonetheless, as we had found ErbB1 abundantly expressed in the cell bodies of small, nociceptive DRG cells, some deployment to peripheral nerve terminals would be anticipated. To investigate whether peripherally localised ErbB1 might play a role in nerve injury-induced sensitisation of nociceptors, we carried out intraplantar injections in both naïve and CCI rats and assessed mechanical hypersensitivity by measuring von Frey PWT scores. Table 3 shows that

intraplantar injection of EGF amplified the ipsilateral hypersensitivity in CCI animals but not in naïve controls. No changes were seen in contralateral PWT values and contralateral injection of EGF had no effect on either contralateral or ipsilateral PWT values. These findings suggest that the effect observed upon ipsilateral injection was a local, not systemically mediated, action and that some event brought about by nerve injury (perhaps local neuroinflammatory processes) was required to prime the nociceptors before an active role of ErbB1 was revealed. The effect of EGF was not mimicked by neuregulin1-β1 EGF domain (NRG1; a selective ErbB3/ErbB4 ligand, matching our evidence for minimal expression of these proteins in small nociceptive DRG cells. The EGF-evoked amplification of hypersensitivity was however prevented by intraplantar co-injection of erlotinib, confirming the anticipated targeting of ErbB1, and also by mubritinib, consistent with our other evidence for ErbB1 acting by way of ErbB1:ErbB2 heterodimers. Pilot experiments in CIPN mice showed similar marked amplification of hypersensitivity lasting from 20-80min following intraplantar injection of EGF (80ng), but no discernible effect in naïve controls.

Evidence for ErbB1 transactivation by intracellular signalling from other receptors following CCI

ErbB1 can act as a hub for transactivation by signals from diverse G protein-coupled receptors (GPCRs), chemokine-, and orphan-receptors (Wang 2016, Kose 2017). Gq-, Gi- and Gs-linked GPCRs can lead to ErbB1 transactivation by a mechanism involving Src and the recruitment of signalling adapter molecules including Grb2 and Gab1 (Daub, Wallasch et al. 1997, Maudsley, Pierce et al. 2000, Drube, Stirnweiss et al. 2006, Qian, Peng et al. 2016). While activation of Gi-linked GPCRs, such as for lysophosphatidic acid, is reported to lead to Src-dependent tyrosine phosphorylation of ErbB1, ErbB2 phosphorylation was not directly increased (Luttrell, Della Rocca et al. 1997). This is consistent with the idea of Src-dependent targeting of ErbB1, rather than ErbB2, representing the primary step in the transactivation of ErbB1:ErbB2 heterodimers by diverse upstream regulators. Src phosphorylation of ErbB1 specifically at Tyr845 leads to activation of ErbB1 signalling (Tice, Biscardi et al. 1999, Baumdick, Gelleri et al. 2018). Similarly, another Src family kinase, Yes, phosphorylates ErbB1 at sites including Tyr845 (but not Tyr1068), causing activation of downstream signalling, while the receptor is located intracellularly in endosomes (Su, Bryant et al. 2010). Multiple candidate activators; inflammatory mediators, chemokines and cytokines are released during the local neuroinflammation following nerve injury (White, Sun et al. 2005, Uceyler, Tscharke et al. 2007, Sacerdote, Franchi et al. 2008, Ji, Xu et al. 2014, Zhu, Cao et al. 2014). GPCRs for peptides (such as bradykinin), lipids (such as prostaglandins), proteases (such as thrombin) and chemokines (such as CCL2), as well as receptors for cytokines, such as interleukin-1β and TNF-α, can all activate Src-family kinases (Viviani, Bartesaghi et al. 2003, van Vliet, Bukczynska et al. 2005, Davis, Tabarean et al. 2006, Hardyman, Wilkinson et al. 2013, Ghosh, Green et al. 2016, Kose 2017, Zhang, Han et al. 2017, Yao, Fang et

al. 2019); a signalling event reported to occur in primary afferents during neuropathic pain (Chen, Walwyn et al. 2014, Lam, Momeni et al. 2018).

To explore whether Src-dependent transactivation of ErbB1 was important in nerve injury-induced hypersensitivity, we firstly assessed the effect of selective inhibitors of Src on CCI-induced hypersensitivity in paw withdrawal thresholds from von Frey filaments. The potent Src inhibitor, dasatinib (O'Hare, Walters et al. 2005), at a dose of 3mg/kg ip, and the Src family-specific kinase inhibitor, A419259 (Wilson, Schreiner et al. 2002), at a dose of 15mg/kg ip, both caused clear reversal of CCI-induced hypersensitivity, with complete reversal of hypersensitivity at peak and statistically significant reversal for 60min and 50min in each case (Fig. 4A). The amplification of mechanical hypersensitivity caused by intraplantar injection of 100ng EGF ipsilateral to CCI (48.1±14.0% reduction in PWT, Table 3) was also prevented by local co-administration of 0.73ng dasatinib (2.8±13.4% reduction in PWT, n=4). These observations strongly support the idea of a key role for Src throughout primary nociceptive neurons in bringing about neuropathic hypersensitivity (and are consistent with previous reports). In future studies, outwith the scope of current work, it would be of interest to assess the possibility of synergistic analgesic effects arising from combined delivery of Src- and ErbB1 inhibitors.

As Src activity is normally restrained due to constitutive phosphorylation at Tyr527 by Csk and disinhibited by intracellular signals leading to dephosphorylation at this locus (Hunter 1987), we investigated the status of phosphorylation at this site, using an antibody specific for phospho-Src (Tyr527). We showed significantly decreased staining in small, ErbB1-positive DRG cells following CCI, which would be predicted to reflect increased Src activity (Fig. 4B). This was unaffected by erlotinib, exactly as would be expected for a signalling process upstream of ErbB1, that could drive its transactivation or priming sensitisation by neuroinflammatory signals.

We further investigated phosphorylation of ErbB1 at the Src-target site, Tyr845. Fig. 4C shows that CCI induced a marked increase in staining with a phospho-ErbB1 (Tyr845)-specific antibody in small, peripherin-positive DRG cells. This was blocked, as expected, by dasatinib treatment, but was unaltered by erlotinib, consistent with this step representing an upstream regulation of ErbB1 that is independent of ErbB1's own catalytic activity.

Downstream signalling by ErbB1 activated following CCI

Following ErbB1 activation, Tyr1068 is amongst the most prominent receptor autophosphorylation/transphosphorylation sites, which forms the major recruitment site for the adapter proteins, Grb2 and Gab1; leading to signalling through ERK MAP kinase and PI 3-kinase/Akt (Rojas, Yao et al. 1996, Olayioye, Neve et al. 2000, Rodrigues, Falasca et al. 2000, Nishida and Hirano 2003, Mattoon, Lamothe et al. 2004). Figure 5A shows that ErbB1 phosphorylation at Tyr1068 was clearly increased following CCI and this was reversed by treatment with erlotinib (10mg/kg, for 1hr), suggesting that Tyr1068 phosphorylation was maintained by an active, rapidly turning-over process following nerve injury. The potent Src inhibitor, dasatinib (3mg/kg) was

similarly effective, consistent with an upstream role of Src in bringing about ErbB1 autophosphorylation (Fig. 5A). Figure 5B displays the subcellular distribution of phospho-ErbB1 (Tyr1068) immunoreactivity in DRG neurons from naïve, CCI and erlotinib-treated CCI animals. Both high power images of individual cells and fluorescence intensity profiles of transects from the nuclear perimeter to the plasma membrane at the cell apex, show that phospho-ErbB1 (Tyr1068) was clearly increased following CCI and this increment was reversed by erlotinib treatment; n=8 in each case. The increase in ErbB1 phosphorylation at Tyr1068 following nerve injury was however, predominantly at an intracellular (perinuclear) site, as opposed to plasma membrane; consistent with its induction by an intracellular signalling process rather than an external ligand. The close molecular engagement of Gab1 with ErbB1 was explicitly demonstrated by Proximity Ligation Assay, which shows ErbB1:Gab1 proximal interaction was significantly increased in peripherin-positive DRG cells following CCI and that this increment was reversed by in vivo treatment with erlotinib or mubritinib (Fig. 5C), consistent with roles of the tyrosine kinase function of both ErbB1 and ErbB2 in Gab1 recruitment. The subcellular distribution of Gab1 immunoreactivity itself was not studied in detail. Trials for antibody specificity were only carried out with naïve tissue and examined at low power, where staining appeared to be distributed throughout the cytoplasm. Whether this distribution might be altered in CCI tissue was not assessed.

Two downstream signalling cascades are activated following ErbB1 phosphorylation at Tyr1068; the PI 3-kinase/Akt and ERK MAP kinase pathways (Olayioye, Neve et al. 2000). Akt is activated as a consequence of PIP_3 generation by PI 3-kinase, which may occur as a result of its Gab1-dependent recruitment to phospho-ErbB1 (Tyr1068). The activation state of Akt can be monitored by its obligatory phosphorylation at Ser473 (Sarbassov, Guertin et al. 2005). Figure 6A shows that phospho-Akt (Ser473) staining in small, ErbB1-positive DRG cells was significantly increased following CCI and that this increment was fully reversed by erlotinib (10mg/kg ip, 1hr), the highly selective Akt inhibitor, ipatasertib (GDC-0068) (Lin, Sampath et al. 2013) (20mg/kg ip, 1hr) or the Src inhibitor, dasatinib (3mg/kg ip, 1 hr). Figure 6B shows that two selective Akt inhibitors of distinct structure, ipatasertib and afuresertib, both reversed CCI-induced mechanical hypersensitivity in the von Frey paw withdrawal test, at doses providing effective target coverage in vivo (20mg/kg ip and 3.3mg/kg ip, respectively) (Lin, Sampath et al. 2013, Dumble, Crouthamel et al. 2014). Both agents caused significant reversal ($p<0.01$) of hypersensitivity for at least 160min following administration, with mean±SEM percentage reversal of hypersensitivity from 20-140min of 87.6±6.8%, n=6 and 75.5±8.5%, n=5, respectively. These observations indicate that Akt is activated in ErbB1-expressing small DRG cells following CCI and that this is prevented by erlotinib blockade of ErbB1 signalling or dasatinib inhibition of the upstream ErbB1 regulator, Src. Highly selective Akt inhibitors also cause marked and sustained reversal of CCI-induced mechanical hypersensitivity. These findings suggest that activation of Akt by ErbB1 plays a key role in hypersensitivity following nerve injury. It is notable that the

functional lifetime of ErbB1 and its co-immunoprecipitation with Gab1 and the p85 subunit of PI 3-kinase are reported to be increased by the co-expression of ErbB2 (Hartman, Zhao et al. 2013). Whether co-administration of ErbB1/ErbB2 inhibitors with blockers of Akt might lead to further synergistic enhancement of analgesia would be interesting to explore in follow-on studies.

ERK MAP kinase is also activated upon ErbB1 autophosphorylation at Tyr1068, through recruitment of the adapter Grb2, or potentially indirectly through a Gab1/SHP-2 complex (Nishida and Hirano 2003), to trigger a kinase cascade leading to MEK and ERK. Activation of ERK was monitored by its obligatory phosphorylation by MEK at Thr202 and Tyr204 (Robinson and Cobb 1997). While the majority of DRG cells positive for phospho-ERK (Thr202/Tyr204) were also ErbB1-positive, a sizeable fraction of this ERK phosphorylation occurred in cells that did not stain for ErbB1 (25.2±5.3%, n=4), and this proportion was unaltered following CCI, or CCI plus erlotinib treatment. Correspondingly, highly selective blockers of ERK MAP kinase, (ravoxertinib, GDC-0994) (Blake, Burkard et al. 2016) or its upstream regulator, MEK, (AZD-8330) (Wallace, Lyssikatos et al. 2005), produced only modest reversal of CCI-induced mechanical hypersensitivity. The mean±SEM values for percentage reversal of CCI-induced hypersensitivity in the von Frey test were 9.7±2.6% (n=4) and 35.8±4.6% (n=11), over 20-140min following administration, for 30mg/kg ravoxertinib and for 1.25mg/kg AZD-8330 (doses that have been documented to provide effective target coverage in vivo). In comparison with the Akt inhibitor results, these observations suggest a relatively minor involvement of ERK in driving the hypersensitivity measured here. This corresponds to reports of rather transient ERK activation in DRG and dorsal horn neurons, following nerve injury (Obata, Yamanaka et al. 2004, Zhuang, Gerner et al. 2005, Ji, Gereau et al. 2009). While EGF treatment of cultured DRG neurons does cause activating phosphorylation of Shc (an intermediary adapter) for the ERK MAP kinase pathway (Ganju, O'Bryan et al. 1998), ERK itself is reported to be only minimally activated (Andres, Meyer et al. 2010).

ErbB1-dependent activation of Akt targets downstream vesicular trafficking

Among the range of Akt substrates discovered in an unbiased search using an antibody raised against the consensus Akt phosphorylation motif (Kane, Sano et al. 2002) was AS160 (TBC1D4). AS160 is now known to act as a Rab-GAP and participate (upon its phosphorylation and inhibition by Akt at Thr642) in insulin-induced translocation of GLUT4 storage vesicles in adipocytes (Sano, Kane et al. 2003). We hypothesised that following nerve injury, ErbB1 activation of Akt might similarly regulate trafficking of targets relevant to neuronal excitability in sensory neurons. Figure 7A shows that the percentage of ErbB1-positive DRG cells staining for phospho-AS160 (Thr642) was markedly increased following CCI and that this increment was reversed by treatment for 1hr with either erlotinib (10mg/kg ip) or ipatasertib (20mg/kg ip), n=4 in each case; fully consistent with our hypothesis. Levels of pan-AS160 staining in ErbB1-positive DRG cells were unaltered following CCI (69.7±3.6% in naïve, and 71.6±2.4% in CCI, n=4 in each case). Even in low power

images of phospho-AS160 (Thr642) staining, it was obvious that the marked CCI-induced increase was intracellularly localised in a prominent perinuclear ring of fluorescence. High power images and transect fluorescence intensity analysis of phospho-AS160 (Thr642) staining in individual ErbB1-positive DRG cells confirmed this, with a marked (3-fold) increase in maximal intensity following CCI that occurred entirely within 2μm of the nuclear perimeter (Fig. 7B, n=8 in each case). The CCI-induced increment was reversed by erlotinib, mubritinib (15mg/kg ip, 1 hr) or ipatasertib treatment, confirming the involvement of ErbB1, ErbB2 and Akt in this response. AS160 and its Akt-phosphorylated form have been identified at both intracellular and plasma membrane locations in various cell types (Larance, Ramm et al. 2005, Ng, Ramm et al. 2010, Zheng and Cartee 2016), although here, in nociceptive afferent neurons, as in muscle for example (Zheng and Cartee 2016), the location is almost entirely intracellular.

AS160 has been shown to interact directly with LRP1, a chaperone/cargo protein in GLUT4 storage vesicles, that is essential for GLUT4 trafficking to the plasma membrane (Jedrychowski, Gartner et al. 2010, Brewer, Habtemichael et al. 2014). Interestingly, LRP1 has been identified as a key factor in the trafficking of multiple cargoes to the plasma membrane, including β1 integrin and voltage-sensitive ion channels (Salicioni, Gaultier et al. 2004, Lillis, Van Duyn et al. 2008, Parkyn, Vermeulen et al. 2008, Kadurin, Rothwell et al. 2017, Au, Ying et al. 2018). As such a role could potentially play a part in increased nociceptor excitability following nerve injury, we investigated the subcellular distribution of LRP1 immunoreactivity in DRG cells after CCI. Figure 7C shows example high power images and transect fluorescence intensity analysis of LRP1 staining in individual ErbB1-positive DRG cells. LRP1-immunoreactivity was found in small clusters, consistent with a vesicular localisation, which in naïve animals was limited to the inner, perinuclear half of the transect range. In CCI animals, a significant increase in LRP1 staining (with greater clustering) was observed in the outer portion of the transect range and this increment was reversed by treatment with erlotinib or ipatasertib, again defining ErbB1 and Akt involvement in the response (n=9 in each case).

CCI-induced ion channel trafficking in nociceptors through ErbB1 activation of Akt

Numerous ion channels could contribute to altered excitability and action potential generation in nociceptors if they show increased localisation at the plasma membrane following injury. The voltage-sensitive Na^+ channels, $Na_v1.7/1.8/1.9$, are selectively expressed in nociceptors and are thought to play key roles in threshold setting, and in the generation and repetitive firing of action potentials (Dib-Hajj, Black et al. 2015, Dib-Hajj, Geha et al. 2017, Hoffmann, Kistner et al. 2017). Molecular genetics of human hereditary channelopathies with altered pain sensation has directly implicated each of these channels in pain processing, including hypersensitive neuropathic pain states (Dib-Hajj, Geha et al. 2017, Huang, Vanoye et al. 2017). They each show a predominantly intracellular location under basal conditions, suggesting

that their trafficking to the plasma membrane could well lead to increased excitability (Amaya, Decosterd et al. 2000, Okuse, Malik-Hall et al. 2002, Bao 2015). Analysis of $Na_v1.7/1.8/1.9$ expression using specific antibodies showed very high proportions of expression in ErbB1-positive small DRG cells (97.1±5.8%, 71.6±6.3% and 90.3±6.6%, respectively, n=4 in each case). While CCI caused no discernible change in $Na_v1.7$ or $Na_v1.8$ expression levels, $Na_v1.9$ expression and subcellular deployment were significantly altered. We observed a slight reduction in the number of ErbB1-positive DRG cells co-expressing $Na_v1.9$ to 75.3±7.9% of ErbB1-positive cells ($p<0.05$, t-test), but a marked redeployment of the channel towards the plasma membrane (Fig. 8A). A partial reduction in expression of $Na_v1.9$ following sciatic, but not trigeminal nerve injury has been reported previously (Dib-Hajj, Fjell et al. 1999, Luiz, Kopach et al. 2015), while expression is increased in a bone cancer model, which likely incorporates a nerve injury component (Qiu, Jiang et al. 2012). Nerve injury-induced trafficking of $Na_v1.9$, which has a long-lasting impact on nociceptor firing threshold (Hoffmann, Kistner et al. 2017), has not previously been reported. Figure 8A shows high power images of individual ErbB1-positive DRG cells and transect fluorescence intensity analysis indicating marked recruitment of $Na_v1.9$ to sites adjacent to the apical plasma membrane (transect bins 43-49 out of 50) following CCI and its efficient reversal by treatment with erlotinib or ipatasertib (n=8 in each case). It was not possible to readily assess whether $Na_v1.9$ blockade would reverse CCI-induced pain hypersensitivity in the current experiments, as no highly selective small molecule $Na_v1.9$ inhibitors are available (Dib-Hajj, Black et al. 2015, Lin, Santos et al. 2016). Similar (but less marked) results were observed with $Na_v1.8$, indicating significant CCI-induced recruitment to transect bins 46-50 and reversal by erlotinib treatment (n=9 in each case), while no significant changes were detected in $Na_v1.7$ distribution (Supplementary Figure). Figure 8B shows that Proximity Ligation Assay using specific $Na_v1.9$ and LRP1 antibodies, identified a close molecular interaction of these two proteins in peripherin-positive DRG cells, which was significantly increased following CCI, and reversed by treatment with erlotinib. This fully supports the idea of LRP1 driving $Na_v1.9$ translocation to the plasma membrane following CCI, through an ErbB1, Akt and AS160-dependent process.

Several voltage-sensitive Ca^{2+} channel types are also expressed in DRG neurons, particularly L-type, generally involving $Ca_v1.2$ or $Ca_v1.3$ α1-subunits, and also N-type, involving $Ca_v2.2$, which between them contribute the majority of voltage-dependent Ca^{2+} current (Heinke, Balzer et al. 2004, Woodall, Richards et al. 2008, Bourinet, Altier et al. 2014). $Ca_v1.2$ and $Ca_v2.2$ have both been shown to undergo PI 3-kinase/Akt-dependent trafficking to the plasma membrane of transfected fibroblasts and DRG neurons (Viard, Butcher et al. 2004), so could potentially play a part in the ErbB1-dependent hypersensitivity identified following nerve injury. We focused here on $Ca_v1.2$, as intrathecal administration of L-type Ca^{2+} channel blockers (affecting DRG as well as spinal cord (Cao, Qian et al. 2016)) produces analgesia in chronic pain states (Vanegas and Schaible 2000, Yaksh 2006), while knockdown of Cav1.2 specifically reverses neuropathy-associated mechanical hypersensitivity (Fossat,

Dobremez et al. 2010). In contrast, $Ca_v1.3$ knockout mice lack any pain phenotype (Clark, Nagano et al. 2003). $Ca_v1.2$ is also of particular interest in relation to nociceptor excitability due to its subcellular localisation, not only at the plasma membrane and intracellularly, but also in the Axon Initial Segment (AIS), where it may play a role in excitability setting (Brandao, Dell'Acqua et al. 2012). A large proportion of $Ca_v1.2$-positive cells were also ErbB1-positive, and this was unaltered following nerve injury (74.1±3.7% naïve, and 66.5±3.9% CCI, n=4 in each case). The subcellular distribution of $Ca_v1.2$ however, was strikingly altered following nerve injury. Figure 8C shows high power images of individual cells and fluorescence intensity analysis of cell transects. This indicates remarkable trafficking of $Ca_v1.2$ to the apical plasma membrane and proximal stem axon following CCI, which was reversed by treatment with erlotinib or ipatasertib (n=8 in each case). Nerve injury-induced translocation of $Ca_v1.2$ to such sites in nociceptors could contribute importantly to increased excitability. The reversal of this response by erlotinib and ipatasertib indicates its dependence on the ErbB1/Akt pathway we have elucidated above.

Discussion

Our results provide powerful evidence that highly selective small molecule inhibitors of the tyrosine kinase function of ErbB1 (TKIs) reverse hypersensitivity in rodent neuropathic pain models. This represents robust corroboration of previous clinical findings with both ErbB1 antibody reagents, such as cetuximab or panitumumab, and small molecule ErbB1-selective TKIs, such as erlotinib and gefitinib (Kersten and Cameron 2012, Kersten, Cameron et al. 2013, Kersten, Cameron et al. 2015). It was not possible to test cetuximab or panitumumab here due to their humanised/human immune origins. Our results using the CCI model of neuropathic mechanical pain hypersensitivity in rats (von Frey paw withdrawal threshold) gave a mean IC_{50} value of 1.4mg/kg ip for erlotinib, similar estimated potencies for gefitinib and AG 1478, and robust analgesic effects of several structurally distinct ErbB1-selective TKIs (Table 2). These observations were reproduced in the mouse CIPN model, which showed mean IC_{50} values of 3.2, 2.4 and 3.0mg/kg ip for erlotinib, gefitinib and AG 1478, respectively. The effective analgesic doses here are in the range of approved human dosing. Similar analgesic effects of small molecule ErbB1-selective TKIs have been reported using various inflammatory and neuropathic pain models in mice and the CCD, chronic DRG compression, model in rats (Martin, Smith et al. 2017, Wang, Liu et al. 2019). In many cases though, the mean IC_{50} values reported were notably higher, both in inflammatory pain models (formalin phase-2 and Complete Freund's Adjuvant), and particularly in neuropathic pain models (Spared Nerve Injury and CCI), where IC_{50}s for gefitinib and AG 1478 ranged from 77 to around 300mg/kg (Martin, Smith et al. 2017). The basis for this disparity is unclear, although the analgesic signal is fully corroborated.

The present study provides substantive evidence for the highly selective expression of ErbB1 in small unmyelinated nociceptors. In the CCI model here, ErbB1 expression is unaltered following nerve injury, in contrast to findings from the CCD

(DRG compression) model (Wang, Liu et al. 2019). We found a high degree of co-localisation of ErbB1 with ErbB2, but not ErbB3 or ErbB4, in small unmyelinated nociceptors. Our study further delivers fundamental new insights by showing that ErbB1 is likely to act as a heterodimer with ErbB2 in driving neuropathic pain hypersensitivity. The key evidence arises from converging experimental approaches; proximity ligation showing direct ErbB1:ErbB2 interaction in DRG, analgesia induced by either ErbB1 and ErbB2 inhibitors (both systemically and peripherally), crossed blockade of an activation marker by inhibiting the partner receptor, and importantly, definitive synergism in the analgesia produced by co-administration of ErbB1 and ErbB2 inhibitors. This synergistic co-operation of ErbB1 and ErbB2 inhibitors in delivering analgesic efficacy against neuropathic pain identifies clear translational potential; highlighting a strategy for enhanced pain relief with lesser side effects than might be achieved by an EGFR inhibitor alone.

Our evidence that Src could well play a key role in triggering pro-excitatory ErbB1 processes in nociceptive afferents is consistent with reports of Src activation in DRG (including in TRPV1-positive afferents) in both neuropathic and inflammatory pain models (Alessandri-Haber, Dina et al. 2004, Jin, Morsy et al. 2004, Zhang, Huang et al. 2005, Liu, Liu et al. 2015). Src is readily activated in DRG by cytokines (IL-1β and CXCL12) (Igwe 2003, Rivat, Sebaihi et al. 2014), which would support the hypothesis that ErbB1 activation in CCI here may result from intracellular transactivation, potentially as a result of nerve injury-induced neuroinflammation. Src phosphorylation of ErbB1 at Tyr845 leads to facilitated or direct activation of ErbB1 signalling (Tice, Biscardi et al. 1999, Baumdick, Gelleri et al. 2018), thereby obviating the need for increased availability of an extracellular EGF-like ligand. Nevertheless, genetic association of a SNP in the gene locus for epiregulin (an ErbB1 and ErbB4 receptor ligand) in patient cohorts with chronic temporomandibular disorder (TMD) pain has been identified (Martin, Smith et al. 2017), although acute pain seems to be inversely correlated (Verma, Khoury et al. 2020). Both inflammatory and neuropathic pain models in mice result in increased blood levels of epiregulin and its intrathecal administration produces modest hypersensitivity in baseline thermal and mechanical responses as well as a dose-dependent increase in licking/biting behaviour in the second phase of the formalin test (Martin, Smith et al. 2017). However, the facilitation of formalin responses was not replicated by any of 4 other ErbB1 agonist-ligands, despite the binding affinity of epiregulin to ErbB family receptors (including ErbB1 homodimers and ErbB1:ErbB2 heterodimers) being lower than that of all other EGF family ligands (Toyoda, Komurasaki et al. 1995, Shelly, Pinkas-Kramarski et al. 1998, Jones, Akita et al. 1999, Sato, Nakamura et al. 2003, Freed, Bessman et al. 2017). The application of epiregulin to dorsal nerve roots in rats showed disparate effects on the spontaneous or C-fibre-evoked activity of dorsal horn neurons (Kongstorp, Schjolberg et al. 2019), matching the dichotomous molecular genetics findings (Martin, Smith et al. 2017, Verma, Khoury et al. 2020). Similarly, while systemic infusion of an epiregulin-neutralising antibody speeded the recovery from hypersensitivity in a nerve injury model, this had mixed effects in an inflammatory model and exacerbated

capsaicin-evoked pain responses (Verma, Khoury et al. 2020). With respect to the specific role of ErbB1, although attenuation of epiregulin facilitation of phase-2 formalin responses by the ErbB1-selective TKI, AG 1478, was reported (Martin, Smith et al. 2017), the fact that this itself reduces formalin responses, complicates interpretation. Similarly, although epiregulin facilitation of formalin responses was absent in (heterozygous) mutant mice with a large deletion of the ErbB1 extracellular domain, the mutants showed significantly altered basal formalin responses. Overall, while systemic epiregulin levels increase in chronic pain models and may indeed contribute to hypersensitivity, there is limited explicit evidence that this relates specifically to ErbB1 in primary nociceptive afferents.

To explore the role of ErbB1 in the peripheral terminals of nociceptors, we carried out intraplantar injections of EGF and assessed mechanical paw withdrawal thresholds (Table 3). EGF showed no discernible effect in naïve animals, in agreement with previous observations (Andres, Meyer et al. 2010, Ferrari, Bogen et al. 2010, Araldi, Ferrari et al. 2018), but a clear amplification of ipsilateral hypersensitivity after nerve injury. This suggests that ErbB1 plays a role in nociceptive processing only in chronic injury-induced hypersensitive states. The EGF response was specific to the injured limb, reversed by local erlotinib, mubritinib or dasatinib (indicating ErbB1, ErbB2 and Src involvement) and was not mimicked by neuregulin-1-β1 EGF domain (indicating lack of ErbB3/4 involvement). Interestingly, the prolongation of intradermal PGE_2-induced mechanical hypersensitivity caused by repeated administration of μ-opioid receptor agonist, is reported to be attenuated by inhibitors of both ErbB1 and Src (Araldi, Ferrari et al. 2018), emphasising a key role of ErbB1 in GPCR-induced pain hypersensitivity. In that model, intradermal EGF did not on its own affect pain responses, as described here. Responses to PGE_2 were unaltered 5 days after EGF administration, which would align with our observations that concurrent nerve injury is required to reveal a sensitising effect of ErbB1 activation and support the hypothesis that intracellular signalling plays a key role in this connection.

A number of reports have described the activation of Akt in DRG neurons in chronic pain hypersensitivity induced by nerve injury (Xu, Tu et al. 2007, Shi, Huang et al. 2009), chemotherapeutic-evoked neuropathy (Jiang, Zhang et al. 2016, Li, Chen et al. 2016), inflammation (Liang, Tao et al. 2013), bone cancer (Guan, Fu et al. 2015) and intradermal injection of capsaicin, ephrin or formalin (Sun, Yan et al. 2007, Guan, Lu et al. 2010, Martin, Smith et al. 2017). In many cases, administration of PI 3-kinase or Akt inhibitors attenuated pain hypersensitivity, matching our observations here with the second generation highly selective Akt inhibitors, ipatasertib and afuresertib. Various reports have also outlined changes in mTOR and protein translational machinery (significant downstream targets of Akt) in neuropathic, inflammatory and formalin-induced pain models, with analgesic effects seen due to blockers of different elements (Xu, Zhao et al. 2010, Obara, Tochiki et al. 2011, Liang, Tao et al. 2013, Khoutorsky, Bonin et al. 2015, Martin, Smith et al. 2017). Epiregulin-induced enhancement of formalin-induced nocifensive behaviour was attenuated by inhibitors

of PI 3-kinase (but not MEK) and accompanied by increased Akt phosphorylation in DRG (Martin, Smith et al. 2017), potentially relating to ErbB1 activation. Epiregulin-induced pain hypersensitivity was also diminished by inhibitors of mTOR and in mutant mice with disrupted elements of the protein translational machinery, indicating a clear functional role. In the current study we investigated whether alternative rapid Akt-dependent processes such as ion channel trafficking may be key to the role of ErbB1 in neuropathic pain and help explain the rapid analgesic effects of ErbB1 inhibitors.

Akt has important cellular roles in the regulation of vesicular trafficking, for example in insulin-induced rapid translocation of the GLUT4 glucose transporter to the plasma membrane of adipocytes (Hill, Clark et al. 1999). The substrates for Akt phosphorylation include AS160 (TBC1D4), a Rab-GAP (GTPase-activating protein), which signals GLUT4 translocation by terminating vesicle retention upon its inactivating phosphorylation by Akt (Kane, Sano et al. 2002, Sano, Kane et al. 2003, Fujita, Hatakeyama et al. 2010). AS160 has a predominantly peri-nuclear subcellular localisation, associated with GLUT4 storage vesicles, from which it dissociates following insulin stimulation (Larance, Ramm et al. 2005). Akt-phosphorylated AS160 (at Thr642) has been identified at both intracellular and plasma membrane sites after insulin stimulation of adipocytes (Ng, Ramm et al. 2010), although in muscle its localisation is entirely intracellular (Zheng and Cartee 2016), as we found here associated with ErbB1-dependant nociceptive hypersensitivity following nerve injury. An AS160 paralogue, TBC1D1, and AS250 (a Ral-GAP) may also contribute to Akt regulation of GLUT4 trafficking (Sakamoto and Holman 2008, Peck, Chavez et al. 2009, Chen, Leto et al. 2011, Leto and Saltiel 2012). We further showed that the AS160-interacting protein and vesicular chaperone/co-cargo, LRP1 (Jedrychowski, Gartner et al. 2010), which participates in the plasma membrane trafficking of various surface-deployed proteins, such as $Ca_v2.2$ (Kadurin, Rothwell et al. 2017), undergoes clustering and localisation closer to the plasma membrane following CCI. Crucially these changes were prevented by selective blockers of ErbB1 or Akt.

In addition, we demonstrated increased ErbB1- and Akt-dependent trafficking of $Na_v1.9$ and $Na_v1.8$ (but not $Na_v1.7$) to DRG somata plasma membrane following CCI (Fig. 8A, Supplementary Figure), a process that potentially could also occur in peripheral nociceptor endings. This matches human molecular genetics evidence associating these channels with hereditary painful neuropathies, and their disruption with insensitivity to pain (Dib-Hajj, Geha et al. 2017, Bennett, Clark et al. 2019). The electrophysiological characteristics of $Na_v1.8$ point to a role in rapid re-priming and maintenance of repetitive firing (Dib-Hajj, Geha et al. 2017, Bennett, Clark et al. 2019). The activation of $Na_v1.9$ by weak stimuli at hyperpolarised voltages and very delayed time-course of inactivation are consistent with a role in threshold setting of excitability (Dib-Hajj, Geha et al. 2017, Bennett, Clark et al. 2019). Many, but not all, knockdown, knockout and pharmacological studies indicate a role for $Na_v1.8$ in both inflammatory and neuropathic pain (Porreca, Lai et al. 1999, Kerr, Souslova et al. 2001, Lai, Hunter et al. 2003, Nassar, Levato et al. 2005, Joshi, Mikusa et al. 2006, Dong, Goregoaker et al. 2007). Differences in findings may relate to the characteristics of particular mutant mouse lines and compensatory changes (Leo, D'Hooge et al. 2010). Although

no truly selective pharmacological selective agents are yet available (Dib-Hajj, Black et al. 2015, Lin, Santos et al. 2016), knockout/deletion studies have implicated $Na_v1.9$ in inflammatory pain, but also in neuropathic and basal pain (Porreca, Lai et al. 1999, Priest, Murphy et al. 2005, Amaya, Wang et al. 2006, Maingret, Coste et al. 2008, Leo, D'Hooge et al. 2010, Hockley, Boundouki et al. 2014, Osorio, Korogod et al. 2014, Lolignier, Bonnet et al. 2015, Luiz, Kopach et al. 2015, Hoffmann, Kistner et al. 2017). Very little is known however, of the processes involved in their deployment at the plasma membrane of DRG neurons. There is evidence that contactin and FHF1B interact directly with $Na_v1.9$ and could play a role (Liu, Dib-Hajj et al. 2001, Liu, Dib-Hajj et al. 2001), although FHF1B and contactin are also implicated in the function/trafficking of $Na_v1.5/1.3$ (Liu, Dib-Hajj et al. 2003, Shah, Rush et al. 2004). The heterologous expression of functional $Na_v1.9$ has proved difficult to achieve and is likely to require $Na_v\beta$ subunits as well as probably additional, unknown factors (Goral, Leipold et al. 2015, Lin, Santos et al. 2016). Similarly, little is known of $Na_v1.8$ trafficking and its control, although interaction with annexin light chain p11 has been reported as a key factor (Okuse, Malik-Hall et al. 2002, Foulkes, Nassar et al. 2006). Annexin light chain p11 is also implicated in the plasma membrane trafficking of epithelial Na^+ (ENaC) channels and related ASIC1a channels (Donier, Rugiero et al. 2005, Cheung, Ismail et al. 2019), both of which can be driven by PI 3-kinase/Akt signalling (Markadieu, Blero et al. 2004, Duan, Liu et al. 2012). The question of why $Na_v1.9$ deployment at the plasma membrane is relatively low under basal conditions was addressed in a recent study that compared key trafficking motifs in $Na_v1.9$ with those in $Na_v1.7$ (Sizova, Huang et al. 2020). Evidence for distinct trafficking signals between $Na_v1.9$ and $Na_v1.7$ fits well with our observations that the trafficking of $Na_v1.9$ (and $Na_v1.8$), but not $Na_v1.7$ to DRG cell plasma membrane can be upregulated by an ErbB1-dependent mechanism in neuropathic pain. The ErbB1-dependent trafficking of $Na_v1.9$ (and $Na_v1.8$) to key locations for neuronal excitability may be crucial to neuropathic hypersensitivity.

We further demonstrated striking, ErbB1- and Akt-dependent trafficking of $Ca_v1.2$ to the plasma membrane and axon initial segment/proximal axon of small peripherin-positive DRG cells following CCI (Fig. 8C). This matches evidence for the preferential expression of $Ca_v1.2$ (together with known protein partners) in the soma, plasma membrane and axon initial segment/proximal axon of small, peripherin-positive C-fibre afferents (Brandao, Dell'Acqua et al. 2012) and may, together with the well documented clustering of Na_v channels in this region (Zhou, Lambert et al. 1998), contribute to increased excitability. Indeed, selective $Ca_v1.2$ blockers or $Ca_v1.2$ knockdown produce analgesia in a number of chronic pain models (Vanegas and Schaible 2000, Yaksh 2006, Fossat, Dobremez et al. 2010) (Vanegas and Schaible, 2000; Yaksh, 2006; Fossat, Dobremez et al., 2010). Furthermore, numerous reports describe growth factor-induced trafficking of channels (including TRP, K_{Ca} and both L- and N-type Ca^{2+} channels) to the plasma membrane in various cell types including neurons and the crucial role of PI 3-kinase/Akt signalling in this (Blair and Marshall 1997, Kanzaki, Zhang et al. 1999, Bezzerides, Ramsey et al. 2004, Viard, Butcher et

al. 2004, Chae, Martin-Caraballo et al. 2005). In addition to the Akt-dependent targeting of the Rab-GAP AS160 and disinhibition of LRP1-associated trafficking identified here (as also identified in GLUT4 translocation (Leto and Saltiel 2012), trafficking of $Ca_v1.2$ and 2.2 has been shown to depend on both β and $\alpha 2\delta$ channel subunits, the latter of which interact directly with LRP1 (Viard, Butcher et al. 2004, Hoppa, Lana et al. 2012, Kadurin, Rothwell et al. 2017, Nieto-Rostro, Ramgoolam et al. 2018). Nerve injury-induced trafficking of $Ca_v1.2$ to functionally important subcellular locations in DRG neurons, including the plasma membrane, proximal axon and potentially, even synaptic release sites (Hoppa, Lana et al. 2012) could play a crucial part in nociceptive hypersensitivity. Other channel-interacting proteins, such as CRMP2, are reported to modulate trafficking of channels, including $Na_v1.7$ and $Ca_v2.2$ (Brittain, Piekarz et al. 2009, Chi, Schmutzler et al. 2009, Chew and Khanna 2018).

The pseudo-polar morphology of DRG neurons is thought to be responsible for an increased probability of action potential failure at the bifurcation, especially for high frequency firing (Luscher, Lipp et al. 1996, Nascimento, Mar et al. 2018). Peripheral nerve injury leads to a reduction in this low-pass filtering and may thereby contribute to neuropathic pain hypersensitivity (Gemes, Koopmeiners et al. 2013). Ion channel recruitment to a potential axon initial segment-like zone in the proximal stem axon and soma plasma membrane, particularly in small diameter DRG neurons, may thus exert an important influence over spike propagation (Nascimento, Mar et al. 2018). Both Na^+ and Ca^{2+} currents contribute to action potentials in DRG cells (Kostyuk, Veselovsky et al. 1981, Heyer and Macdonald 1982) and intracellular Ca^{2+} levels may additionally facilitate spike propagation (Luscher, Lipp et al. 1996), so the nerve injury-associated translocation of Na^+ and Ca^{2+} channels here could potentially play a part in enhanced action potential generation along the axon of nociceptors.

Overall, the work presented here corroborates and provides a mechanistic basis for previous clinical observations in neuropathic pain patients. Increased recruitment of $Na_v1.9$, $Na_v1.8$ and $Ca_v1.2$ to the apical plasma membrane and proximal stem axon of primary afferent nociceptive neurons following nerve injury may be crucial to the increased excitability and excessive firing that is likely to underlie pain hypersensitivity. These events, in small diameter nociceptive DRG neurons, are driven by ErbB1, acting in synergy with ErbB2, and their downstream signalling through Akt to regulate vesicular trafficking, emphasizing the potential value of targeting ErbB1 and ErbB2 to suppress these processes and achieve analgesia for neuropathic pain.

Acknowledgements

We are grateful to Martin Michaelis for his consistently wise advice, to Anisha Kubasik-Thayil from the IMPACT Confocal Imaging Facility for expert imaging assistance and to the staff of Biomedical Research Resources (BRR) for their ongoing technical support.

Declaration of interest

None.

Role of Funding Source

The funders played no role in the design of experiments and the analysis or interpretation of data.

Author contributions

Rory Mitchell: Conceptualization, Methodology, Investigation, Formal Analysis, Visualization, Writing (Original Draft), Writing (Review and Editing), Supervision, Project administration, Funding acquisition. **Marta Mikolajczak:** Methodology, Investigation, Formal Analysis, Visualization, Constructive feedback. **Christian Kersten:** Constructive feedback, Writing (Review and Editing). **Sue Fleetwood-Walker:** Conceptualization, Methodology, Investigation, Formal Analysis, Visualization, Writing (Original Draft), Writing (Review and Editing), Supervision, Project administration, Funding acquisition.

References

Alessandri-Haber, N., O. A. Dina, J. J. Yeh, C. A. Parada, D. B. Reichling and J. D. Levine (2004). "Transient receptor potential vanilloid 4 is essential in chemotherapy-induced neuropathic pain in the rat." J Neurosci **24**(18): 4444-4452.

Amaya, F., I. Decosterd, T. A. Samad, C. Plumpton, S. Tate, R. J. Mannion, M. Costigan and C. J. Woolf (2000). "Diversity of expression of the sensory neuron-specific TTX-resistant voltage-gated sodium ion channels SNS and SNS2." Mol Cell Neurosci **15**(4): 331-342.

Amaya, F., H. Wang, M. Costigan, A. J. Allchorne, J. P. Hatcher, J. Egerton, T. Stean, V. Morisset, D. Grose, M. J. Gunthorpe, I. P. Chessell, S. Tate, P. J. Green and C. J. Woolf (2006). "The voltage-gated sodium channel Na(v)1.9 is an effector of peripheral inflammatory pain hypersensitivity." J Neurosci **26**(50): 12852-12860.

Anastassiadis, T., S. W. Deacon, K. Devarajan, H. Ma and J. R. Peterson (2011). "Comprehensive assay of kinase catalytic activity reveals features of kinase inhibitor selectivity." Nat Biotechnol **29**(11): 1039-1045.

Andres, C., S. Meyer, O. A. Dina, J. D. Levine and T. Hucho (2010). "Quantitative automated microscopy (QuAM) elucidates growth factor specific signalling in pain sensitization." Mol Pain **6**: 98.

Araldi, D., L. F. Ferrari and J. D. Levine (2018). "Role of GPCR (mu-opioid)-receptor tyrosine kinase (epidermal growth factor) crosstalk in opioid-induced hyperalgesic priming (type II)." Pain **159**(5): 864-875.

Au, D. T., Z. Ying, E. O. Hernandez-Ochoa, W. E. Fondrie, B. Hampton, M. Migliorini, R. Galisteo, M. F. Schneider, A. Daugherty, D. L. Rateri, D. K. Strickland and S. C. Muratoglu (2018). "LRP1 (Low-Density Lipoprotein Receptor-Related Protein 1) Regulates Smooth Muscle Contractility by Modulating Ca(2+) Signaling and Expression of Cytoskeleton-Related Proteins." Arterioscler Thromb Vasc Biol **38**(11): 2651-2664.

Bao, L. (2015). "Trafficking regulates the subcellular distribution of voltage-gated sodium channels in primary sensory neurons." Mol Pain **11**: 61.

Baumdick, M., M. Gelleri, C. Uttamapinant, V. Beranek, J. W. Chin and P. I. H. Bastiaens (2018). "A conformational sensor based on genetic code expansion reveals an autocatalytic component in EGFR activation." Nat Commun **9**(1): 3847.

Bennett, D. L., A. J. Clark, J. Huang, S. G. Waxman and S. D. Dib-Hajj (2019). "The Role of Voltage-Gated Sodium Channels in Pain Signaling." Physiol Rev **99**(2): 1079-1151.

Bennett, G. J. and Y. K. Xie (1988). "A peripheral mononeuropathy in rat that produces disorders of pain sensation like those seen in man." Pain **33**(1): 87-107.
Berenbaum, M. C. (1981). "Criteria for analyzing interactions between biologically active agents." Adv Cancer Res **35**: 269-335.
Berger, C., U. Krengel, E. Stang, E. Moreno and I. H. Madshus (2011). "Nimotuzumab and cetuximab block ligand-independent EGF receptor signaling efficiently at different concentrations." J Immunother **34**(7): 550-555.
Bezzerides, V. J., I. S. Ramsey, S. Kotecha, A. Greka and D. E. Clapham (2004). "Rapid vesicular translocation and insertion of TRP channels." Nat Cell Biol **6**(8): 709-720.
Blair, L. A. and J. Marshall (1997). "IGF-1 modulates N and L calcium channels in a PI 3-kinase-dependent manner." Neuron **19**(2): 421-429.
Blake, J. F., M. Burkard, J. Chan, H. Chen, K. J. Chou, D. Diaz, D. A. Dudley, J. J. Gaudino, S. E. Gould, J. Grina, T. Hunsaker, L. Liu, M. Martinson, D. Moreno, L. Mueller, C. Orr, P. Pacheco, A. Qin, K. Rasor, L. Ren, K. Robarge, S. Shahidi-Latham, J. Stults, F. Sullivan, W. Wang, J. Yin, A. Zhou, M. Belvin, M. Merchant, J. Moffat and J. B. Schwarz (2016). "Discovery of (S)-1-(1-(4-Chloro-3-fluorophenyl)-2-hydroxyethyl)-4-(2-((1-methyl-1H-pyrazol-5-y l)amino)pyrimidin-4-yl)pyridin-2(1H)-one (GDC-0994), an Extracellular Signal-Regulated Kinase 1/2 (ERK1/2) Inhibitor in Early Clinical Development." J Med Chem **59**(12): 5650-5660.
Borisy, A. A., P. J. Elliott, N. W. Hurst, M. S. Lee, J. Lehar, E. R. Price, G. Serbedzija, G. R. Zimmermann, M. A. Foley, B. R. Stockwell and C. T. Keith (2003). "Systematic discovery of multicomponent therapeutics." Proc Natl Acad Sci U S A **100**(13): 7977-7982.
Bourinet, E., C. Altier, M. E. Hildebrand, T. Trang, M. W. Salter and G. W. Zamponi (2014). "Calcium-permeable ion channels in pain signaling." Physiol Rev **94**(1): 81-140.
Brandao, K. E., M. L. Dell'Acqua and S. R. Levinson (2012). "A-kinase anchoring protein 150 expression in a specific subset of TRPV1- and CaV 1.2-positive nociceptive rat dorsal root ganglion neurons." J Comp Neurol **520**(1): 81-99.
Brewer, P. D., E. N. Habtemichael, I. Romenskaia, C. C. Mastick and A. C. Coster (2014). "Insulin-regulated Glut4 translocation: membrane protein trafficking with six distinctive steps." J Biol Chem **289**(25): 17280-17298.
Brittain, J. M., A. D. Piekarz, Y. Wang, T. Kondo, T. R. Cummins and R. Khanna (2009). "An atypical role for collapsin response mediator protein 2 (CRMP-2) in neurotransmitter release via interaction with presynaptic voltage-gated calcium channels." J Biol Chem **284**(45): 31375-31390.
Burke, P. M. and H. S. Wiley (1999). "Human mammary epithelial cells rapidly exchange empty EGFR between surface and intracellular pools." J Cell Physiol **180**(3): 448-460.
Cairns, B. E. (2010). "Pathophysiology of TMD pain--basic mechanisms and their implications for pharmacotherapy." J Oral Rehabil **37**(6): 391-410.
Cao, C., X. Huang, Y. Han, Y. Wan, L. Birnbaumer, G. S. Feng, J. Marshall, M. Jiang and W. M. Chu (2009). "Galpha(i1) and Galpha(i3) are required for epidermal growth factor-mediated activation of the Akt-mTORC1 pathway." Sci Signal **2**(68): ra17.
Cao, D. L., B. Qian, Z. J. Zhang, Y. J. Gao and X. B. Wu (2016). "Chemokine receptor CXCR2 in dorsal root ganglion contributes to the maintenance of inflammatory pain." Brain Res Bull **127**: 219-225.
Cavanaugh, D. J., H. Lee, L. Lo, S. D. Shields, M. J. Zylka, A. I. Basbaum and D. J. Anderson (2009). "Distinct subsets of unmyelinated primary sensory fibers mediate

behavioral responses to noxious thermal and mechanical stimuli." Proc Natl Acad Sci U S A **106**(22): 9075-9080.
Chae, K. S., M. Martin-Caraballo, M. Anderson and S. E. Dryer (2005). "Akt activation is necessary for growth factor-induced trafficking of functional K(Ca) channels in developing parasympathetic neurons." J Neurophysiol **93**(3): 1174-1182.
Chang, J. Y., P. Parra-Bueno, T. Laviv, E. M. Szatmari, S. R. Lee and R. Yasuda (2017). "CaMKII Autophosphorylation Is Necessary for Optimal Integration of Ca(2+) Signals during LTP Induction, but Not Maintenance." Neuron **94**(4): 800-808 e804.
Chen, W., W. Walwyn, H. S. Ennes, H. Kim, J. A. McRoberts and J. C. Marvizon (2014). "BDNF released during neuropathic pain potentiates NMDA receptors in primary afferent terminals." Eur J Neurosci **39**(9): 1439-1454.
Chen, X. W., D. Leto, T. Xiong, G. Yu, A. Cheng, S. Decker and A. R. Saltiel (2011). "A Ral GAP complex links PI 3-kinase/Akt signaling to RalA activation in insulin action." Mol Biol Cell **22**(1): 141-152.
Cheung, T. T., N. A. S. Ismail, R. Moir, N. Arora, F. J. McDonald and S. B. Condliffe (2019). "Annexin II Light Chain p11 Interacts With ENaC to Increase Functional Activity at the Membrane." Front Physiol **10**: 7.
Chew, L. A. and R. Khanna (2018). "CRMP2 and voltage-gated ion channels: potential roles in neuropathic pain." Neuronal Signal **2**(1).
Chi, X. X., B. S. Schmutzler, J. M. Brittain, Y. Wang, C. M. Hingtgen, G. D. Nicol and R. Khanna (2009). "Regulation of N-type voltage-gated calcium channels (Cav2.2) and transmitter release by collapsin response mediator protein-2 (CRMP-2) in sensory neurons." J Cell Sci **122**(Pt 23): 4351-4362.
Clark, N. C., N. Nagano, F. M. Kuenzi, W. Jarolimek, I. Huber, D. Walter, G. Wietzorrek, S. Boyce, D. M. Kullmann, J. Striessnig and G. R. Seabrook (2003). "Neurological phenotype and synaptic function in mice lacking the CaV1.3 alpha subunit of neuronal L-type voltage-dependent Ca2+ channels." Neuroscience **120**(2): 435-442.
Daub, H., C. Wallasch, A. Lankenau, A. Herrlich and A. Ullrich (1997). "Signal characteristics of G protein-transactivated EGF receptor." EMBO J **16**(23): 7032-7044.
Davis, C. N., I. Tabarean, S. Gaidarova, M. M. Behrens and T. Bartfai (2006). "IL-1beta induces a MyD88-dependent and ceramide-mediated activation of Src in anterior hypothalamic neurons." J Neurochem **98**(5): 1379-1389.
Davis, M. I., J. P. Hunt, S. Herrgard, P. Ciceri, L. M. Wodicka, G. Pallares, M. Hocker, D. K. Treiber and P. P. Zarrinkar (2011). "Comprehensive analysis of kinase inhibitor selectivity." Nat Biotechnol **29**(11): 1046-1051.
Dawson, J. P., M. B. Berger, C. C. Lin, J. Schlessinger, M. A. Lemmon and K. M. Ferguson (2005). "Epidermal growth factor receptor dimerization and activation require ligand-induced conformational changes in the dimer interface." Mol Cell Biol **25**(17): 7734-7742.
Dib-Hajj, S. D., J. A. Black and S. G. Waxman (2015). "NaV1.9: a sodium channel linked to human pain." Nat Rev Neurosci **16**(9): 511-519.
Dib-Hajj, S. D., J. Fjell, T. R. Cummins, Z. Zheng, K. Fried, R. LaMotte, J. A. Black and S. G. Waxman (1999). "Plasticity of sodium channel expression in DRG neurons in the chronic constriction injury model of neuropathic pain." Pain **83**(3): 591-600.
Dib-Hajj, S. D., P. Geha and S. G. Waxman (2017). "Sodium channels in pain disorders: pathophysiology and prospects for treatment." Pain **158 Suppl 1**: S97-S107.

Dong, X., S. Han, M. J. Zylka, M. I. Simon and D. J. Anderson (2001). "A diverse family of GPCRs expressed in specific subsets of nociceptive sensory neurons." Cell **106**(5): 619-632.
Dong, X. W., S. Goregoaker, H. Engler, X. Zhou, L. Mark, J. Crona, R. Terry, J. Hunter and T. Priestley (2007). "Small interfering RNA-mediated selective knockdown of Na(V)1.8 tetrodotoxin-resistant sodium channel reverses mechanical allodynia in neuropathic rats." Neuroscience **146**(2): 812-821.
Donier, E., F. Rugiero, K. Okuse and J. N. Wood (2005). "Annexin II light chain p11 promotes functional expression of acid-sensing ion channel ASIC1a." J Biol Chem **280**(46): 38666-38672.
Downward, J. (1994). "The GRB2/Sem-5 adaptor protein." FEBS Lett **338**(2): 113-117.
Drube, S., J. Stirnweiss, C. Valkova and C. Liebmann (2006). "Ligand-independent and EGF receptor-supported transactivation: lessons from beta2-adrenergic receptor signalling." Cell Signal **18**(10): 1633-1646.
Duan, B., D. S. Liu, Y. Huang, W. Z. Zeng, X. Wang, H. Yu, M. X. Zhu, Z. Y. Chen and T. L. Xu (2012). "PI3-kinase/Akt pathway-regulated membrane insertion of acid-sensing ion channel 1a underlies BDNF-induced pain hypersensitivity." J Neurosci **32**(18): 6351-6363.
Dumble, M., M. C. Crouthamel, S. Y. Zhang, M. Schaber, D. Levy, K. Robell, Q. Liu, D. J. Figueroa, E. A. Minthorn, M. A. Seefeld, M. B. Rouse, S. K. Rabindran, D. A. Heerding and R. Kumar (2014). "Discovery of novel AKT inhibitors with enhanced anti-tumor effects in combination with the MEK inhibitor." PLoS One **9**(6): e100880.
Fabian, M. A., W. H. Biggs, 3rd, D. K. Treiber, C. E. Atteridge, M. D. Azimioara, M. G. Benedetti, T. A. Carter, P. Ciceri, P. T. Edeen, M. Floyd, J. M. Ford, M. Galvin, J. L. Gerlach, R. M. Grotzfeld, S. Herrgard, D. E. Insko, M. A. Insko, A. G. Lai, J. M. Lelias, S. A. Mehta, Z. V. Milanov, A. M. Velasco, L. M. Wodicka, H. K. Patel, P. P. Zarrinkar and D. J. Lockhart (2005). "A small molecule-kinase interaction map for clinical kinase inhibitors." Nat Biotechnol **23**(3): 329-336.
Ferrari, L. F., O. Bogen and J. D. Levine (2010). "Nociceptor subpopulations involved in hyperalgesic priming." Neuroscience **165**(3): 896-901.
Ferrer, I., S. Alcantara, J. Ballabriga, M. Olive, R. Blanco, R. Rivera, M. Carmona, M. Berruezo, S. Pitarch and A. M. Planas (1996). "Transforming growth factor-alpha (TGF-alpha) and epidermal growth factor-receptor (EGF-R) immunoreactivity in normal and pathologic brain." Prog Neurobiol **49**(2): 99-123.
Finnerup, N. B., S. H. Sindrup and T. S. Jensen (2010). "The evidence for pharmacological treatment of neuropathic pain." Pain **150**(3): 573-581.
Fornaro, M., J. M. Lee, S. Raimondo, S. Nicolino, S. Geuna and M. Giacobini-Robecchi (2008). "Neuronal intermediate filament expression in rat dorsal root ganglia sensory neurons: an in vivo and in vitro study." Neuroscience **153**(4): 1153-1163.
Fossat, P., E. Dobremez, R. Bouali-Benazzouz, A. Favereaux, S. S. Bertrand, K. Kilk, C. Leger, J. R. Cazalets, U. Langel, M. Landry and F. Nagy (2010). "Knockdown of L calcium channel subtypes: differential effects in neuropathic pain." J Neurosci **30**(3): 1073-1085.
Foulkes, T., M. A. Nassar, T. Lane, E. A. Matthews, M. D. Baker, V. Gerke, K. Okuse, A. H. Dickenson and J. N. Wood (2006). "Deletion of annexin 2 light chain p11 in nociceptors causes deficits in somatosensory coding and pain behavior." J Neurosci **26**(41): 10499-10507.
Fredriksson, S., M. Gullberg, J. Jarvius, C. Olsson, K. Pietras, S. M. Gustafsdottir, A. Ostman and U. Landegren (2002). "Protein detection using proximity-dependent DNA ligation assays." Nat Biotechnol **20**(5): 473-477.

Freed, D. M., N. J. Bessman, A. Kiyatkin, E. Salazar-Cavazos, P. O. Byrne, J. O. Moore, C. C. Valley, K. M. Ferguson, D. J. Leahy, D. S. Lidke and M. A. Lemmon (2017). "EGFR Ligands Differentially Stabilize Receptor Dimers to Specify Signaling Kinetics." Cell **171**(3): 683-695 e618.
Fujita, H., H. Hatakeyama, T. M. Watanabe, M. Sato, H. Higuchi and M. Kanzaki (2010). "Identification of three distinct functional sites of insulin-mediated GLUT4 trafficking in adipocytes using quantitative single molecule imaging." Mol Biol Cell **21**(15): 2721-2731.
Ganju, P., J. P. O'Bryan, C. Der, J. Winter and I. F. James (1998). "Differential regulation of SHC proteins by nerve growth factor in sensory neurons and PC12 cells." Eur J Neurosci **10**(6): 1995-2008.
Garrett, T. P., N. M. McKern, M. Lou, T. C. Elleman, T. E. Adams, G. O. Lovrecz, M. Kofler, R. N. Jorissen, E. C. Nice, A. W. Burgess and C. W. Ward (2003). "The crystal structure of a truncated ErbB2 ectodomain reveals an active conformation, poised to interact with other ErbB receptors." Mol Cell **11**(2): 495-505.
Garry, E. M., A. Moss, A. Delaney, F. O'Neill, J. Blakemore, J. Bowen, H. Husi, R. Mitchell, S. G. Grant and S. M. Fleetwood-Walker (2003). "Neuropathic sensitization of behavioral reflexes and spinal NMDA receptor/CaM kinase II interactions are disrupted in PSD-95 mutant mice." Curr Biol **13**(4): 321-328.
Gemes, G., A. Koopmeiners, M. Rigaud, P. Lirk, D. Sapunar, M. L. Bangaru, D. Vilceanu, S. R. Garrison, M. Ljubkovic, S. J. Mueller, C. L. Stucky and Q. H. Hogan (2013). "Failure of action potential propagation in sensory neurons: mechanisms and loss of afferent filtering in C-type units after painful nerve injury." J Physiol **591**(4): 1111-1131.
Ghosh, B., M. V. Green, K. A. Krogh and S. A. Thayer (2016). "Interleukin-1beta activates an Src family kinase to stimulate the plasma membrane Ca2+ pump in hippocampal neurons." J Neurophysiol **115**(4): 1875-1885.
Goldstein, M. E., S. B. House and H. Gainer (1991). "NF-L and peripherin immunoreactivities define distinct classes of rat sensory ganglion cells." J Neurosci Res **30**(1): 92-104.
Gomez-Pinilla, F., D. J. Knauer and M. Nieto-Sampedro (1988). "Epidermal growth factor receptor immunoreactivity in rat brain. Development and cellular localization." Brain Res **438**(1-2): 385-390.
Goral, R. O., E. Leipold, E. Nematian-Ardestani and S. H. Heinemann (2015). "Heterologous expression of NaV1.9 chimeras in various cell systems." Pflugers Arch **467**(12): 2423-2435.
Graus-Porta, D., R. R. Beerli, J. M. Daly and N. E. Hynes (1997). "ErbB-2, the preferred heterodimerization partner of all ErbB receptors, is a mediator of lateral signaling." EMBO J **16**(7): 1647-1655.
Guan, X., Q. Fu, B. Xiong, Z. Song, B. Shu, H. Bu, B. Xu, A. Manyande, F. Cao and Y. Tian (2015). "Activation of PI3Kgamma/Akt pathway mediates bone cancer pain in rats." J Neurochem **134**(3): 590-600.
Guan, X. H., X. F. Lu, H. X. Zhang, J. R. Wu, Y. Yuan, Q. Bao, D. Y. Ling and J. L. Cao (2010). "Phosphatidylinositol 3-kinase mediates pain behaviors induced by activation of peripheral ephrinBs/EphBs signaling in mice." Pharmacol Biochem Behav **95**(3): 315-324.
Harding, J. and B. Burtness (2005). "Cetuximab: an epidermal growth factor receptor chemeric human-murine monoclonal antibody." Drugs Today (Barc) **41**(2): 107-127.
Hardyman, M. A., E. Wilkinson, E. Martin, N. P. Jayasekera, C. Blume, E. J. Swindle, N. Gozzard, S. T. Holgate, P. H. Howarth, D. E. Davies and J. E. Collins (2013). "TNF-

alpha-mediated bronchial barrier disruption and regulation by src-family kinase activation." J Allergy Clin Immunol **132**(3): 665-675 e668.
Hartman, Z., H. Zhao and Y. M. Agazie (2013). "HER2 stabilizes EGFR and itself by altering autophosphorylation patterns in a manner that overcomes regulatory mechanisms and promotes proliferative and transformation signaling." Oncogene **32**(35): 4169-4180.
Heinke, B., E. Balzer and J. Sandkuhler (2004). "Pre- and postsynaptic contributions of voltage-dependent Ca2+ channels to nociceptive transmission in rat spinal lamina I neurons." Eur J Neurosci **19**(1): 103-111.
Heyer, E. J. and R. L. Macdonald (1982). "Calcium- and sodium-dependent action potentials of mouse spinal cord and dorsal root ganglion neurons in cell culture." J Neurophysiol **47**(4): 641-655.
Hill, M. M., S. F. Clark, D. F. Tucker, M. J. Birnbaum, D. E. James and S. L. Macaulay (1999). "A role for protein kinase Bbeta/Akt2 in insulin-stimulated GLUT4 translocation in adipocytes." Mol Cell Biol **19**(11): 7771-7781.
Hockley, J. R., G. Boundouki, V. Cibert-Goton, C. McGuire, P. K. Yip, C. Chan, M. Tranter, J. N. Wood, M. A. Nassar, L. A. Blackshaw, Q. Aziz, G. J. Michael, M. D. Baker, W. J. Winchester, C. H. Knowles and D. C. Bulmer (2014). "Multiple roles for NaV1.9 in the activation of visceral afferents by noxious inflammatory, mechanical, and human disease-derived stimuli." Pain **155**(10): 1962-1975.
Hoffmann, T., K. Kistner, R. W. Carr, M. A. Nassar, P. W. Reeh and C. Weidner (2017). "Reduced excitability and impaired nociception in peripheral unmyelinated fibers from Nav1.9-null mice." Pain **158**(1): 58-67.
Holgado-Madruga, M., D. R. Emlet, D. K. Moscatello, A. K. Godwin and A. J. Wong (1996). "A Grb2-associated docking protein in EGF- and insulin-receptor signalling." Nature **379**(6565): 560-564.
Hoppa, M. B., B. Lana, W. Margas, A. C. Dolphin and T. A. Ryan (2012). "alpha2delta expression sets presynaptic calcium channel abundance and release probability." Nature **486**(7401): 122-125.
Hu, P. and E. M. McLachlan (2003). "Distinct functional types of macrophage in dorsal root ganglia and spinal nerves proximal to sciatic and spinal nerve transections in the rat." Exp Neurol **184**(2): 590-605.
Huang, J., C. G. Vanoye, A. Cutts, Y. P. Goldberg, S. D. Dib-Hajj, C. J. Cohen, S. G. Waxman and A. L. George, Jr. (2017). "Sodium channel NaV1.9 mutations associated with insensitivity to pain dampen neuronal excitability." J Clin Invest **127**(7): 2805-2814.
Huerta, J. J., R. Diaz-Trelles, F. J. Naves, M. M. Llamosas, M. E. Del Valle and J. A. Vega (1996). "Epidermal growth factor receptor in adult human dorsal root ganglia." Anat Embryol (Berl) **194**(3): 253-257.
Hunter, T. (1987). "A tail of two src's: mutatis mutandis." Cell **49**(1): 1-4.
Igwe, O. J. (2003). "c-Src kinase activation regulates preprotachykinin gene expression and substance P secretion in rat sensory ganglia." Eur J Neurosci **18**(7): 1719-1730.
Jedrychowski, M. P., C. A. Gartner, S. P. Gygi, L. Zhou, J. Herz, K. V. Kandror and P. F. Pilch (2010). "Proteomic analysis of GLUT4 storage vesicles reveals LRP1 to be an important vesicle component and target of insulin signaling." J Biol Chem **285**(1): 104-114.
Ji, R. R., R. W. t. Gereau, M. Malcangio and G. R. Strichartz (2009). "MAP kinase and pain." Brain Res Rev **60**(1): 135-148.

Ji, R. R., Z. Z. Xu and Y. J. Gao (2014). "Emerging targets in neuroinflammation-driven chronic pain." Nat Rev Drug Discov **13**(7): 533-548.
Jiang, S. P., Z. D. Zhang, L. M. Kang, Q. H. Wang, L. Zhang and H. P. Chen (2016). "Celecoxib reverts oxaliplatin-induced neuropathic pain through inhibiting PI3K/Akt2 pathway in the mouse dorsal root ganglion." Exp Neurol **275 Pt 1**: 11-16.
Jimeno, A., B. Rubio-Viqueira, M. L. Amador, D. Oppenheimer, N. Bouraoud, P. Kulesza, V. Sebastiani, A. Maitra and M. Hidalgo (2005). "Epidermal growth factor receptor dynamics influences response to epidermal growth factor receptor targeted agents." Cancer Res **65**(8): 3003-3010.
Jin, X., N. Morsy, J. Winston, P. J. Pasricha, K. Garrett and H. I. Akbarali (2004). "Modulation of TRPV1 by nonreceptor tyrosine kinase, c-Src kinase." Am J Physiol Cell Physiol **287**(2): C558-563.
Jones, J. T., R. W. Akita and M. X. Sliwkowski (1999). "Binding specificities and affinities of egf domains for ErbB receptors." FEBS Lett **447**(2-3): 227-231.
Joshi, S. K., J. P. Mikusa, G. Hernandez, S. Baker, C. C. Shieh, T. Neelands, X. F. Zhang, W. Niforatos, K. Kage, P. Han, D. Krafte, C. Faltynek, J. P. Sullivan, M. F. Jarvis and P. Honore (2006). "Involvement of the TTX-resistant sodium channel Nav 1.8 in inflammatory and neuropathic, but not post-operative, pain states." Pain **123**(1-2): 75-82.
Junttila, T. T., R. W. Akita, K. Parsons, C. Fields, G. D. Lewis Phillips, L. S. Friedman, D. Sampath and M. X. Sliwkowski (2009). "Ligand-independent HER2/HER3/PI3K complex is disrupted by trastuzumab and is effectively inhibited by the PI3K inhibitor GDC-0941." Cancer Cell **15**(5): 429-440.
Kadurin, I., S. W. Rothwell, B. Lana, M. Nieto-Rostro and A. C. Dolphin (2017). "LRP1 influences trafficking of N-type calcium channels via interaction with the auxiliary alpha2delta-1 subunit." Sci Rep **7**: 43802.
Kane, S., H. Sano, S. C. Liu, J. M. Asara, W. S. Lane, C. C. Garner and G. E. Lienhard (2002). "A method to identify serine kinase substrates. Akt phosphorylates a novel adipocyte protein with a Rab GTPase-activating protein (GAP) domain." J Biol Chem **277**(25): 22115-22118.
Kanzaki, M., Y. Q. Zhang, H. Mashima, L. Li, H. Shibata and I. Kojima (1999). "Translocation of a calcium-permeable cation channel induced by insulin-like growth factor-I." Nat Cell Biol **1**(3): 165-170.
Kavuri, S. M., N. Jain, F. Galimi, F. Cottino, S. M. Leto, G. Migliardi, A. C. Searleman, W. Shen, J. Monsey, L. Trusolino, S. A. Jacobs, A. Bertotti and R. Bose (2015). "HER2 activating mutations are targets for colorectal cancer treatment." Cancer Discov **5**(8): 832-841.
Kerr, B. J., V. Souslova, S. B. McMahon and J. N. Wood (2001). "A role for the TTX-resistant sodium channel Nav 1.8 in NGF-induced hyperalgesia, but not neuropathic pain." Neuroreport **12**(14): 3077-3080.
Kersten, C. and M. G. Cameron (2012). "Cetuximab alleviates neuropathic pain despite tumour progression." BMJ Case Rep **2012**.
Kersten, C., M. G. Cameron, A. G. Bailey, M. T. Fallon, B. J. Laird, V. Paterson, R. Mitchell, S. M. Fleetwood-Walker, F. Daly and S. Mjaland (2019). "Relief of Neuropathic Pain Through Epidermal Growth Factor Receptor Inhibition: A Randomized Proof-of-Concept Trial." Pain Med **20**(12): 2495-2505.
Kersten, C., M. G. Cameron, B. Laird and S. Mjaland (2015). "Epidermal growth factor receptor-inhibition (EGFR-I) in the treatment of neuropathic pain." Br J Anaesth **115**(5): 761-767.

Kersten, C., M. G. Cameron and S. Mjaland (2013). "Epithelial growth factor receptor (EGFR)-inhibition for relief of neuropathic pain-A case series." Scand J Pain **4**(1): 3-7.
Khoutorsky, A., R. P. Bonin, R. E. Sorge, C. G. Gkogkas, S. A. Pawlowski, S. M. Jafarnejad, M. H. Pitcher, T. Alain, J. Perez-Sanchez, E. W. Salter, L. Martin, A. Ribeiro-da-Silva, Y. De Koninck, F. Cervero, J. S. Mogil and N. Sonenberg (2015). "Translational control of nociception via 4E-binding protein 1." Elife **4**.
Kim, E. S., F. R. Khuri and R. S. Herbst (2001). "Epidermal growth factor receptor biology (IMC-C225)." Curr Opin Oncol **13**(6): 506-513.
Kongstorp, M., T. Schjolberg, D. P. Jacobsen, F. Haugen and J. Gjerstad (2019). "Epiregulin is released from intervertebral disks and induces spontaneous activity in pain pathways." Pain Rep **4**(2): e718.
Kose, M. (2017). "GPCRs and EGFR - Cross-talk of membrane receptors in cancer." Bioorg Med Chem Lett **27**(16): 3611-3620.
Kostyuk, P. G., N. S. Veselovsky and S. A. Fedulova (1981). "Ionic currents in the somatic membrane of rat dorsal root ganglion neurons-II. Calcium currents." Neuroscience **6**(12): 2431-2437.
Kumagai, T., M. Katsumata, A. Hasegawa, K. Furuuchi, T. Funakoshi, I. Kawase and M. I. Greene (2003). "Role of extracellular subdomains of p185c-neu and the epidermal growth factor receptor in ligand-independent association and transactivation." Proc Natl Acad Sci U S A **100**(16): 9220-9225.
Lai, J., J. C. Hunter and F. Porreca (2003). "The role of voltage-gated sodium channels in neuropathic pain." Curr Opin Neurobiol **13**(3): 291-297.
Lam, D., Z. Momeni, M. Theaker, S. Jagadeeshan, Y. Yamamoto, J. P. Ianowski and V. A. Campanucci (2018). "RAGE-dependent potentiation of TRPV1 currents in sensory neurons exposed to high glucose." PLoS One **13**(2): e0193312.
Larance, M., G. Ramm, J. Stockli, E. M. van Dam, S. Winata, V. Wasinger, F. Simpson, M. Graham, J. R. Junutula, M. Guilhaus and D. E. James (2005). "Characterization of the role of the Rab GTPase-activating protein AS160 in insulin-regulated GLUT4 trafficking." J Biol Chem **280**(45): 37803-37813.
Lengyel, I., K. Voss, M. Cammarota, K. Bradshaw, V. Brent, K. P. Murphy, K. P. Giese, J. A. Rostas and T. V. Bliss (2004). "Autonomous activity of CaMKII is only transiently increased following the induction of long-term potentiation in the rat hippocampus." Eur J Neurosci **20**(11): 3063-3072.
Leo, S., R. D'Hooge and T. Meert (2010). "Exploring the role of nociceptor-specific sodium channels in pain transmission using Nav1.8 and Nav1.9 knockout mice." Behav Brain Res **208**(1): 149-157.
Leto, D. and A. R. Saltiel (2012). "Regulation of glucose transport by insulin: traffic control of GLUT4." Nat Rev Mol Cell Biol **13**(6): 383-396.
Li, D., L. Ambrogio, T. Shimamura, S. Kubo, M. Takahashi, L. R. Chirieac, R. F. Padera, G. I. Shapiro, A. Baum, F. Himmelsbach, W. J. Rettig, M. Meyerson, F. Solca, H. Greulich and K. K. Wong (2008). "BIBW2992, an irreversible EGFR/HER2 inhibitor highly effective in preclinical lung cancer models." Oncogene **27**(34): 4702-4711.
Li, D., H. Chen, X. H. Luo, Y. Sun, W. Xia and Y. C. Xiong (2016). "CX3CR1-Mediated Akt1 Activation Contributes to the Paclitaxel-Induced Painful Peripheral Neuropathy in Rats." Neurochem Res **41**(6): 1305-1314.
Li, S., K. R. Schmitz, P. D. Jeffrey, J. J. Wiltzius, P. Kussie and K. M. Ferguson (2005). "Structural basis for inhibition of the epidermal growth factor receptor by cetuximab." Cancer Cell **7**(4): 301-311.

Liang, L., B. Tao, L. Fan, M. Yaster, Y. Zhang and Y. X. Tao (2013). "mTOR and its downstream pathway are activated in the dorsal root ganglion and spinal cord after peripheral inflammation, but not after nerve injury." Brain Res **1513**: 17-25.
Lillis, A. P., L. B. Van Duyn, J. E. Murphy-Ullrich and D. K. Strickland (2008). "LDL receptor-related protein 1: unique tissue-specific functions revealed by selective gene knockout studies." Physiol Rev **88**(3): 887-918.
Lin, J., D. Sampath, M. A. Nannini, B. B. Lee, M. Degtyarev, J. Oeh, H. Savage, Z. Guan, R. Hong, R. Kassees, L. B. Lee, T. Risom, S. Gross, B. M. Liederer, H. Koeppen, N. J. Skelton, J. J. Wallin, M. Belvin, E. Punnoose, L. S. Friedman and K. Lin (2013). "Targeting activated Akt with GDC-0068, a novel selective Akt inhibitor that is efficacious in multiple tumor models." Clin Cancer Res **19**(7): 1760-1772.
Lin, Z., S. Santos, K. Padilla, D. Printzenhoff and N. A. Castle (2016). "Biophysical and Pharmacological Characterization of Nav1.9 Voltage Dependent Sodium Channels Stably Expressed in HEK-293 Cells." PLoS One **11**(8): e0161450.
Liu, C., S. D. Dib-Hajj and S. G. Waxman (2001). "Fibroblast growth factor homologous factor 1B binds to the C terminus of the tetrodotoxin-resistant sodium channel rNav1.9a (NaN)." J Biol Chem **276**(22): 18925-18933.
Liu, C. H., T. C. Chen, G. Y. Chau, Y. H. Jan, C. H. Chen, C. N. Hsu, K. T. Lin, Y. L. Juang, P. J. Lu, H. C. Cheng, M. H. Chen, C. F. Chang, Y. S. Ting, C. Y. Kao, M. Hsiao and C. Y. Huang (2013). "Analysis of protein-protein interactions in cross-talk pathways reveals CRKL protein as a novel prognostic marker in hepatocellular carcinoma." Mol Cell Proteomics **12**(5): 1335-1349.
Liu, C. J., S. D. Dib-Hajj, J. A. Black, J. Greenwood, Z. Lian and S. G. Waxman (2001). "Direct interaction with contactin targets voltage-gated sodium channel Na(v)1.9/NaN to the cell membrane." J Biol Chem **276**(49): 46553-46561.
Liu, C. J., S. D. Dib-Hajj, M. Renganathan, T. R. Cummins and S. G. Waxman (2003). "Modulation of the cardiac sodium channel Nav1.5 by fibroblast growth factor homologous factor 1B." J Biol Chem **278**(2): 1029-1036.
Liu, S., Y. P. Liu, Z. J. Huang, Y. K. Zhang, A. A. Song, P. C. Ma and X. J. Song (2015). "Wnt/Ryk signaling contributes to neuropathic pain by regulating sensory neuron excitability and spinal synaptic plasticity in rats." Pain **156**(12): 2572-2584.
Lolignier, S., C. Bonnet, C. Gaudioso, J. Noel, J. Ruel, M. Amsalem, J. Ferrier, L. Rodat-Despoix, V. Bouvier, Y. Aissouni, L. Prival, E. Chapuy, F. Padilla, A. Eschalier, P. Delmas and J. Busserolles (2015). "The Nav1.9 channel is a key determinant of cold pain sensation and cold allodynia." Cell Rep **11**(7): 1067-1078.
Lou, L. L., S. J. Lloyd and H. Schulman (1986). "Activation of the multifunctional Ca2+/calmodulin-dependent protein kinase by autophosphorylation: ATP modulates production of an autonomous enzyme." Proc Natl Acad Sci U S A **83**(24): 9497-9501.
Lowenstein, E. J., R. J. Daly, A. G. Batzer, W. Li, B. Margolis, R. Lammers, A. Ullrich, E. Y. Skolnik, D. Bar-Sagi and J. Schlessinger (1992). "The SH2 and SH3 domain-containing protein GRB2 links receptor tyrosine kinases to ras signaling." Cell **70**(3): 431-442.
Luiz, A. P., O. Kopach, S. Santana-Varela and J. N. Wood (2015). "The role of Nav1.9 channel in the development of neuropathic orofacial pain associated with trigeminal neuralgia." Mol Pain **11**: 72.
Luscher, C., P. Lipp, H. R. Luscher and E. Niggli (1996). "Control of action potential propagation by intracellular Ca2+ in cultured rat dorsal root ganglion cells." J Physiol **490 (Pt 2)**: 319-324.
Luttrell, L. M., G. J. Della Rocca, T. van Biesen, D. K. Luttrell and R. J. Lefkowitz (1997). "Gbetagamma subunits mediate Src-dependent phosphorylation of the

epidermal growth factor receptor. A scaffold for G protein-coupled receptor-mediated Ras activation." J Biol Chem **272**(7): 4637-4644.
Maingret, F., B. Coste, F. Padilla, N. Clerc, M. Crest, S. M. Korogod and P. Delmas (2008). "Inflammatory mediators increase Nav1.9 current and excitability in nociceptors through a coincident detection mechanism." J Gen Physiol **131**(3): 211-225.
Markadieu, N., D. Blero, A. Boom, C. Erneux and R. Beauwens (2004). "Phosphatidylinositol 3,4,5-trisphosphate: an early mediator of insulin-stimulated sodium transport in A6 cells." Am J Physiol Renal Physiol **287**(2): F319-328.
Martin, L. J., S. B. Smith, A. Khoutorsky, C. A. Magnussen, A. Samoshkin, R. E. Sorge, C. Cho, N. Yosefpour, S. Sivaselvachandran, S. Tohyama, T. Cole, T. M. Khuong, E. Mir, D. G. Gibson, J. S. Wieskopf, S. G. Sotocinal, J. S. Austin, C. B. Meloto, J. H. Gitt, C. Gkogkas, N. Sonenberg, J. D. Greenspan, R. B. Fillingim, R. Ohrbach, G. D. Slade, C. Knott, R. Dubner, A. G. Nackley, A. Ribeiro-da-Silva, G. G. Neely, W. Maixner, D. V. Zaykin, J. S. Mogil and L. Diatchenko (2017). "Epiregulin and EGFR interactions are involved in pain processing." J Clin Invest **127**(9): 3353-3366.
Mattoon, D. R., B. Lamothe, I. Lax and J. Schlessinger (2004). "The docking protein Gab1 is the primary mediator of EGF-stimulated activation of the PI-3K/Akt cell survival pathway." BMC Biol **2**: 24.
Maudsley, S., K. L. Pierce, A. M. Zamah, W. E. Miller, S. Ahn, Y. Daaka, R. J. Lefkowitz and L. M. Luttrell (2000). "The beta(2)-adrenergic receptor mediates extracellular signal-regulated kinase activation via assembly of a multi-receptor complex with the epidermal growth factor receptor." J Biol Chem **275**(13): 9572-9580.
Miller, K. E., B. A. Richards and R. M. Kriebel (2002). "Glutamine-, glutamine synthetase-, glutamate dehydrogenase- and pyruvate carboxylase-immunoreactivities in the rat dorsal root ganglion and peripheral nerve." Brain Res **945**(2): 202-211.
Moasser, M. M., A. Basso, S. D. Averbuch and N. Rosen (2001). "The tyrosine kinase inhibitor ZD1839 ("Iressa") inhibits HER2-driven signaling and suppresses the growth of HER2-overexpressing tumor cells." Cancer Res **61**(19): 7184-7188.
Moriki, T., H. Maruyama and I. N. Maruyama (2001). "Activation of preformed EGF receptor dimers by ligand-induced rotation of the transmembrane domain." J Mol Biol **311**(5): 1011-1026.
Moulder, S. L., V. F. Borges, T. Baetz, T. McSpadden, G. Fernetich, R. K. Murthy, R. Chavira, K. Guthrie, E. Barrett and S. K. Chia (2017). "Phase I Study of ONT-380, a HER2 Inhibitor, in Patients with HER2(+)-Advanced Solid Tumors, with an Expansion Cohort in HER2(+) Metastatic Breast Cancer (MBC)." Clin Cancer Res **23**(14): 3529-3536.
Moyer, J. D., E. G. Barbacci, K. K. Iwata, L. Arnold, B. Boman, A. Cunningham, C. DiOrio, J. Doty, M. J. Morin, M. P. Moyer, M. Neveu, V. A. Pollack, L. R. Pustilnik, M. M. Reynolds, D. Sloan, A. Theleman and P. Miller (1997). "Induction of apoptosis and cell cycle arrest by CP-358,774, an inhibitor of epidermal growth factor receptor tyrosine kinase." Cancer Res **57**(21): 4838-4848.
Nagasawa, J., A. Mizokami, K. Koshida, S. Yoshida, K. Naito and M. Namiki (2006). "Novel HER2 selective tyrosine kinase inhibitor, TAK-165, inhibits bladder, kidney and androgen-independent prostate cancer in vitro and in vivo." Int J Urol **13**(5): 587-592.
Nascimento, A. I., F. M. Mar and M. M. Sousa (2018). "The intriguing nature of dorsal root ganglion neurons: Linking structure with polarity and function." Prog Neurobiol **168**: 86-103.
Nassar, M. A., A. Levato, L. C. Stirling and J. N. Wood (2005). "Neuropathic pain develops normally in mice lacking both Na(v)1.7 and Na(v)1.8." Mol Pain **1**: 24.

Ng, Y., G. Ramm, J. G. Burchfield, A. C. Coster, J. Stockli and D. E. James (2010). "Cluster analysis of insulin action in adipocytes reveals a key role for Akt at the plasma membrane." J Biol Chem **285**(4): 2245-2257.
Nieto-Rostro, M., K. Ramgoolam, W. S. Pratt, A. Kulik and A. C. Dolphin (2018). "Ablation of alpha2delta-1 inhibits cell-surface trafficking of endogenous N-type calcium channels in the pain pathway in vivo." Proc Natl Acad Sci U S A **115**(51): E12043-E12052.
Nishida, K. and T. Hirano (2003). "The role of Gab family scaffolding adapter proteins in the signal transduction of cytokine and growth factor receptors." Cancer Sci **94**(12): 1029-1033.
O'Hare, T., D. K. Walters, E. P. Stoffregen, T. Jia, P. W. Manley, J. Mestan, S. W. Cowan-Jacob, F. Y. Lee, M. C. Heinrich, M. W. Deininger and B. J. Druker (2005). "In vitro activity of Bcr-Abl inhibitors AMN107 and BMS-354825 against clinically relevant imatinib-resistant Abl kinase domain mutants." Cancer Res **65**(11): 4500-4505.
Obara, I., K. K. Tochiki, S. M. Geranton, F. B. Carr, B. M. Lumb, Q. Liu and S. P. Hunt (2011). "Systemic inhibition of the mammalian target of rapamycin (mTOR) pathway reduces neuropathic pain in mice." Pain **152**(11): 2582-2595.
Obata, K., H. Yamanaka, K. Kobayashi, Y. Dai, T. Mizushima, H. Katsura, T. Fukuoka, A. Tokunaga and K. Noguchi (2004). "Role of mitogen-activated protein kinase activation in injured and intact primary afferent neurons for mechanical and heat hypersensitivity after spinal nerve ligation." J Neurosci **24**(45): 10211-10222.
Okuse, K., M. Malik-Hall, M. D. Baker, W. Y. Poon, H. Kong, M. V. Chao and J. N. Wood (2002). "Annexin II light chain regulates sensory neuron-specific sodium channel expression." Nature **417**(6889): 653-656.
Olayioye, M. A., R. M. Neve, H. A. Lane and N. E. Hynes (2000). "The ErbB signaling network: receptor heterodimerization in development and cancer." EMBO J **19**(13): 3159-3167.
Osorio, N., S. Korogod and P. Delmas (2014). "Specialized functions of Nav1.5 and Nav1.9 channels in electrogenesis of myenteric neurons in intact mouse ganglia." J Neurosci **34**(15): 5233-5244.
Parkyn, C. J., E. G. Vermeulen, R. C. Mootoosamy, C. Sunyach, C. Jacobsen, C. Oxvig, S. Moestrup, Q. Liu, G. Bu, A. Jen and R. J. Morris (2008). "LRP1 controls biosynthetic and endocytic trafficking of neuronal prion protein." J Cell Sci **121**(Pt 6): 773-783.
Pearson, R. J., Jr. and S. L. Carroll (2004). "ErbB transmembrane tyrosine kinase receptors are expressed by sensory and motor neurons projecting into sciatic nerve." J Histochem Cytochem **52**(10): 1299-1311.
Peck, G. R., J. A. Chavez, W. G. Roach, B. A. Budnik, W. S. Lane, H. K. Karlsson, J. R. Zierath and G. E. Lienhard (2009). "Insulin-stimulated phosphorylation of the Rab GTPase-activating protein TBC1D1 regulates GLUT4 translocation." J Biol Chem **284**(44): 30016-30023.
Pedersen, M. W., N. Pedersen, L. H. Ottesen and H. S. Poulsen (2005). "Differential response to gefitinib of cells expressing normal EGFR and the mutant EGFRvIII." Br J Cancer **93**(8): 915-923.
Perez-Torres, M., M. Guix, A. Gonzalez and C. L. Arteaga (2006). "Epidermal growth factor receptor (EGFR) antibody down-regulates mutant receptors and inhibits tumors expressing EGFR mutations." J Biol Chem **281**(52): 40183-40192.
Pollack, V. A., D. M. Savage, D. A. Baker, K. E. Tsaparikos, D. E. Sloan, J. D. Moyer, E. G. Barbacci, L. R. Pustilnik, T. A. Smolarek, J. A. Davis, M. P. Vaidya, L. D. Arnold, J. L. Doty, K. K. Iwata and M. J. Morin (1999). "Inhibition of epidermal growth factor

receptor-associated tyrosine phosphorylation in human carcinomas with CP-358,774: dynamics of receptor inhibition in situ and antitumor effects in athymic mice." J Pharmacol Exp Ther **291**(2): 739-748.
Porreca, F., J. Lai, D. Bian, S. Wegert, M. H. Ossipov, R. M. Eglen, L. Kassotakis, S. Novakovic, D. K. Rabert, L. Sangameswaran and J. C. Hunter (1999). "A comparison of the potential role of the tetrodotoxin-insensitive sodium channels, PN3/SNS and NaN/SNS2, in rat models of chronic pain." Proc Natl Acad Sci U S A **96**(14): 7640-7644.
Priest, B. T., B. A. Murphy, J. A. Lindia, C. Diaz, C. Abbadie, A. M. Ritter, P. Liberator, L. M. Iyer, S. F. Kash, M. G. Kohler, G. J. Kaczorowski, D. E. MacIntyre and W. J. Martin (2005). "Contribution of the tetrodotoxin-resistant voltage-gated sodium channel NaV1.9 to sensory transmission and nociceptive behavior." Proc Natl Acad Sci U S A **102**(26): 9382-9387.
Qian, Y., K. Peng, C. Qiu, M. Skibba, Y. Huang, Z. Xu, Y. Zhang, J. Hu, D. Liang, C. Zou, Y. Wang and G. Liang (2016). "Novel Epidermal Growth Factor Receptor Inhibitor Attenuates Angiotensin II-Induced Kidney Fibrosis." J Pharmacol Exp Ther **356**(1): 32-42.
Qiu, F., Y. Jiang, H. Zhang, Y. Liu and W. Mi (2012). "Increased expression of tetrodotoxin-resistant sodium channels Nav1.8 and Nav1.9 within dorsal root ganglia in a rat model of bone cancer pain." Neurosci Lett **512**(2): 61-66.
Ricci, A., L. Lanfrancone, R. Chiari, G. Belardo, C. Pertica, P. G. Natali, P. G. Pelicci and O. Segatto (1995). "Analysis of protein-protein interactions involved in the activation of the Shc/Grb-2 pathway by the ErbB-2 kinase." Oncogene **11**(8): 1519-1529.
Rivat, C., S. Sebaihi, J. Van Steenwinckel, S. Fouquet, P. Kitabgi, M. Pohl, S. Melik Parsadaniantz and A. Reaux-Le Goazigo (2014). "Src family kinases involved in CXCL12-induced loss of acute morphine analgesia." Brain Behav Immun **38**: 38-52.
Rivera-Oliver, M., E. Moreno, Y. Alvarez-Bagnarol, C. Ayala-Santiago, N. Cruz-Reyes, G. C. Molina-Castro, S. Clemens, E. I. Canela, S. Ferre, V. Casado and M. Diaz-Rios (2019). "Adenosine A1-Dopamine D1 Receptor Heteromers Control the Excitability of the Spinal Motoneuron." Mol Neurobiol **56**(2): 797-811.
Robinson, M. J. and M. H. Cobb (1997). "Mitogen-activated protein kinase pathways." Curr Opin Cell Biol **9**(2): 180-186.
Rodrigues, G. A., M. Falasca, Z. Zhang, S. H. Ong and J. Schlessinger (2000). "A novel positive feedback loop mediated by the docking protein Gab1 and phosphatidylinositol 3-kinase in epidermal growth factor receptor signaling." Mol Cell Biol **20**(4): 1448-1459.
Rojas, M., S. Yao and Y. Z. Lin (1996). "Controlling epidermal growth factor (EGF)-stimulated Ras activation in intact cells by a cell-permeable peptide mimicking phosphorylated EGF receptor." J Biol Chem **271**(44): 27456-27461.
Roskoski, R., Jr. (2014). "ErbB/HER protein-tyrosine kinases: Structures and small molecule inhibitors." Pharmacol Res **87**: 42-59.
Rusnak, D. W., K. Lackey, K. Affleck, E. R. Wood, K. J. Alligood, N. Rhodes, B. R. Keith, D. M. Murray, W. B. Knight, R. J. Mullin and T. M. Gilmer (2001). "The effects of the novel, reversible epidermal growth factor receptor/ErbB-2 tyrosine kinase inhibitor, GW2016, on the growth of human normal and tumor-derived cell lines in vitro and in vivo." Mol Cancer Ther **1**(2): 85-94.
Sacerdote, P., S. Franchi, A. E. Trovato, A. E. Valsecchi, A. E. Panerai and M. Colleoni (2008). "Transient early expression of TNF-alpha in sciatic nerve and dorsal root

ganglia in a mouse model of painful peripheral neuropathy." Neurosci Lett **436**(2): 210-213.
Sakamoto, K. and G. D. Holman (2008). "Emerging role for AS160/TBC1D4 and TBC1D1 in the regulation of GLUT4 traffic." Am J Physiol Endocrinol Metab **295**(1): E29-37.
Salicioni, A. M., A. Gaultier, C. Brownlee, M. K. Cheezum and S. L. Gonias (2004). "Low density lipoprotein receptor-related protein-1 promotes beta1 integrin maturation and transport to the cell surface." J Biol Chem **279**(11): 10005-10012.
Sano, H., S. Kane, E. Sano, C. P. Miinea, J. M. Asara, W. S. Lane, C. W. Garner and G. E. Lienhard (2003). "Insulin-stimulated phosphorylation of a Rab GTPase-activating protein regulates GLUT4 translocation." J Biol Chem **278**(17): 14599-14602.
Sarbassov, D. D., D. A. Guertin, S. M. Ali and D. M. Sabatini (2005). "Phosphorylation and regulation of Akt/PKB by the rictor-mTOR complex." Science **307**(5712): 1098-1101.
Sato, K., T. Nakamura, M. Mizuguchi, K. Miura, M. Tada, T. Aizawa, T. Gomi, K. Miyamoto and K. Kawano (2003). "Solution structure of epiregulin and the effect of its C-terminal domain for receptor binding affinity." FEBS Lett **553**(3): 232-238.
Sawano, A., S. Takayama, M. Matsuda and A. Miyawaki (2002). "Lateral propagation of EGF signaling after local stimulation is dependent on receptor density." Dev Cell **3**(2): 245-257.
Schworer, C. M., R. J. Colbran and T. R. Soderling (1986). "Reversible generation of a Ca2+-independent form of Ca2+(calmodulin)-dependent protein kinase II by an autophosphorylation mechanism." J Biol Chem **261**(19): 8581-8584.
Shah, B. S., A. M. Rush, S. Liu, L. Tyrrell, J. A. Black, S. D. Dib-Hajj and S. G. Waxman (2004). "Contactin associates with sodium channel Nav1.3 in native tissues and increases channel density at the cell surface." J Neurosci **24**(33): 7387-7399.
Shelly, M., R. Pinkas-Kramarski, B. C. Guarino, H. Waterman, L. M. Wang, L. Lyass, M. Alimandi, A. Kuo, S. S. Bacus, J. H. Pierce, G. C. Andrews and Y. Yarden (1998). "Epiregulin is a potent pan-ErbB ligand that preferentially activates heterodimeric receptor complexes." J Biol Chem **273**(17): 10496-10505.
Shi, F., S. E. Telesco, Y. Liu, R. Radhakrishnan and M. A. Lemmon (2010). "ErbB3/HER3 intracellular domain is competent to bind ATP and catalyze autophosphorylation." Proc Natl Acad Sci U S A **107**(17): 7692-7697.
Shi, T. J., P. Huang, J. Mulder, S. Ceccatelli and T. Hokfelt (2009). "Expression of p-Akt in sensory neurons and spinal cord after peripheral nerve injury." Neurosignals **17**(3): 203-212.
Sizova, D. V., J. Huang, E. J. Akin, M. Estacion, C. Gomis-Perez, S. G. Waxman and S. D. Dib-Hajj (2020). "A 49-residue sequence motif in the C terminus of Nav1.9 regulates trafficking of the channel to the plasma membrane." J Biol Chem **295**(4): 1077-1090.
Soderberg, O., M. Gullberg, M. Jarvius, K. Ridderstrale, K. J. Leuchowius, J. Jarvius, K. Wester, P. Hydbring, F. Bahram, L. G. Larsson and U. Landegren (2006). "Direct observation of individual endogenous protein complexes in situ by proximity ligation." Nat Methods **3**(12): 995-1000.
Solca, F. F., A. Baum, E. Langkopf, G. Dahmann, K. H. Heider, F. Himmelsbach and J. C. van Meel (2004). "Inhibition of epidermal growth factor receptor activity by two pyrimidopyrimidine derivatives." J Pharmacol Exp Ther **311**(2): 502-509.
Su, T., D. M. Bryant, F. Luton, M. Verges, S. M. Ulrich, K. C. Hansen, A. Datta, D. J. Eastburn, A. L. Burlingame, K. M. Shokat and K. E. Mostov (2010). "A kinase cascade

leading to Rab11-FIP5 controls transcytosis of the polymeric immunoglobulin receptor." Nat Cell Biol **12**(12): 1143-1153.
Sun, R., J. Yan and W. D. Willis (2007). "Activation of protein kinase B/Akt in the periphery contributes to pain behavior induced by capsaicin in rats." Neuroscience **144**(1): 286-294.
Tao, R. H. and I. N. Maruyama (2008). "All EGF(ErbB) receptors have preformed homo- and heterodimeric structures in living cells." J Cell Sci **121**(Pt 19): 3207-3217.
Tice, D. A., J. S. Biscardi, A. L. Nickles and S. J. Parsons (1999). "Mechanism of biological synergy between cellular Src and epidermal growth factor receptor." Proc Natl Acad Sci U S A **96**(4): 1415-1420.
Toyoda, H., T. Komurasaki, D. Uchida, Y. Takayama, T. Isobe, T. Okuyama and K. Hanada (1995). "Epiregulin. A novel epidermal growth factor with mitogenic activity for rat primary hepatocytes." J Biol Chem **270**(13): 7495-7500.
Traxler, P., J. Green, H. Mett, U. Sequin and P. Furet (1999). "Use of a pharmacophore model for the design of EGFR tyrosine kinase inhibitors: isoflavones and 3-phenyl-4(1H)-quinolones." J Med Chem **42**(6): 1018-1026.
Tzahar, E., R. Pinkas-Kramarski, J. D. Moyer, L. N. Klapper, I. Alroy, G. Levkowitz, M. Shelly, S. Henis, M. Eisenstein, B. J. Ratzkin, M. Sela, G. C. Andrews and Y. Yarden (1997). "Bivalence of EGF-like ligands drives the ErbB signaling network." EMBO J **16**(16): 4938-4950.
Uceyler, N., A. Tscharke and C. Sommer (2007). "Early cytokine expression in mouse sciatic nerve after chronic constriction nerve injury depends on calpain." Brain Behav Immun **21**(5): 553-560.
van Vliet, C., P. E. Bukczynska, M. A. Puryer, C. M. Sadek, B. J. Shields, M. L. Tremblay and T. Tiganis (2005). "Selective regulation of tumor necrosis factor-induced Erk signaling by Src family kinases and the T cell protein tyrosine phosphatase." Nat Immunol **6**(3): 253-260.
Vanegas, H. and H. Schaible (2000). "Effects of antagonists to high-threshold calcium channels upon spinal mechanisms of pain, hyperalgesia and allodynia." Pain **85**(1-2): 9-18.
Verma, V., S. Khoury, M. Parisien, C. Cho, W. Maixner, L. J. Martin and L. Diatchenko (2020). "The dichotomous role of epiregulin in pain." Pain.
Verveer, P. J., F. S. Wouters, A. R. Reynolds and P. I. Bastiaens (2000). "Quantitative imaging of lateral ErbB1 receptor signal propagation in the plasma membrane." Science **290**(5496): 1567-1570.
Viard, P., A. J. Butcher, G. Halet, A. Davies, B. Nurnberg, F. Heblich and A. C. Dolphin (2004). "PI3K promotes voltage-dependent calcium channel trafficking to the plasma membrane." Nat Neurosci **7**(9): 939-946.
Viviani, B., S. Bartesaghi, F. Gardoni, A. Vezzani, M. M. Behrens, T. Bartfai, M. Binaglia, E. Corsini, M. Di Luca, C. L. Galli and M. Marinovich (2003). "Interleukin-1beta enhances NMDA receptor-mediated intracellular calcium increase through activation of the Src family of kinases." J Neurosci **23**(25): 8692-8700.
Wallace, E. M., J. P. Lyssikatos, T. Yeh, J. D. Winkler and K. Koch (2005). "Progress towards therapeutic small molecule MEK inhibitors for use in cancer therapy." Curr Top Med Chem **5**(2): 215-229.
Wang, S., S. Liu, L. Xu, X. Zhu, W. Liu, L. Tian, Y. Chen, Y. Wang, B. V. P. Nagendra, S. Jia, L. Liang and F. Q. Huo (2019). "The upregulation of EGFR in the dorsal root ganglion contributes to chronic compression of dorsal root ganglions-induced neuropathic pain in rats." Mol Pain **15**: 1744806919857297.

Wang, Z. (2016). "Transactivation of Epidermal Growth Factor Receptor by G Protein-Coupled Receptors: Recent Progress, Challenges and Future Research." Int J Mol Sci **17**(1).
Weiss, A. and J. Schlessinger (1998). "Switching signals on or off by receptor dimerization." Cell **94**(3): 277-280.
White, F. A., J. Sun, S. M. Waters, C. Ma, D. Ren, M. Ripsch, J. Steflik, D. N. Cortright, R. H. Lamotte and R. J. Miller (2005). "Excitatory monocyte chemoattractant protein-1 signaling is up-regulated in sensory neurons after chronic compression of the dorsal root ganglion." Proc Natl Acad Sci U S A **102**(39): 14092-14097.
Wiley, H. S. (2003). "Trafficking of the ErbB receptors and its influence on signaling." Exp Cell Res **284**(1): 78-88.
Wilson, M. B., S. J. Schreiner, H. J. Choi, J. Kamens and T. E. Smithgall (2002). "Selective pyrrolo-pyrimidine inhibitors reveal a necessary role for Src family kinases in Bcr-Abl signal transduction and oncogenesis." Oncogene **21**(53): 8075-8088.
Woodall, A. J., M. A. Richards, D. J. Turner and E. M. Fitzgerald (2008). "Growth factors differentially regulate neuronal Cav channels via ERK-dependent signalling." Cell Calcium **43**(6): 562-575.
Xian, C. J. and X. F. Zhou (1999). "Neuronal-glial differential expression of TGF-alpha and its receptor in the dorsal root ganglia in response to sciatic nerve lesion." Exp Neurol **157**(2): 317-326.
Xu, J. T., H. Y. Tu, W. J. Xin, X. G. Liu, G. H. Zhang and C. H. Zhai (2007). "Activation of phosphatidylinositol 3-kinase and protein kinase B/Akt in dorsal root ganglia and spinal cord contributes to the neuropathic pain induced by spinal nerve ligation in rats." Exp Neurol **206**(2): 269-279.
Xu, J. T., X. Zhao, M. Yaster and Y. X. Tao (2010). "Expression and distribution of mTOR, p70S6K, 4E-BP1, and their phosphorylated counterparts in rat dorsal root ganglion and spinal cord dorsal horn." Brain Res **1336**: 46-57.
Yaksh, T. L. (2006). "Calcium channels as therapeutic targets in neuropathic pain." J Pain **7**(1 Suppl 1): S13-30.
Yao, M., W. Fang, C. Smart, Q. Hu, S. Huang, N. Alvarez, P. Fields and N. Cheng (2019). "CCR2 Chemokine Receptors Enhance Growth and Cell-Cycle Progression of Breast Cancer Cells through SRC and PKC Activation." Mol Cancer Res **17**(2): 604-617.
Yu, X., K. D. Sharma, T. Takahashi, R. Iwamoto and E. Mekada (2002). "Ligand-independent dimer formation of epidermal growth factor receptor (EGFR) is a step separable from ligand-induced EGFR signaling." Mol Biol Cell **13**(7): 2547-2557.
Zhang, Q., Y. Liu, F. Gao, Q. Ding, C. Cho, W. Hur, Y. Jin, T. Uno, C. A. Joazeiro and N. Gray (2006). "Discovery of EGFR selective 4,6-disubstituted pyrimidines from a combinatorial kinase-directed heterocycle library." J Am Chem Soc **128**(7): 2182-2183.
Zhang, X., J. Huang and P. A. McNaughton (2005). "NGF rapidly increases membrane expression of TRPV1 heat-gated ion channels." EMBO J **24**(24): 4211-4223.
Zhang, Y., Y. Han, Y. Zhao, Y. Lv, Y. Hu, Y. Tan, X. Bi, B. Yu and J. Kou (2017). "DT-13 Ameliorates TNF-alpha-Induced Vascular Endothelial Hyperpermeability via Non-Muscle Myosin IIA and the Src/PI3K/Akt Signaling Pathway." Front Immunol **8**: 925.
Zhao, M., K. Isami, S. Nakamura, H. Shirakawa, T. Nakagawa and S. Kaneko (2012). "Acute cold hypersensitivity characteristically induced by oxaliplatin is caused by the enhanced responsiveness of TRPA1 in mice." Mol Pain **8**: 55.
Zheng, X. and G. D. Cartee (2016). "Insulin-induced Effects on the Subcellular Localization of AKT1, AKT2 and AS160 in Rat Skeletal Muscle." Sci Rep **6**: 39230.

Zhou, D., S. Lambert, P. L. Malen, S. Carpenter, L. M. Boland and V. Bennett (1998). "AnkyrinG is required for clustering of voltage-gated Na channels at axon initial segments and for normal action potential firing." J Cell Biol **143**(5): 1295-1304.
Zhu, X., S. Cao, M. D. Zhu, J. Q. Liu, J. J. Chen and Y. J. Gao (2014). "Contribution of chemokine CCL2/CCR2 signaling in the dorsal root ganglion and spinal cord to the maintenance of neuropathic pain in a rat model of lumbar disc herniation." J Pain **15**(5): 516-526.
Zhuang, Z. Y., P. Gerner, C. J. Woolf and R. R. Ji (2005). "ERK is sequentially activated in neurons, microglia, and astrocytes by spinal nerve ligation and contributes to mechanical allodynia in this neuropathic pain model." Pain **114**(1-2): 149-159.

Figure Legends

Figure 1: The highly selective ErbB1 inhibitor, erlotinib, reverses nerve injury-induced hypersensitivity in reflex pain behaviours and increases a biomarker of cellular activation in nociceptors. A) - C) show time courses of reflex pain behaviours in the CCI neuropathic pain model, following administration of erlotinib (10mg/kg, ip). All values are shown as mean±SEM. A) shows effects on mechanical hypersensitivity (assessed by von Frey filament Paw Withdrawal Thresholds PWT, n=5). B) shows effects on noxious thermal hypersensitivity (assessed by Hargreaves' infra-red test Paw Withdrawal Latencies PWL, n=5). C) shows effects on noxious cold hypersensitivity (seen as increased Suspended Paw Elevation Times from 4^{o}C shallow water bath; n=4). Ipsilateral hypersensitivity was significantly reversed by erlotinib for 140-160min in each case; ††p<0.01 by One-Way Repeated Measures ANOVA with Dunnett's post-hoc test, while no significant effects were observed on contralateral responses. D) shows immunofluorescence staining for an unbiased activity reporter (phospho-CaMKII (Thr286), reflecting increased intracellular Ca^{2+} concentrations) in DRG neurons from naïve and CCI animals, as well as the effect of treatment with erlotinib (10mg/kg, ip, 1 hr). Both typical immunofluorescence images and quantitative analysis show that phospho-CaMKII (Thr286) staining in peripherin-positive (nociceptive) DRG neurons was increased following CCI and this was reversed by erlotinib (n=4 in each case). One-Way ANOVA with Tukey's post-hoc test revealed a significant increase due to CCI (*p<0.05) and its significant reversal by erlotinib (†p<0.05). Scale bars represent 50μm. Typical numbers of positive cells counted per section were 197 for peripherin and 76 for phospho-CaMKII (Thr286).

Figure 2: ErbB1 expression in DRG is limited to small, unmyelinated nociceptive neurons and colocalises with ErbB2, but not ErbB3 or ERbB4. A) shows typical images of immunofluorescence staining using a highly characterised ErbB1 antibody (mouse monoclonal [EGFR1], ab30) that does not cross-react with other ErbB family members, compared to peripherin (a marker of unmyelinated C-fibre nociceptors). Very high concurrence of staining was observed in DRG from either naïve or CCI animals. Numbers of positive cells counted per section were typically 134 for peripherin and 112 for ErbB1. Around 80% of peripherin-positive cells expressed

ErbB1 in both naïve and CCI conditions and this result was corroborated with a second, similarly specific ErbB1 antibody (rabbit monoclonal [E235], ab32077). The n values were 18 and 4, respectively. B) shows typical images of staining for ErbB1 versus the myelinated afferent marker, NF-200; the satellite glial cell marker, glutamine synthetase; and the microglial/invading macrophage marker, CD68. Minimal co-localisation with ErbB1 (<14%) was observed in each case, in DRG from either naïve or CCI animals. Numbers of positive cells counted per section were typically 120 for ErbB1, 95 for NF-200, 182 for glutamine synthetase, and 66 for CD68, n=4 in each case. C) shows typical examples of staining using highly characterised antibodies (that do not cross-react with other ErbB family members) for ErbB2 (rabbit polyclonal, 06-562), ErbB3 (mouse monoclonal, H3.105.5) and ErbB4 (mouse monoclonal, H4.77.16) versus peripherin or ErbB1 (ab30). Abundant staining for ErbB2 was seen in a very high proportion (>90%) of peripherin-positive cells with little staining of other cells. There was a similarly high concurrence of ErbB2 staining with ErbB1, again limited to small DRG cells. ErbB2 was expressed in 93.9±1.0% and 96.4±1.1% of ErbB1-positive cells from naïve and CCI DRG, respectively. Only occasional staining was observed for ErbB3 or ErbB4 in DRG and this was almost entirely associated with peripherin-negative cellular profiles. Less than 8% of peripherin-positive cells showed staining for ErbB3 or ErbB4. Numbers of positive cells counted per section were typically 191 for peripherin, 187 for ErbB1, 188 for ErbB2, 11 for ErbB3, and 14 for ErbB4, n=4 in each case. Scale bars represent 50μm.

Figure 3: ErbB2 inhibitors reverse nerve injury-induced mechanical hypersensitivity and act synergistically with selective ErbB1 inhibitors, matching evidence for direct ErbB1:ErbB2 interaction in small nociceptive DRG neurons. A) and B) show effects of the highly selective ErbB2 inhibitors, mubritinib (15mg/kg, ip) and tucatinib (15mg/kg, ip) in A), and the dual ErbB1/ErbB2 inhibitors, lapatinib (20mg/kg, ip) and afatinib (2.5mg/kg, ip) in B), on mechanical hypersensitivity following CCI, as assessed by von Frey filament PWT values (n=4-6). Ipsilateral hypersensitivity was significantly reversed for up to 140-180min in each case; †-††p<0.05-0.01 by One-Way Repeated Measures ANOVA with Dunnett's post-hoc test, while no significant effects were observed on contralateral responses. C) shows typical images from a Proximity Ligation Assay, with specific antibodies for ErbB1 (ab30) and ErbB2 (06-562). Close target proximity is reported as orange fluorescence. Sections were counterstained for peripherin (green) using conventional immunofluorescence. Nerve injury induced a clear (>2-fold) increase in the percentage of peripherin-positive cells that showed ErbB1:ErbB2 proximity fluorescence compared to naïve. Typical numbers of positive cells counted per section were 117 for peripherin and 40 for ErbB1:ErbB2 proximity ligation, n=4 in each case. The statistical significance of changes was assessed by unpaired two-tailed t-test; **p<0.01, showing a significant CCI-induced increase in ErbB1:ErbB2 heterodimerisation compared to naïve. Scale bars represent 50μm. D) shows typical images of immunofluorescence staining for a prominent auto-/trans-phosphorylation site in ErbB2, phospho-ErbB2

(Tyr1221/2), identified by a specific rabbit monoclonal antibody [6B12], compared to ErbB1, identified using ab30, in DRG from naïve, CCI and CCI animals treated with erlotinib, 10mg/kg ip, 1hr. The percentage of ErbB1-positive cells showing phospho-ErbB2 (Tyr1221/2) staining was more than 2.5-fold increased following CCI and this was reversed by erlotinib. One-Way ANOVA with Tukey's post-hoc test revealed a significant increase due to CCI (***$p<0.01$) and its significant reversal following erlotinib treatment (††$p<0.01$), n=4 in each case. Numbers of positive cells counted per section were typically 189 for ErbB1 and 53 for phospho-ErbB2 (Tyr1221/2). Scale bars represent 50μm. E) shows effects of selective ErbB1 and ErbB2 inhibitors, in combination, on mechanical hypersensitivity following CCI, as assessed by von Frey PWT scores. Low doses of erlotinib (0.33mg/kg, ip) and mubritinib (1.0mg/kg, ip), selected to produce just discernible levels of analgesia alone, were tested in combination. One-Way Repeated Measures ANOVA with Dunnett's post-hoc test indicated statistically significant attenuation due to erlotinib at 20 and 40min following administration, for mubritinib at 20min and for the combination throughout the 20-100min period; ††$p<0.01$; n=4 in each case. F) shows formal assessment of analgesic synergy between mubritinib (1.0mg/kg, ip) and erlotinib across a range of erlotinib doses (ip), using Bliss Additivism effect-based modelling to predict expected combination outcomes. Comparison of observed versus expected combination dose-response curves by Extra Sum of Squares F test indicated a significant difference, reflected in a more than 3.8-fold reduction in EC_{50} value (mean [95% CI] from 1.09 [1.06/1.14]) to 0.28 [0.25/0.31]mg/kg, †††$p<0.001$ (n=4-5 for each point). G) shows the effects of individual and combined treatment with further (structurally distinct) selective ErbB1 and ErbB2 blockers, falnidamol (0.33mg/kg, ip) and tucatinib (1.0mg/kg, ip), respectively, against nerve injury-induced hypersensitivity. The observed analgesic effect was significantly greater than the predicted combination effect according to Bliss Additivism modelling ($p<0.001$, Student's t-test, n=4).

Figure 4: Nerve injury-induced mechanical hypersensitivity involves Src-mediated transactivation of ErbB1 in small nociceptive DRG neurons. A) shows effects of the selective Src/Abl inhibitor, dasatinib (3mg/kg, ip) and the highly selective Src inhibitor, A419259 (15mg/kg, ip) on mechanical hypersensitivity following CCI, as assessed by von Frey filament PWT scores (n=4 in each case). Ipsilateral hypersensitivity was significantly reversed for 60min and 50min, respectively, with complete reversal at peak in both cases; ††$p<0.01$ by One-Way Repeated Measures ANOVA with Dunnett's post-hoc test. No significant changes were seen in contralateral responses. B) shows typical images of immunofluorescence staining for phospho-Src (Tyr527); a site targeted by Csk that constitutively suppresses Src activity (using a specific rabbit polyclonal antibody) versus ErbB1 (identified using ab30). Staining for phospho-Src (Tyr527) was observed in a clear majority of ErbB1-positive DRG cells in naïve animals, but this was approximately halved following CCI and the change was unaffected by erlotinib treatment (10mg/kg ip, 1hr). The statistical significance of changes was assessed by One-Way ANOVA with Tukey's post-hoc

test; **p<0.01 compared to naïve, n=4 in each case. Numbers of positive cells counted per section were 197 for ErbB1 and 47 for phospho-Src (Tyr527). Src activation by dephosphorylation at Tyr527 during CCI appeared to be independent of ErbB1 functional activity. C) shows typical examples of staining for phospho-ErbB1(Tyr845); a site prominently targeted by Src (using a specific mouse monoclonal antibody, clone 12A3) versus peripherin. Staining for phospho-ErbB1 (Tyr845) in peripherin-positive DRG cells was increased almost 3-fold following CCI, compared to that in naïve animals, but this was virtually unaltered following erlotinib (10mg/kg ip, 1hr), despite being completely reversed following dasatinib (3mg/kg ip, 1hr). The statistical significance of changes was assessed by One-Way ANOVA with Tukey's post-hoc test. **p<0.01, increase compared to naïve and ††p<0.01, decrease compared to CCI, n=4 in each case. Numbers of positive cells counted per section were typically 231 for peripherin and 105 for phospho-ErbB1(Tyr845). Nerve injury clearly increased ErbB1 phosphorylation at Tyr845 (the target site for upstream Src), and correspondingly, this was reversed by dasatanib, but not by erlotinib, indicating that the event was not downstream of ErbB1 activation. Scale bars represent 50μm in each case.

Figure 5: Nerve injury induces autophosphorylation of ErbB1 at Tyr1068 with an intracellular peri-nuclear localisation and recruitment of Gab1, a linker to PI 3-kinase/Akt signalling. A) shows typical images of dual immunofluorescence staining for phospho-ErbB1 (Tyr1068), an auto-/trans-phosphorylation site responsible for recruiting the signalling adapters Grb2 and Gab1 (using a specific rabbit monoclonal antibody [D7A5] versus ErbB1 (identified using ab30), in DRG from naïve, CCI and CCI animals treated with erlotinib (10mg/kg ip, 1hr) or dasatinib (3mg/kg ip, 1hr). The percentage of ErbB1-positive cells showing phospho-ErbB1 (Tyr1068) staining was clearly increased following CCI and this was fully reversed by erlotinib or dasatinib. One-Way ANOVA with Tukey's post-hoc test revealed a significant increase due to CCI (*p<0.05) and its significant reversal following erlotinib or dasatinib (††p<0.01 and †p<0.05, respectively), n=4 in each case. Numbers of positive cells counted per section were typically 62 for ErbB1, and 36 for phospho-ErbB1(Tyr1068). B) shows cellular transect analysis of high power individual DRG cell images to reveal the intracellular localisation of the increased phosphorylation of ErbB1 at Tyr1068 following nerve injury and the effect of erlotinib. Scale bar represents 5μm. A transect from the nuclear perimeter to the neuronal apex of each cell (identified in yellow in this example) was divided into 50 equal bins and the fluorescence intensity was recorded at each. The graph shows mean±SEM fluorescence intensity values plotted against bin number for typical individual DRG cells (n=8 in each case). The statistical significance of changes was assessed by Two-Way Repeated Measures ANOVA with Bonferroni's post-hoc test; *-***p<0.05-p<0.001 for CCI compared to naïve; †-†††p<0.05-p<0.001 for CCI plus erlotinib compared to CCI alone. Low basal levels of phospho-ErbB1 (Tyr1068) immunofluorescence were observed across the transects. Nerve injury induced a marked increase in ErbB1 phosphorylation at Tyr1068 at a perinuclear (not plasma membrane) location and this increment was fully reversed by

erlotinib treatment, consistent with ErbB1 activation occurring here via a ligand-independent intracellular process. C) shows typical images of a Proximity Ligation Assay, with specific antibodies for ErbB1 (ab30) and Gab1 (rabbit polyclonal, 06-579), reporting proximity as orange fluorescence. Sections were counterstained for peripherin (green) using conventional immunofluorescence. Nerve injury induced a clear increase in the percentage of peripherin-positive cells that showed ErbB1:Gab1 proximity fluorescence compared to naïve and this was reversed by erlotinib (10mg/kg ip, 1hr) or mubritinib (15mg/kg ip, 1hr). Scale bar represents 50μm. Numbers of positive cells counted per section were typically 126 for peripherin and 42 for ErbB1:Gab1 proximity ligation, n=4 in each case. The statistical significance of changes was assessed by One-Way ANOVA with Tukey's post-hoc test; *p<0.05 showing a significant CCI-induced increase in Gab1 recruitment to ErbB1 compared to naïve, and †p<0.05 showing significant reversal.

Figure 6: ErbB1-mediated activation of Akt following nerve injury and reversal of mechanical hypersensitivity by highly selective Akt inhibitors. A) shows typical images of immunofluorescence staining for phospho-Akt (Ser473); a phosphorylation site reflecting its activation (using a specific rabbit monoclonal antibody [EP2109Y]) versus ErbB1 (identified using ab30), in DRG from naïve, CCI and CCI animals treated with erlotinib (10mg/kg ip, 1hr), the Akt inhibitor, ipatasertib (20mg/kg ip, 1hr) or the Src inhibitor, dasatinib (3mg/kg ip, 1hr). The percentage of ErbB1-positive cells showing phospho-Akt (Ser473) staining was clearly increased following CCI and this was reversed by erlotinib, ipatasertib or dasatinib. One-Way ANOVA with Tukey's post-hoc test revealed a significant increase due to CCI (*p<0.05) and its significant reversal following erlotinib, ipatasertib or dasatinib (††p<0.01 or †p<0.05), n=4 in each case. Scale bar represents 50μm. Numbers of positive cells counted per section were typically 140 for ErbB1, and 74 for phospho-Akt (Ser473). B) shows effects of the selective Akt inhibitors, ipatasertib (20mg/kg ip) and afuresertib (3.3mg/kg ip) on mechanical hypersensitivity following CCI, as assessed by von Frey filament PWT scores (n=6 and 5, respectively). Ipsilateral hypersensitivity was significantly reversed for 160 and 180min, respectively, with complete reversal at peak in both cases; ††p<0.01 by One-Way Repeated Measures ANOVA with Dunnett's post-hoc test. No significant changes were seen in contralateral responses.

Figure 7: Nerve injury induces ErbB1-, ErbB2- and Akt-dependent intracellular phosphorylation of the vesicular trafficking regulator, AS160 and translocation of the AS160 partner (and vesicular chaperone) LRP1. A) shows typical images of immunofluorescence staining for phospho-AS160 (Thr642), an Akt-target site reflecting AS160 inhibition, which terminates its vesicular anchoring role (using a specific rabbit polyclonal antibody, BS4293) versus ErbB1 (identified using ab30), in DRG from naïve, CCI and CCI animals treated with erlotinib (10mg/kg ip, 1hr) or ipatasertib (20mg/kg ip, 1hr). The percentage of ErbB1-positive cells showing phospho-AS160 (Thr642) staining was clearly increased following CCI and this was

reversed by erlotinib or ipatasertib. One-Way ANOVA with Tukey's post-hoc test revealed a significant increase due to CCI (***p<0.001) and its significant reversal following erlotinib (††p<0.01) or ipatasertib (†p<0.05), n=4 in each case. Scale bar represents 50μm. Numbers of positive cells counted per section were typically 115 for ErbB1, and 79 for phospho-AS160 (Thr642). B) shows cellular transect analysis of high power individual DRG cell images to reveal the subcellular localisation of the increased phosphorylation of AS160 at Thr642 following nerve injury and the effect of treatment with erlotinib, mubritinib (15mg/kg ip, 1hr) or ipatasertib. Scale bar represents 5μm. A transect from the nuclear perimeter to the neuronal apex was constructed for each cell, the proximal part divided into 50 equal bins to encompass all discernible phospho-AS160 (Thr642) staining (0.09μm per bin), and the mean±SEM fluorescence intensity recorded at each. This was plotted against distance from the nuclear perimeter (n=8 in each case). The statistical significance of changes was assessed by Two-Way Repeated Measures ANOVA with Bonferroni's post-hoc test; *-***p<0.05-p<0.001 for CCI compared to naïve and †-†††p<0.05-p<0.001 for CCI plus erlotinib, mubritinib or ipatasertib compared to CCI alone. In basal conditions a low level of phospho-AS160 (Thr642) staining was observed in a ring-like configuration close to the nuclear perimeter. Nerve injury induced a striking (3-fold at peak) increase in phospho-AS160 (Thr642) fluorescence, concentrated at a slightly more distal (but still perinuclear) site compared to naïve, and this change was reversed by erlotinib, mubritinib or ipatasertib. C) shows cellular transect analysis of high power individual DRG cell images to reveal the intracellular localisation of LRP1 (using a specific rabbit monoclonal antibody, [EPR3724], versus ErbB1 (identified using ab30), following nerve injury and the effect of erlotinib or ipatasertib. Scale bar represents 5μm. A transect from the nuclear perimeter to the neuronal apex was divided into 50 equally spaced bins and the fluorescence intensity was recorded at each, for typical individual DRG cells in naïve, CCI and CCI plus erlotinib or CCI plus ipatasertib animals, and the mean ± SEM intensity values plotted against bin number (n=9 in each case). The statistical significance of changes was assessed by Two-Way Repeated Measures ANOVA with Bonferroni's post-hoc test; *p<0.05 for CCI compared to naïve; †p<0.05 for CCI plus erlotinib compared to CCI, and †-††p<0.05-p<0.01 for CCI plus ipatasertib compared to CCI. In basal conditions, scattered clusters of LRP1 fluorescence were seen in a broadly perinuclear location. Nerve injury induced the significant appearance of LRP1 clusters in more distal parts of the transect and this change was reversed by treatment with selective ErbB1 or Akt inhibitors.

Figure 8: Nerve injury induces ErbB1- and Akt-dependent trafficking of $Na_v1.9$ (an LRP1 partner) and $Ca_v1.2$ to the plasma membrane of small DRG neurons. A) shows cellular transect analysis of high power individual DRG cell images to reveal the subcellular localisation of $Na_v1.9$ (using a specific guinea pig polyclonal antibody, AGP-030) in ErbB1-positive DRG cells (identified using ab30) from naïve, CCI and CCI animals treated with erlotinib (10mg/kg ip, 1hr) or ipatasertib (20mg/kg ip, 1hr). Scale bar represents 5μm. The cyan (ErbB1) channel is omitted to enhance clarity of

$Na_v1.9$ distribution. A transect from the nuclear perimeter to the neuronal apex was divided into 50 equal bins and the mean±SEM fluorescence intensity was recorded at each (n=8). The statistical significance of changes was assessed by Two-Way Repeated Measures ANOVA with Bonferroni's post-hoc test; **-***p<0.01-p<0.001 for CCI compared to naïve and †-†††p<0.05-p<0.001 for CCI plus erlotinib or ipatasertib compared to CCI alone. In basal conditions $Na_v1.9$ appeared to be distributed quite uniformly across the transect but following nerve injury there was clearly increased deployment to the plasma membrane or nearby. This CCI-induced relocation of $Na_v1.9$ was fully reversed by treatment with erlotinib or ipatasertib. B) shows typical images of a Proximity Ligation Assay, with specific antibodies for $Na_v1.9$ (rabbit polyclonal ASC-017) and LRP1 (mouse monoclonal [5A6]). Close target proximity is reported as orange fluorescence. Sections were counterstained for peripherin (green) using conventional immunofluorescence, n=4 in each case. One-Way ANOVA with Tukey's post-hoc test revealed a significant increase due to CCI (*p<0.05) and reversal by erlotinib treatment (†p<0.05). These results clearly indicate $Na_v1.9$ association with LRP1 and its translocation to the proximity of the plasma membrane following CCI through an ErbB1-dependent process. C) shows cellular transect analysis of high power individual DRG cell images to reveal the intracellular localisation of $Ca_v1.2$ (using a specific guinea pig polyclonal antibody, AGP-001) versus ErbB1 (identified using ab30), following nerve injury and the effect of treatment with erlotinib or ipatasertib. Scale bar represents 5μm. A transect from the nuclear perimeter to the neuronal apex was divided into 50 bins and the fluorescence intensity was recorded at each, with matched extension beyond the 50^{th} bin at the plasma membrane, where appropriate. Mean±SEM intensity was plotted against bin number for typical DRG cells from naïve, CCI and CCI plus erlotinib or CCI plus ipatasertib animals (n=8 in each case). The statistical significance of changes was assessed by Two-Way Repeated Measures ANOVA with Bonferroni's post-hoc test; **p<0.01-p<0.001 for CCI compared to naïve and †-†††p<0.05-p<0.001 for CCI plus erlotinib or CCI plus ipatasertib compared to CCI. In basal conditions $Ca_v1.2$ fluorescence was expressed broadly but moderately concentrated near plasma membrane. Nerve injury induced a marked and significant increase in $Ca_v1.2$ deployment at the plasma membrane and beyond into proximal regions of the AIS and axon itself. These changes were reversed by treatment with erlotinib or ipatasertib.

Supplementary Figure: CCI nerve injury induces ErbB1-dependent trafficking of $Na_v1.8$, but not $Na_v1.7$ to the plasma membrane of small DRG neurons. The Figure shows cellular transect analysis of high power individual DRG cell images to reveal the subcellular localisation of $Na_v1.8$ and $Na_v1.7$ (using specific rabbit polyclonal antibodies, ASC-016 and ASC-007, respectively) in ErbB1-positive DRG cells (identified using ab30) from naïve, CCI and CCI animals treated with erlotinib (10mg/kg, ip, 1hr). A transect from the nuclear perimeter to the neuronal apex was divided into 50 equal bins and the mean±SEM fluorescence intensity was recorded at each (n=9 and 6, respectively). The statistical significance of changes was

assessed by Two-Way Repeated Measures ANOVA with Bonferroni's post-hoc test; *-**p<0.05-p<0.01 for CCI compared to naïve and †p<0.05 for CCI plus erlotinib compared to CCI alone. In basal conditions, $Na_v1.8$ and $Na_v1.7$ appeared to be distributed quite uniformly across the transect but following nerve injury there was significant deployment of $Na_v1.8$ (although not $Na_v1.7$) to the plasma membrane or nearby. This CCI-induced relocation of $Na_v1.8$ was fully reversed by treatment with erlotinib.

Table 1: Primary antibodies used.

Target	Antibody	Supplier; ID (dilution)
ErbB1 EGF-binding domain **ErbB1** cytoplasmic domain **ErbB1** cytoplasmic domain	mouse monoclonal [EGFR1] * rabbit monoclonal [E235] * mouse monoclonal [8G6.2]	Abcam; ab30 (1:1000) Abcam; ab32077 (1:2000) Merck Millipore; 05-1047 (1:1000)
ErbB2	rabbit polyclonal ** rabbit monoclonal **	Merck Millipore; 06-562 (1:1000) Origene; UMAB36 (1:250)
ErbB3	mouse monoclonal [H3.105.5] †	ThermoFisher; MA5-13008 (1:2000)
ErbB4	mouse monoclonal [H4.77.16] ††	ThermoFisher; MA5-12888 (1:1000)
peripherin	chicken polyclonal	Abcam; ab39374 (1:7500)
NF-200	chicken polyclonal	Merck Millipore; AB5539 (1:15000)
glutamine synthetase	rabbit polyclonal	Abcam; ab49873 (1:8000)
CD68	mouse monoclonal [ED1]	Abcam; ab31630 (1:500)
TRPV1	guinea pig polyclonal	Abcam; ab10295 (1:3000)
phospho-CaMKII (Thr286)	rabbit polyclonal	BioWorld Technology Inc; BS5009 (1:2000)
phospho-Src (Tyr527)	rabbit polyclonal	Cell Signaling Technology; 2105 (1:100)
phospho-ErbB1 (Tyr845)	mouse monoclonal [12A3]	Merck Millipore; 04-283 (1:1000)
phospho-ErbB1 (Tyr1068)	rabbit monoclonal [D7A5]	Cell Signaling Technology; 3777 (1:250)
phospho-ErbB2 (Tyr1221/1222)	rabbit monoclonal [6B12]	Cell Signaling Technology; 2243 (1:200)
phospho-Akt (Ser473)	rabbit monoclonal [EP2109Y]	Abcam; ab81283 (1:400)
phospho-ERK (Thr202/Tyr204)	rabbit monoclonal [D13.14.4E]	Cell Signaling Technology; 4370 (1:250)
phospho-AS160 (Thr642)	rabbit polyclonal	BioWorld Technology Inc; BS4293 (1:420)
pan-AS160	rabbit polyclonal	Merck Millipore; ABS-54 (1:2000)
Gab1	rabbit polyclonal	Merck Millipore; 06-579 (1:2000)
LRP1	rabbit monoclonal [EPR3724] mouse monoclonal [5A6]	Abcam; ab92544 (1:3000) Abcam; ab28320 (1:1250)
$Na_v1.7$	rabbit polyclonal	Alomone; ASC-008 (1:1000)
$Na_v1.8$	rabbit polyclonal	Alomone; ASC-016 (1:1000)
$Na_v1.9$	guinea pig polyclonal rabbit polyclonal	Alomone; AGP-030 (1:2000) Alomone; ASC-017 (1:3000)
$Ca_v1.2$	guinea pig polyclonal	Alomone; AGP-001 (1:6000)

ErbB1: *no cross reaction with ErbB2, 3, 4; ErbB2: **no cross reaction with ErbB1, 3, 4; ErbB3: †no cross reaction with ErbB1, 2, 4; ErbB4: ††no cross reaction with ErbB1, 2, 3.

Table 2: Effects of intraperitoneal injection of a variety of highly selective ErbB1 inhibitors on CCI-induced hypersensitivity in the von Frey Paw Withdrawal Threshold test.

Selective ErbB1 inhibitor	Core pharmacophore	Dose; mg/kg (n)	Mean % reversal of injury-induced reduction in PWT (20-140 min post drug)
erlotinib	quinazoline	0.10 (4) 0.33 (4) 1.0 (4) 3.3 (4) 10 (5)	3.7 ± 1.0 9.9 ± 3.1 42.3 ± 10.3 ** 73.2 ± 6.5 ** 92.2 ± 4.0 **
gefitinib	quinazoline	10 (4)	98.8 ± 4.5 **
AG 1478	quinazoline	3.0 (4)	73.8 ± 7.3 **
falnidamol (BIBX 1382)	pyrimido-pyrimidine	10 (4)	83.9 ± 7.6 **
EGFRi 324674	4,6-substituted pyrimidine	40 (4)	76.3 ± 8.5 **
vehicle	-	N/A (4)	2.7 ± 1.9

Experiments were carried out in animals that displayed marked ipsilateral hypersensitivity to von Frey filaments following CCI carried out 8-12 days previously. Drugs were injected (in 0.2ml per animal) under light isoflurane anaesthesia and after a 20min delay for recovery, Paw Withdrawal Threshold (PWT) testing was carried out at 20min intervals up to 3hr post-injection. The percentage reversal of hypersensitivity (ipsilateral compared to contralateral pre-drug PWT) was meaned over 20-140min post-drug administration. A range of highly selective ErbB1 inhibitors showed robust reversal of hypersensitivity, displaying both concentration-dependence and efficacy from structurally diverse agents. ** indicates significant reversal of hypersensitivity (One-Way ANOVA with Dunnett's post-hoc test or Student's t-test, as appropriate). No significant changes in contralateral PWT were observed for any of the drugs or on either side following vehicle.

Table 3: Effects of intraplantar injection of selective ErbB-receptor-targeting drugs on CCI-induced hypersensitivity in the von Frey Paw Withdrawal Threshold test.

Condition	Intraplantar drug (hindlimb side of administration relative to nerve injury; n)	Mean % reduction in PWT score 20-40 min post-drug (ipsilateral)	Mean % reduction in PWT score 20-40 min post-drug (contralateral)
naive	EGF (4)	-1.9 ± 8.1	-
	vehicle (4)	5.4 ± 7.9	-
CCI	EGF (contra; 6)	-8.4 ± 14.5	-1.0 ± 10.1
	EGF (ipsi; 6)	48.1 ± 14.0 **	1.3 ± 3.9
	EGF + erlotinib (ipsi; 6)	-3.4 ± 8.3	-
	EGF + mubritinib (ipsi; 5)	7.6 ± 13.7	-
	vehicle (ipsi; 4)	3.9 ± 6.1	-
	NRG1 (contra; 4)	-7.0 ± 13.4	-
	NRG1 (ipsi; 4)	-2.9 ± 14.1	-

Experiments were carried out 8-12 days following CCI in animals that displayed marked ipsilateral hypersensitivity to von Frey filaments. Drugs were injected intraplantarly into the interdigital skin (in 50μl per animal) under light isoflurane anaesthesia, and Paw Withdrawal Threshold (PWT) testing recommenced after a 20min delay for recovery and then repeated at 10min intervals up to 70min post-injection. The mean percentage reduction in PWT score over 20-40min post-drug administration was calculated and the statistical significance of changes in ipsilateral or contralateral PWT scores was assessed by One-Way ANOVA with Dunnett's post-hoc test. Injection of EGF (100ng) ipsilateral to CCI caused significant exacerbation of injury-induced hypersensitivity (**$p<0.01$) from 20-40min following administration. This effect was reversed by co-injection of the ErbB1 inhibitor, erlotinib (2.2ng) or the ErbB2 inhibitor, mubritinib (7.0ng), which had no discernible effects alone. The ErbB3/4-selective agonist, neuregulin1-β1 EGF domain (NRG1, (100ng) did not mimic the effect of EGF. Contralateral injection of EGF or NRG1 had no effect on ipsilateral PWT values in CCI animals. Either ipsilateral or contralateral injection of EGF had no effect on contralateral PWT values in CCI animals and was also without effect on baseline PWT values in naïve controls. Administration of vehicle alone had no discernible effect.

Figure 1

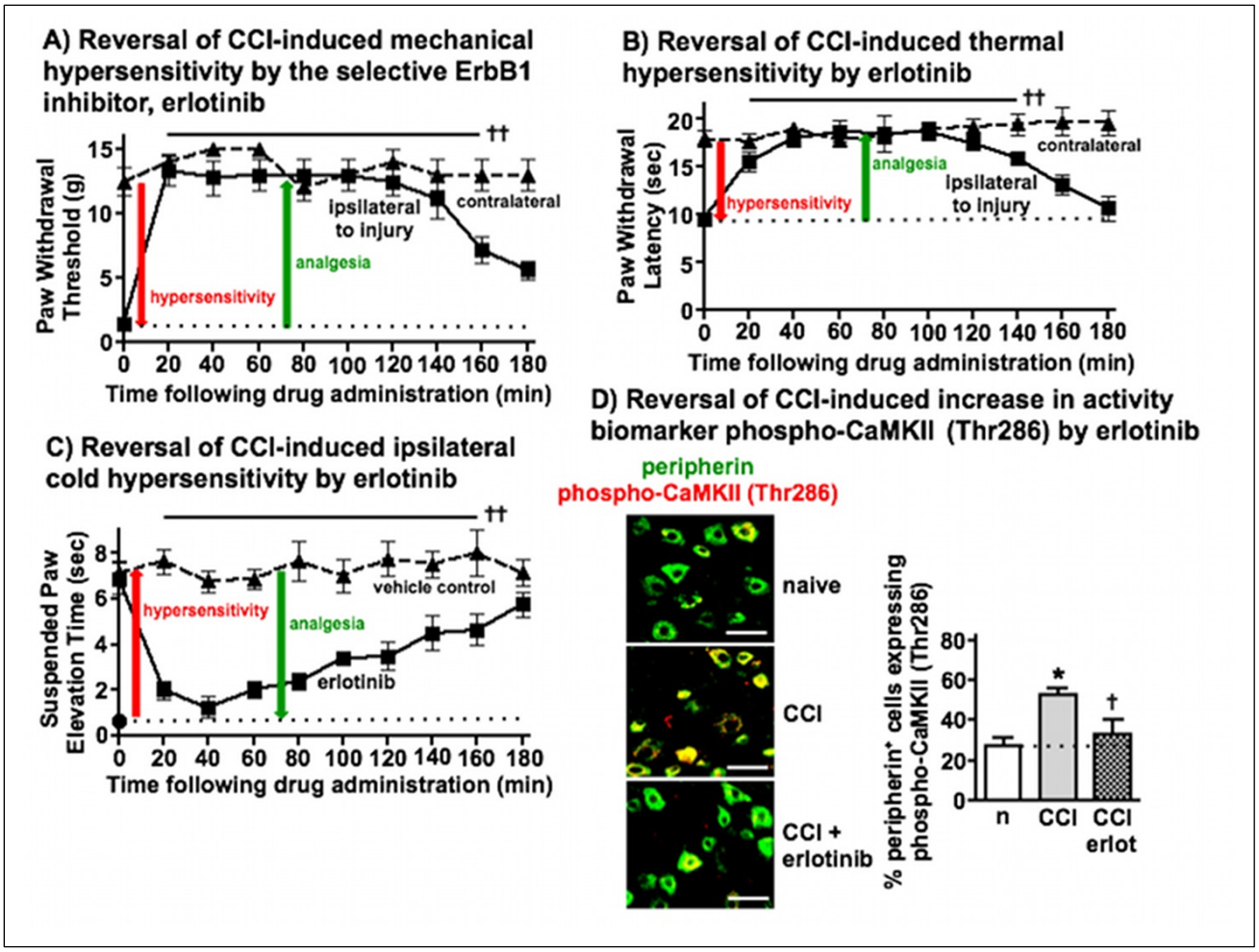
A) Reversal of CCI-induced mechanical hypersensitivity by the selective ErbB1 inhibitor, erlotinib
Paw Withdrawal Threshold (g)
Time following drug administration (min)
hypersensitivity
analgesia
ipsilateral to injury
contralateral
††
B) Reversal of CCI-induced thermal hypersensitivity by erlotinib
Paw Withdrawal Latency (sec)
Time following drug administration (min)
C) Reversal of CCI-induced ipsilateral cold hypersensitivity by erlotinib
Suspended Paw Elevation Time (sec)
vehicle control
erlotinib
D) Reversal of CCI-induced increase in activity biomarker phospho-CaMKII (Thr286) by erlotinib
peripherin
phospho-CaMKII (Thr286)
naive
CCI
CCI + erlotinib
% peripherin+ cells expressing phospho-CaMKII (Thr286)
n
CCI
CCI erlot

Figure 2

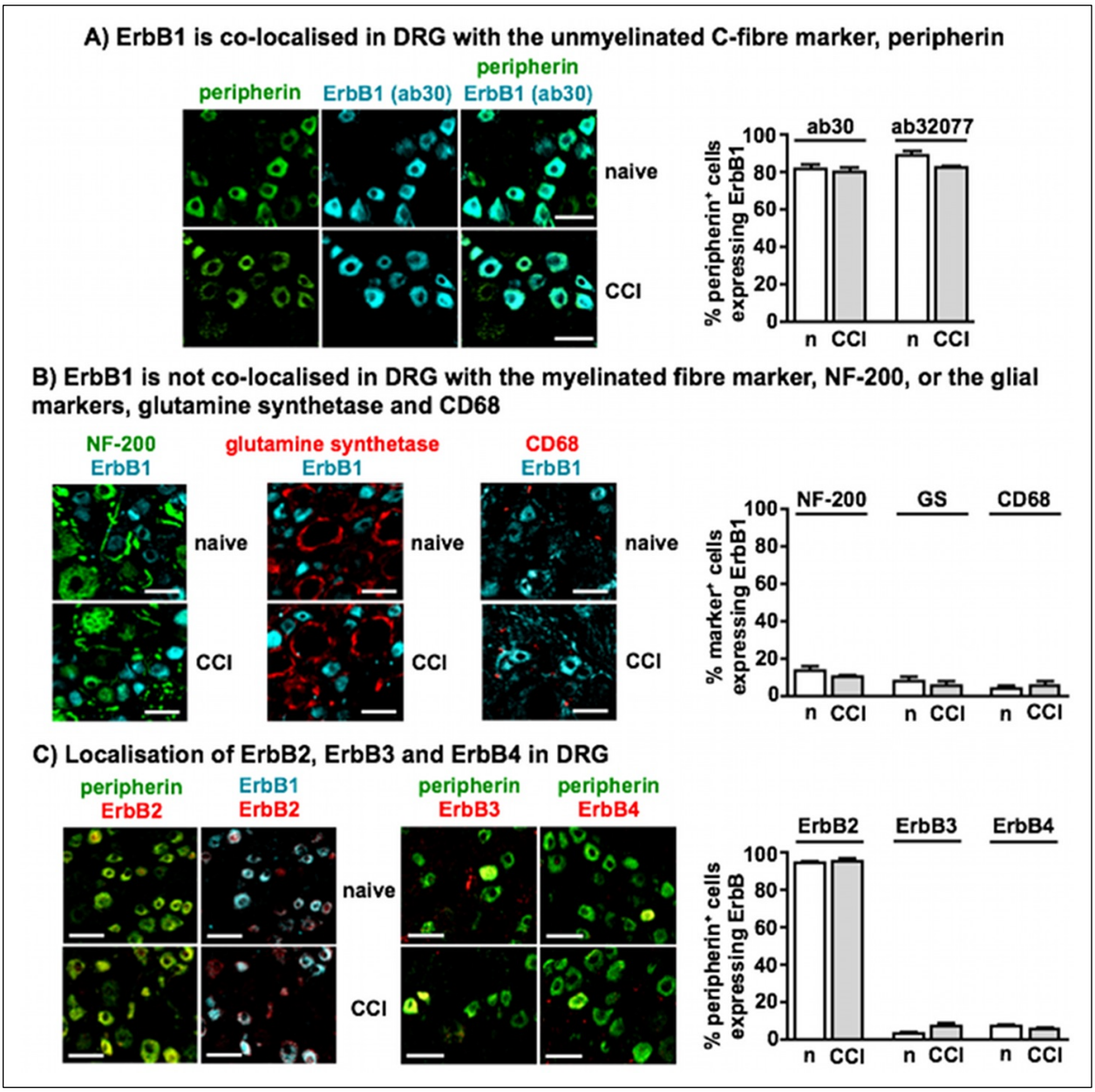
A) ErbB1 is co-localised in DRG with the unmyelinated C-fibre marker, peripherin
peripherin
peripherin
ErbB1 (ab30)
ErbB1 (ab30)
naive
CCI
% peripherin+ cells expressing ErbB1
ab30
ab32077
n
CCI
B) ErbB1 is not co-localised in DRG with the myelinated fibre marker, NF-200, or the glial markers, glutamine synthetase and CD68
NF-200
ErbB1
glutamine synthetase
ErbB1
CD68
ErbB1
% marker+ cells expressing ErbB1
NF-200
GS
CD68
C) Localisation of ErbB2, ErbB3 and ErbB4 in DRG
peripherin
ErbB2
ErbB1
ErbB2
peripherin
ErbB3
peripherin
ErbB4
% peripherin+ cells expressing ErbB
ErbB2
ErbB3
ErbB4

Figure 3

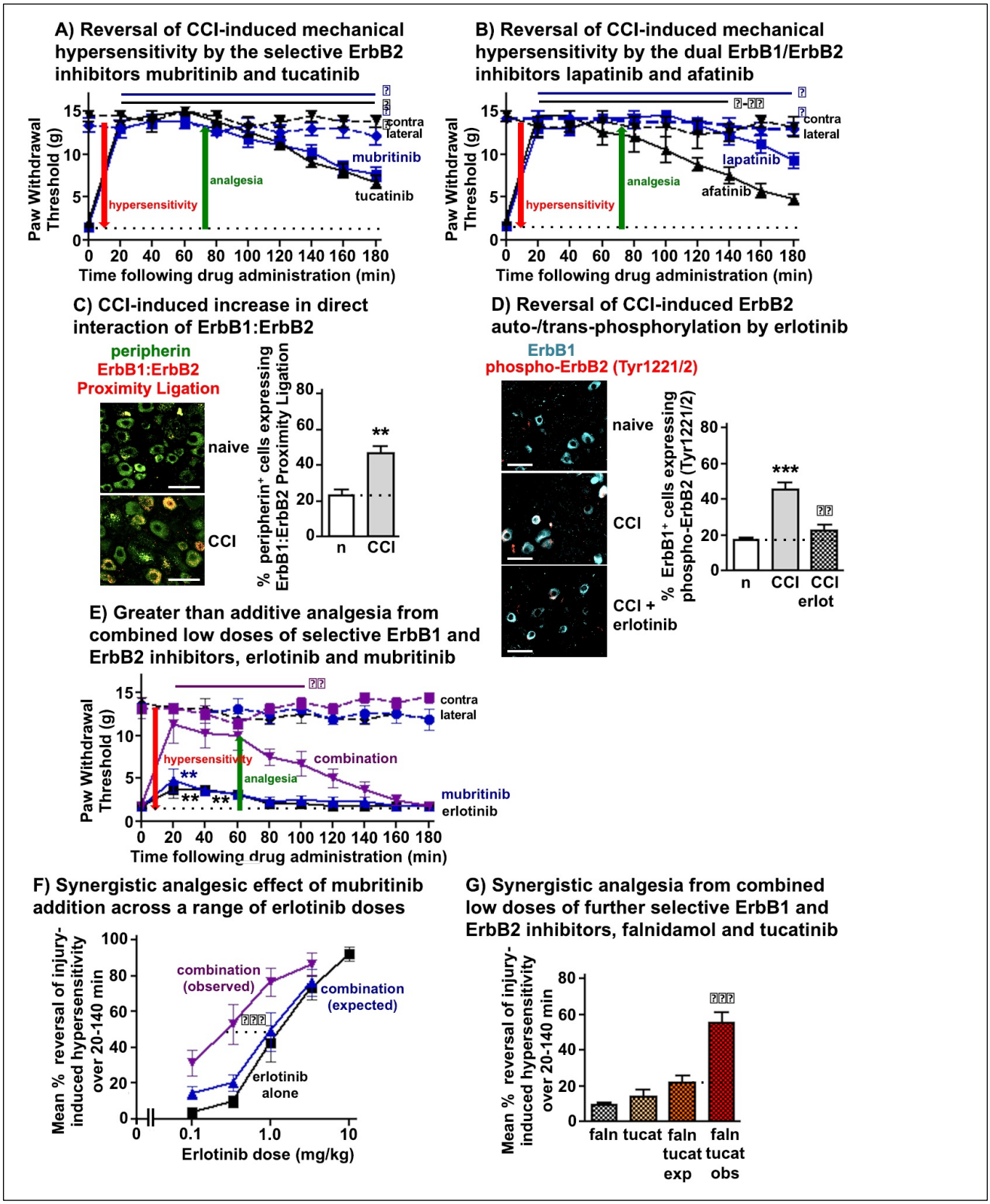
A) Reversal of CCI-induced mechanical hypersensitivity by the selective ErbB2 inhibitors mubritinib and tucatinib
Paw Withdrawal Threshold (g)
contra lateral
mubritinib
tucatinib
hypersensitivity
analgesia
Time following drug administration (min)
B) Reversal of CCI-induced mechanical hypersensitivity by the dual ErbB1/ErbB2 inhibitors lapatinib and afatinib
Paw Withdrawal Threshold (g)
contra lateral
lapatinib
afatinib
hypersensitivity
analgesia
Time following drug administration (min)
C) CCI-induced increase in direct interaction of ErbB1:ErbB2
peripherin
ErbB1:ErbB2
Proximity Ligation
naive
CCI
% peripherin+ cells expressing ErbB1:ErbB2 Proximity Ligation
n
CCI
D) Reversal of CCI-induced ErbB2 auto-/trans-phosphorylation by erlotinib
ErbB1
phospho-ErbB2 (Tyr1221/2)
naive
CCI
CCI + erlotinib
% ErbB1+ cells expressing phospho-ErbB2 (Tyr1221/2)
n
CCI
CCI erlot
E) Greater than additive analgesia from combined low doses of selective ErbB1 and ErbB2 inhibitors, erlotinib and mubritinib
Paw Withdrawal Threshold (g)
contra lateral
hypersensitivity
combination
analgesia
mubritinib
erlotinib
Time following drug administration (min)
F) Synergistic analgesic effect of mubritinib addition across a range of erlotinib doses
Mean % reversal of injury-induced hypersensitivity over 20-140 min
combination (observed)
combination (expected)
erlotinib alone
Erlotinib dose (mg/kg)
G) Synergistic analgesia from combined low doses of further selective ErbB1 and ErbB2 inhibitors, falnidamol and tucatinib
Mean % reversal of injury-induced hypersensitivity over 20-140 min
faln
tucat
faln tucat exp
faln tucat obs

Figure 4

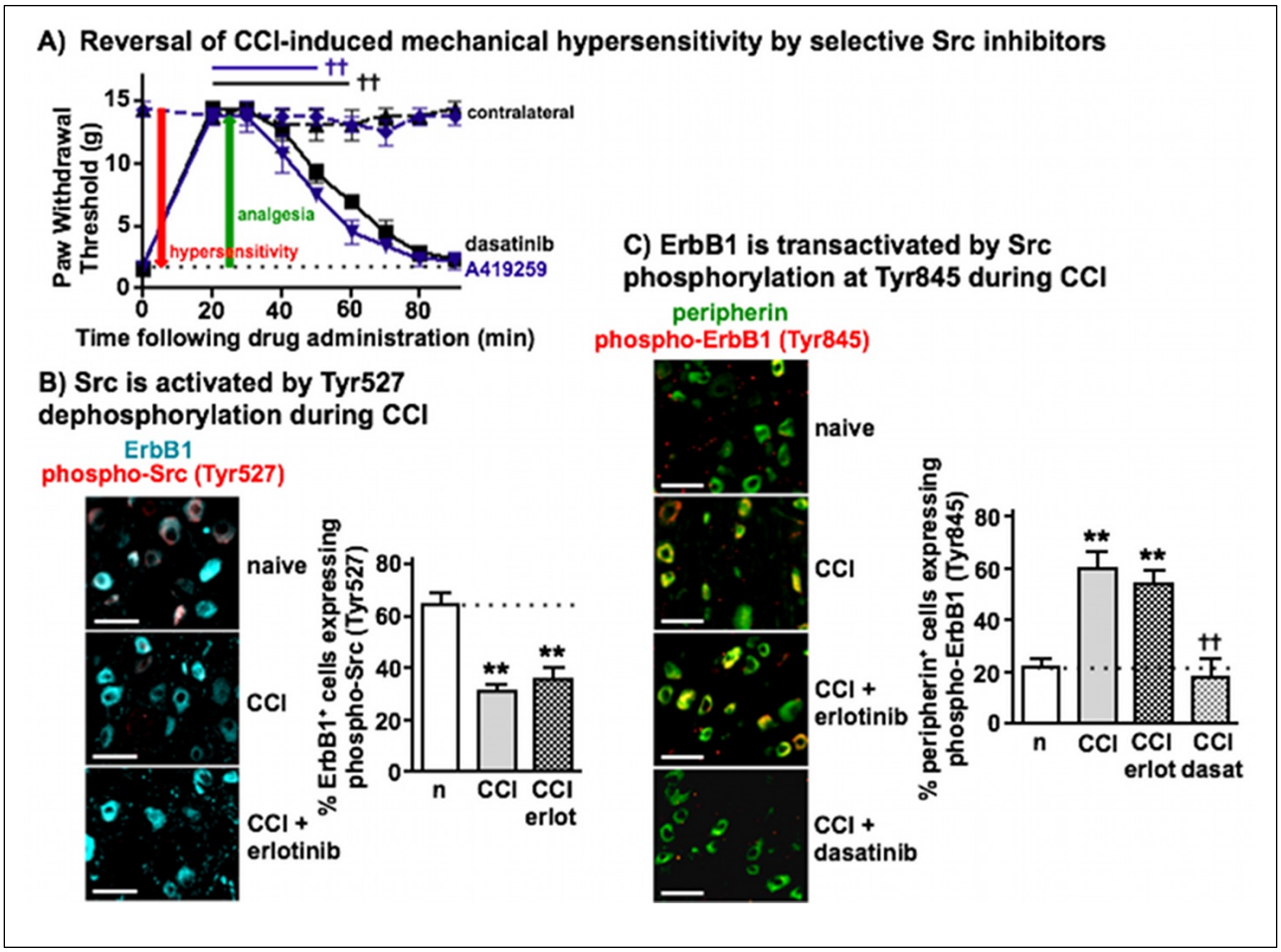
A) Reversal of CCI-induced mechanical hypersensitivity by selective Src inhibitors
Paw Withdrawal Threshold (g)
Time following drug administration (min)
contralateral
dasatinib
A419259
analgesia
hypersensitivity
B) Src is activated by Tyr527 dephosphorylation during CCI
ErbB1
phospho-Src (Tyr527)
naive
CCI
CCI + erlotinib
% ErbB1+ cells expressing phospho-Src (Tyr527)
n
CCI
CCI erlot
C) ErbB1 is transactivated by Src phosphorylation at Tyr845 during CCI
peripherin
phospho-ErbB1 (Tyr845)
naive
CCI
CCI + erlotinib
CCI + dasatinib
% peripherin+ cells expressing phospho-ErbB1 (Tyr845)
n
CCI
CCI erlot
CCI dasat

Figure 5

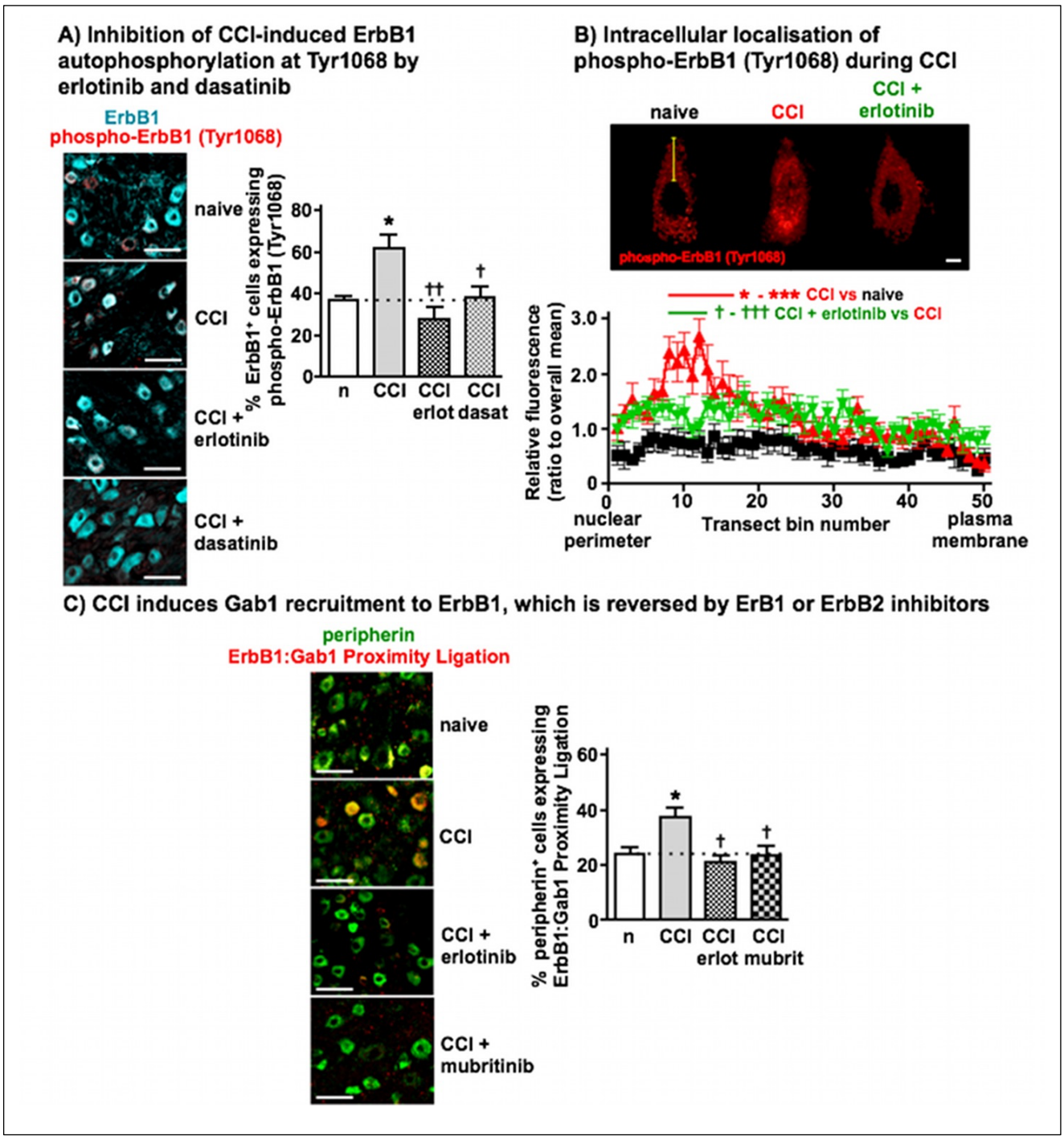
A) Inhibition of CCI-induced ErbB1 autophosphorylation at Tyr1068 by erlotinib and dasatinib
ErbB1
phospho-ErbB1 (Tyr1068)
naive
CCI
CCI + erlotinib
CCI + dasatinib
% ErbB1+ cells expressing phospho-ErbB1 (Tyr1068)
n
CCI
CCI erlot
CCI dasat
B) Intracellular localisation of phospho-ErbB1 (Tyr1068) during CCI
naive
CCI
CCI + erlotinib
phospho-ErbB1 (Tyr1068)
* - *** CCI vs naive
† - ††† CCI + erlotinib vs CCI
Relative fluorescence (ratio to overall mean)
nuclear perimeter
Transect bin number
plasma membrane
C) CCI induces Gab1 recruitment to ErbB1, which is reversed by ErB1 or ErbB2 inhibitors
peripherin
ErbB1:Gab1 Proximity Ligation
naive
CCI
CCI + erlotinib
CCI + mubritinib
% peripherin+ cells expressing ErbB1:Gab1 Proximity Ligation
n
CCI
CCI erlot
CCI mubrit

Figure 6

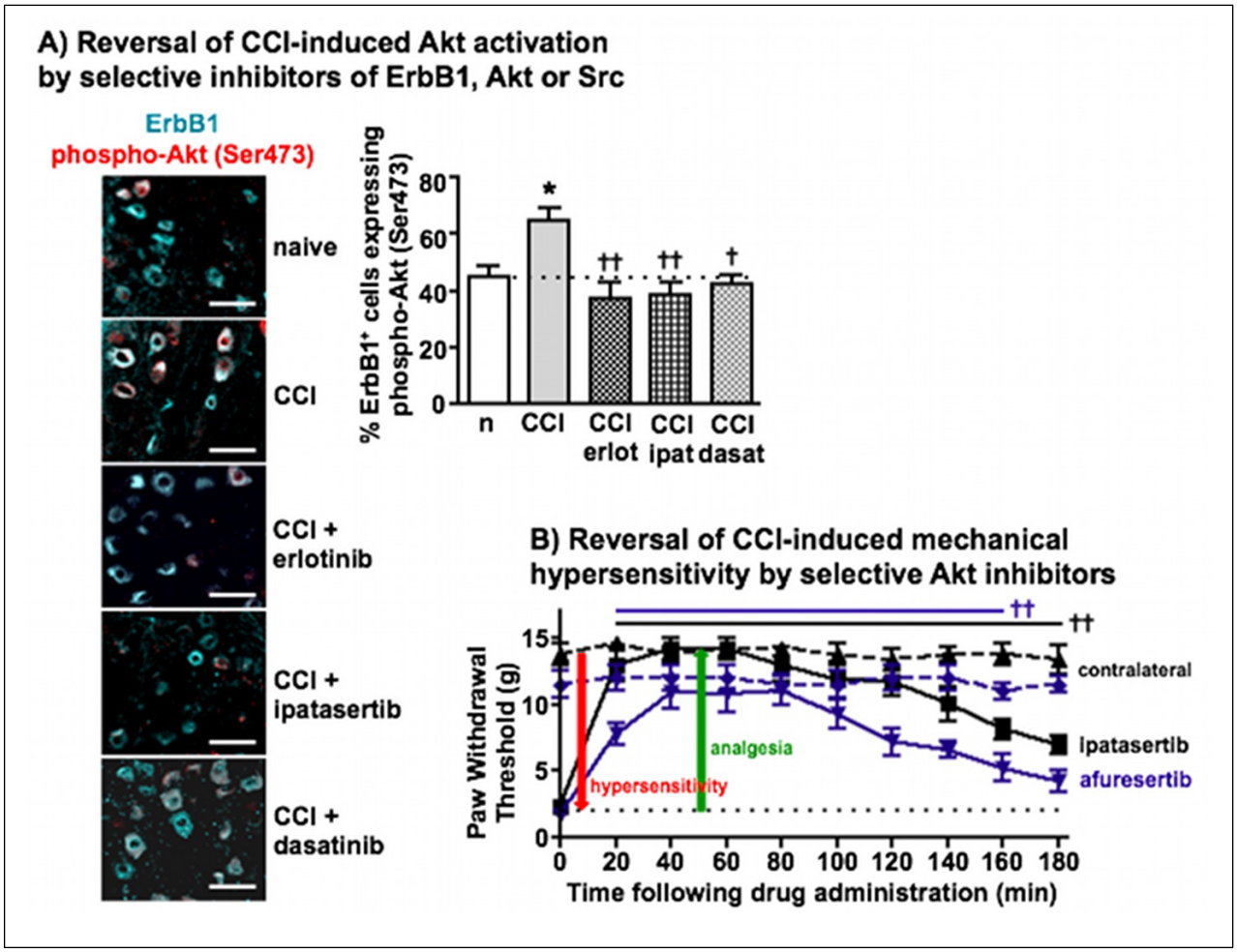
A) Reversal of CCI-induced Akt activation
by selective inhibitors of ErbB1, Akt or Src
ErbB1
phospho-Akt (Ser473)
naive
CCI
CCI +
erlotinib
CCI +
ipatasertib
CCI +
dasatinib
% ErbB1+ cells expressing
phospho-Akt (Ser473)
80
60
40
20
0
*
††
††
†
n
CCI
CCI
erlot
CCI
ipat
CCI
dasat
B) Reversal of CCI-induced mechanical
hypersensitivity by selective Akt inhibitors
Paw Withdrawal
Threshold (g)
15
10
5
0
††
††
contralateral
ipatasertib
afuresertib
analgesia
hypersensitivity
0
20
40
60
80
100
120
140
160
180
Time following drug administration (min)

Figure 7

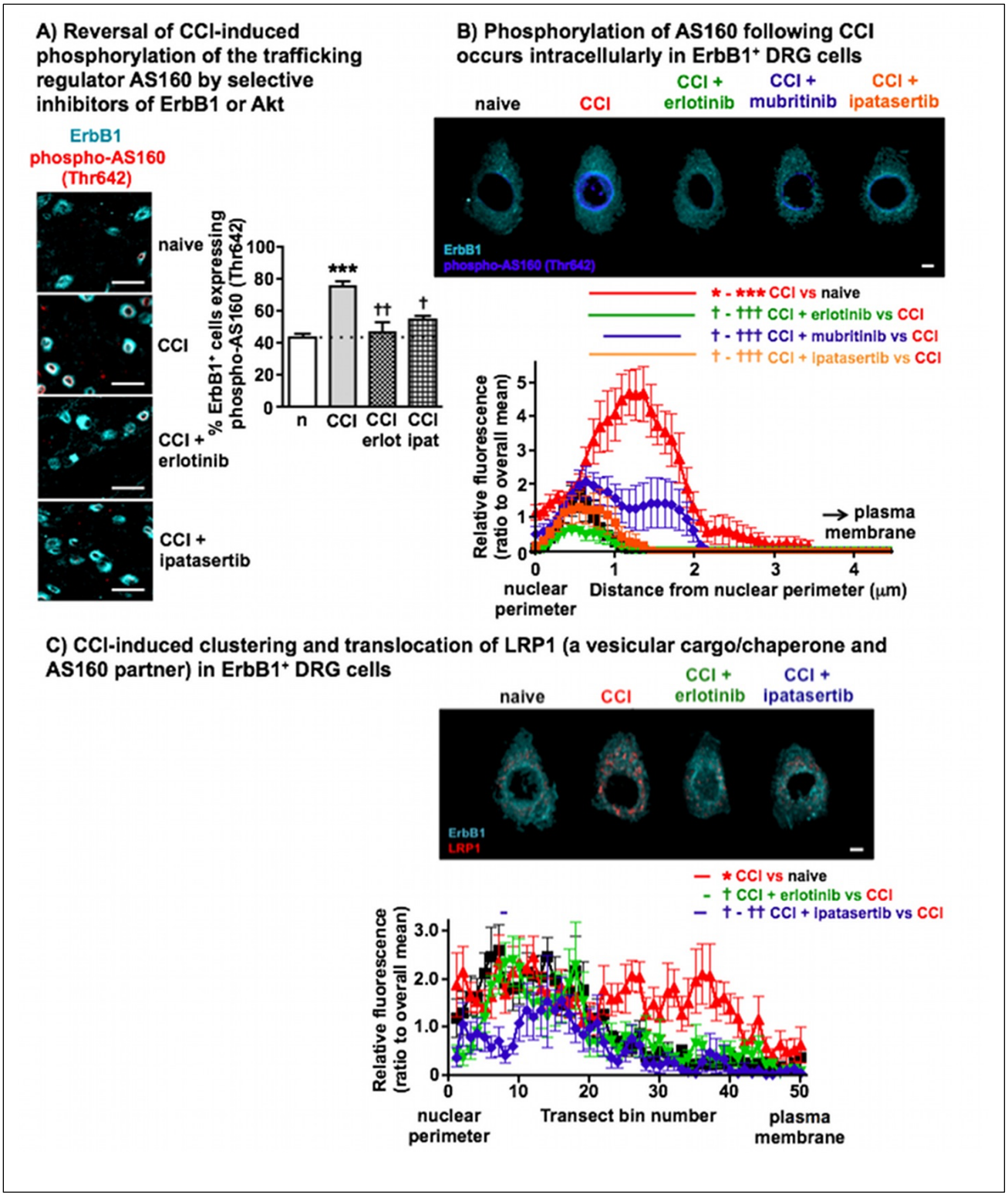
A) Reversal of CCI-induced phosphorylation of the trafficking regulator AS160 by selective inhibitors of ErbB1 or Akt
ErbB1
phospho-AS160 (Thr642)
naive
CCI
CCI + erlotinib
CCI + ipatasertib
% ErbB1+ cells expressing phospho-AS160 (Thr642)
***
††
†
n
CCI
CCI erlot
CCI ipat
B) Phosphorylation of AS160 following CCI occurs intracellularly in ErbB1+ DRG cells
naive
CCI
CCI + erlotinib
CCI + mubritinib
CCI + ipatasertib
ErbB1
phospho-AS160 (Thr642)
* - *** CCI vs naive
† - ††† CCI + erlotinib vs CCI
† - ††† CCI + mubritinib vs CCI
† - ††† CCI + ipatasertib vs CCI
Relative fluorescence (ratio to overall mean)
plasma membrane
nuclear perimeter
Distance from nuclear perimeter (μm)
C) CCI-induced clustering and translocation of LRP1 (a vesicular cargo/chaperone and AS160 partner) in ErbB1+ DRG cells
naive
CCI
CCI + erlotinib
CCI + ipatasertib
ErbB1
LRP1
* CCI vs naive
† CCI + erlotinib vs CCI
† - †† CCI + ipatasertib vs CCI
Relative fluorescence (ratio to overall mean)
nuclear perimeter
Transect bin number
plasma membrane

Figure 8

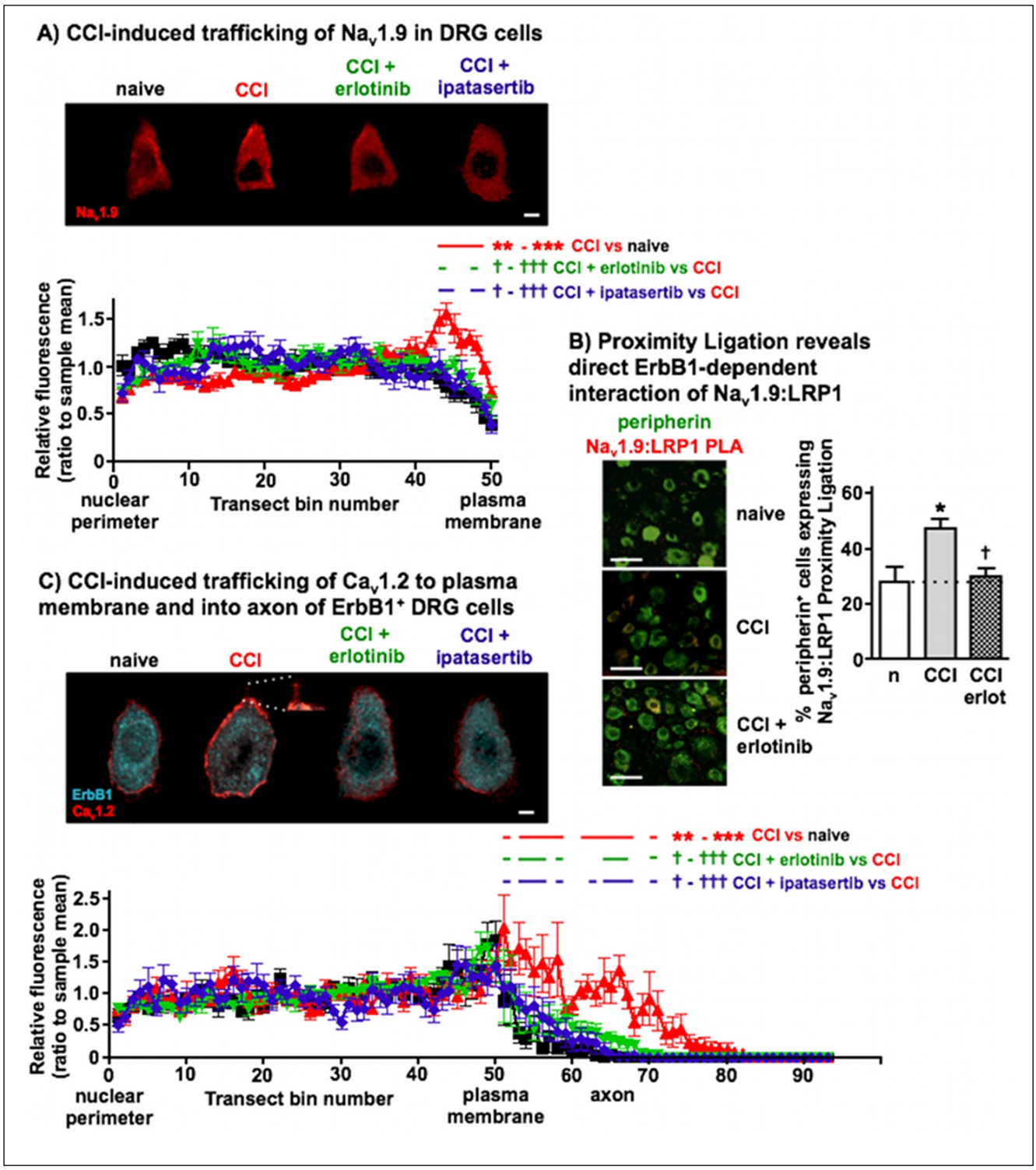
A) CCI-induced trafficking of Nav1.9 in DRG cells
naive
CCI
CCI + erlotinib
CCI + ipatasertib
Nav1.9
** - *** CCI vs naive
† - ††† CCI + erlotinib vs CCI
† - ††† CCI + ipatasertib vs CCI
Relative fluorescence (ratio to sample mean)
nuclear perimeter
Transect bin number
plasma membrane
B) Proximity Ligation reveals direct ErbB1-dependent interaction of Nav1.9:LRP1
peripherin
Nav1.9:LRP1 PLA
naive
CCI
CCI + erlotinib
% peripherin+ cells expressing Nav1.9:LRP1 Proximity Ligation
n
CCI
CCI erlot
C) CCI-induced trafficking of Cav1.2 to plasma membrane and into axon of ErbB1+ DRG cells
ErbB1
Cav1.2
axon

Supplementary Figure